ACTIVATION OF THE ANAPHASE-PROMOTING COMPLEX AS A POSSIBLE TREATMENT STRATEGY FOR HUTCHINSON-GILFORD PROGERIA SYNDROME

A Thesis Submitted to the

College of Graduate and Postdoctoral Studies

in Partial Fulfilment of the Requirements

for the Degree of Master of Science

In the Department of Food and Bioproduct Sciences

University of Saskatchewan

Saskatoon

By

Valeria Carolina Martinez Molina

PERMISSION TO USE

In presenting this thesis/dissertation in partial fulfillment of the requirements for a Postgraduate degree from the University of Saskatchewan, I agree that the Libraries of this University may make it freely available for inspection. I further agree that permission for copying this thesis/dissertation in any manner, in whole or in part, for scholarly purposes may be granted by the professor or professors who supervised my thesis/dissertation work or, in their absence, by the Head of Department or the College in which my thesis/dissertation or parts thereof for financial gain shall not be allowed without my written permission. It is also understood that due recognition shall be given to me and to the University of Saskatchewan in any scholarly use which may be made if any material in my thesis. Requests for permission to copy or to make other uses of materials in this thesis/dissertation in whole or part should be addressed to:

Dean

College of Graduate and Postdoctoral Studies

University of Saskatchewan

116 Thorvaldson Building, 110 Science Place

Saskatoon, Saskatchewan SK S7N 5C9

Canada

OR

Head of the Department of Food and Bioproduct Sciences,

University of Saskatchewan

Room 3E08, Agriculture Building 51 Campus Drive

Saskatoon, Saskatchewan SK S7N 5A8

Canada

ABSTRACT

Numerous factors promote cellular aging, including the accumulation of protein within the nuclear lamina, leading to disrupted gene expression. An extreme example of this is found in children suffering from the premature aging disease, Hutchinson-Gilford Progeria Syndrome (HGPS). HGPS is a rare disease that affects children, causing premature aging and death around the age of 14. It is caused by a mutation in the *LMNA* gene, leading to the production and accumulation of the cytotoxic protein progerin. Progerin has downstream impacts on various cellular functions, such as nuclear morphology, heterochromatin organization, mitosis, DNA replication and repair, and gene transcription. Unfortunately, there is currently no cure for HGPS, and existing treatments still require further development to improve the quality of life for affected children. This research proposes a novel avenue of treatment that focuses on reducing progerin levels within cells by examining the potential of the Anaphase Promoting Complex (APC). The APC is a conserved multiprotein complex that promotes cell cycle progression by targeting proteins such as cyclins for ubiquitin and proteasome-dependent destruction. Moreover, the APC is crucial for mounting cellular stress responses and promoting longevity. Based on the evidence indicating that HGPS is characterized by genomic and proteomic instability, impaired metabolic signaling, mitochondrial dysfunction, and low proteasomal activity, which are cellular functions where the APC plays an important role, we hypothesized that an elevated APC activity would impact progerin levels. Using HGPS primary fibroblasts grown in tissue culture, we observed decreased progerin levels in cells treated with Mad2 inhibitor (M2I-1, an APC activator) compared to cells treated with DMSO (vehicle control). We observed that APC activation via M2I-1 induced morphological changes resulting in a higher proportion of cells resembling non-diseased cells. Likewise, APC activation increased the number of doublings of HGPS fibroblasts, which could be an indicator of cellular repair. APC-progerin interactome, assessed by proximity ligation assays (PLA) and co-immunoprecipitation (Co-IP), showed an interaction between APC subunits and progerin. Additionally, we observed that the proteasome inhibitor MG132 decreased progerin levels in HGPS fibroblasts; when MG132 was combined with M2I-1, progerin levels decreased even further. We concluded that autophagy partly mediates progerin removal after the APC is activated. To further explore this hypothesis, we treated HGPS fibroblasts with chloroquine alone or in combination with M2I-1, MG132, or MG132 and M2I-1. Chloroquine, an autophagy inhibitor, partially inhibited the effect of M2I-1, increasing progerin levels and colocalization with ubiquitin.

These results are remarkable since to remove proteins in HGPS the APC would be associated with autophagy. This research has the potential to benefit children suffering from this devastating disease and the increasing senior population, as aging is a major risk factor for cardiovascular diseases, in particular. Therefore, studying the pathways that link progeria with the normal aging process offers insight into developing potential therapeutic strategies for common diseases associated with aging.

ACKNOWLEDGMENTS

I would like to thank my supervisors, Dr. Christopher Eskiw and Dr. Troy Harkness for giving me the opportunity to travel to Canada to pursue higher education and challenge myself. I want to thank Dr. Eskiw for the guidance and patience in this learning process. I also want to thank my advisory committee members, Dr. Takuji Tanaka, Dr. Yongfeng Ai, and Dr. Kristen Conn, for their time and for providing helpful feedback about this research, special thanks to Ryan Heistad and Dr. Darrell Mousseau for their technical assistance and guidance in conducting co-immuno precipitation experiments.

I also want to thank the members of the Eskiw lab: Zoe Gillespie, Carla Almendariz, Matt Janzen, Fina Nelson, and Morgan Fleming, for their assistance and for creating a positive work environment.

Finally, I want to thank the Canadian Institutes of Health Research (CIHR) for making this project possible.

DEDICATION

I want to dedicate my thesis to my parents, supporting and strengthening me in the most challenging moments, encouraging me to achieve higher education, and believing and seeing the best in me when I could not see it. I am grateful for their support, kind words, and unconditional love. I am also thankful to my partner and his family for being my home and far from home, and for the support during this time.

TABLE OF CONTENTS

1 LITERATURE REVIEW 1
1.1. Nuclear structure and the lamina 1
1.2. Lamina post-translational modifications 3
1.3. Lamina and disease 5
1.4. Hutchinson Gilford Progeria Syndrome HGPS 7
1.4.1 Progerin production 8
1.4.2 Link between HGPS and aging 10
1.5 Mechanism of protein clearance 11
1.5.1 Autophagy 11
1.5.2 The Ubiquitin Proteasome System (UPS) 12
1.5.3 Anaphase Promoting Complex (APC), an important player in the UPS 17
1.6 Understanding aging for a better quality of life: Link between APC aging and HGPS 20
2. HYPOTHESIS AND OBJECTIVES 23
3. MATERIALS AND METHODS 25
3.1 Cell culture 25
3.2 Cell passage 25
3.3 Cell treatments 26
3.4 Western Blotting (WB) 27
3.5 Immunofluorescence 28
3.6 Proximity ligation assay 29
3.7 Immunoprecipitation. 31
3.8 Colocalization 32
3.9 NB1hTert-Δ50 stable cell line 32
3.10 Statistics 33
4. RESULTS 34
4.1 Progerin levels decrease upon APC activation. Western blot levels are dose dependent 34
4.2 Activation of APC with M2I-1 has an impact on progerin levels and cellular morphology. 37
4.3 Impact of APC on population doubling times 42
4.4 Activation of APC with 5 µM of M2I-1 is involved in progerin removal in HGPS primary fibroblasts 44
4.5 Detection of protein-protein interactions between APC proteins and progerin. 53
4.5.1 Progerin and the APC are in proximity 53
4.5.2 Determine interaction between progerin, APC and ubiquitin. 64
4.6 Autophagy plays a role in progerin removal 67
5. DISCUSSION 81

6. CONCLUSIONS 88
7. FUTURE DIRECTIONS. 89
8. LITERATURE CITED 90

LIST OF FIGURES

Figure 1.1 Nuclear lamina localization. 2
Figure 1.2 Lamin A and progerin processing. 9
Figure 1.3 Ubiquitination cascade of target molecule. 14
Figure 1.4 Types of ubiquitin modifications in a substrate**.** 16
Figure 1.5 Representation of macro autophagy process. 12
Figure 4.1 Progerin levels decrease when APC is activated with 5 µM of M2I-1. 36
Figure 4.2 Impact on progerin fluorescent intensity in HGPS cells after APC activation with M2I-1. 38
Figure 4.3 Example of progerin fluorescence of HGPS cells considered for the analysis of progerin fluorescence intensity treated with/without M2I-1. 39
Figure 4.4 Morphology assessment after APC activation. 40
Figure 4.5 Example of cellular shapes corresponding to each category assessed for morphology changes on HGPS cells treated with/without M2I-1. Undieased: untreated 2DD fibroblasts. Diseased progeria cells: HGADFN169 primary fibroblasts 41
Figure 4.6 Doubling times differences between control group and treatment in HGADFN169 and HGADFN167 fibroblasts. 43
Figure 4.7 Evaluation of possible synergetic effects of the APC activator and repurposed drugs Everolimus or Metformin and proteasomal inhibition..... 45
Figure 4.8 Evaluation of synergistic effects of Everolimus and Metformin and M2I-1, and assessment of proteasome inhibition. 47
Figure 4.9 Impact of APC activity modulation on progerin levels in the cell line HGADFN169. 50
Figure 4.10 Analysis of synergetic effects of M2I-1 and Everolimus/Metformin and proteasomal inhibition by immunofluorescence. 52
Figure 4.11 PLA interactions in the control non-diseased cells. 55
Figure 4.12 PLA interaction between APC2 and CDC27 in HGPS HGADFN169 56
Figure 4.13 PLA interactions between APC2 and progerin in HGPS HGADFN169 57
Figure 4.14 PLA interactions between CDC20 and progerin in HGPS HGADFN169fibroblasts after being treated with the APC activator M2I-1 or APC inhibitor apcin. 58

Figure 4.15 Quantification on the number of foci for PLA assay with NB1-hTert as non diseased control cells and HGADFN169 primary fibroblasts. 60
Figure 4.16 PLA interaction in HGADFN169 primary fibroblasts between progerin and ubiquitin. 62
Figure 4.17 Quantification of foci per cell in the PLA reaction progerin-ubiquitin. 63
Figure 4.18 Western blots indicating protein levels of Lamin A/C endogenous interactors. 66
Figure 4.19 Western blot analysis of protein lysates in HGADFN169 HGPS primary fibroblasts. 69
Figure 4.20 Western blot analysis of protein lysates in HGADFN167 HGPS primary fibroblasts. 71
Figure 4.21 Quantification of progerin immunofluorescence levels in HGADFN169 primary fibroblasts with/without autophagy inhibition. 73
Figure 4.22 Assessment of signal colocalization between progerin and ubiquitin evaluated in the nuclei of HGADFN169 primary fibroblasts. 76
Figure 4.23 RGB linear scans to determine colocalization of progerin and ubiquitin. 77
Figure 4.24 Changes in progerin localization upon autophagy inhibition. 79

ABBREVIATION LIST

Aa- Amino acid

AADs- Aging-Associated Diseases

AKT- Serine-threonine protein kinase

AMPK- Adenosine Monophosphate Kinase

APC- Anaphase Promoting Complex

APCIN- APC inhibitor

Atg5- Autophagy Related 5

Atg7- Autophagy Related 7

ATP- Adenosine triphosphate

BAF- Barrier-to-Autointegration Factor

BSA- Bovine Serum Albumin

CAAX- Cysteine-Aliphatic -Aliphatic -Other

CDC20- Cell Division Cycle 20

CDH1- CDC20 Homolog 1

CDK- Cyclin-Dependent Protein Kinases

CDK1- Cyclin-Dependent Kinase 1

CQ- Hydroxychloroquine

CpG-Cytosine phosphate guanine

CR- Caloric Restriction

DAPI-4’,6-diamino-2-phenylindole

DMEM- Dubelco’s Modified Eagles Serum

DMSO- Dimethyl sulfoxide

E1-Ubiquitin-activating enzyme

E2-Ubiquitin-conjugation enzyme

E3-Ubiquitin-ligation enzyme

ECL-Enhanced Chemiluminiscence

EGFP-Enhanced Green Fluorescent Protein

EDM- Emery-Driefuss Muscular Dystrophy

FA- Formaldehyde

FBS- Fetal Bovine Serum

FOXO- Forkhead box

FTI- Farnesyl Inhibitor

GFP - Green Fluorescent Protein

H2AK119ub1- 119-monoubiquitinate histone H2A

H3K27me-trimetylation of lysine 27 on histone H3

HECT- Homologous to E6AP C-Terminus

HECW2- WW Domain-Containing Protein 2

HEPES-4-(2-hydroxyethyl)-1-piperazine ethane sulfonic acid

HGPS- Hutchinson-Gilford Progeria Syndrome

HNF1A- Hepatic Nuclear Factor 1 Alpha

HNTG-HEPES-NaCl-glycerol-Triton X-100

HP1-Heterochromatin Protein 1

HRP-Horse Redish Peroxidase

IF- Immunofluorescence

INM- Inner Nuclear Membrane

LADs- Lamin Associated Domains

LAP1, LAP2B- Lamina-Associated Polypeptides-1 and 2B

LBR- Lamin B Receptor

LC3- protein 1A/AB Light Chain

LMNA-Lamin A/C gene

M2I-1- Mad 2 Inhibitor 1

mTOR-mammalial Target of Rapamycin

NCP: Nuclear Pore Complex

NE- Nuclear Envelope

NL- Nuclear Lamina

ONM- Outer Nuclear Membrane

PBS-Phosphate Buffered Saline

PBST- Phosphate Buffered Saline with Tween 20

PcGs- Polycomb Group Proteins

PCR-Polymerase Chain Reaction

PDT-Population Doubling Time

PKA-Protein Kinase A

PLA- Proximity Ligation Assay

PTM- Post-Transcriptional Modifications

RB- Retinoblastoma Protein

RBR- Ring Between Ring

RE - Restriction Endonuclease

RFC- Relative Centrifugal Field

RGB-Red Green Blue

RING- Really Interesting New Gene

RIPA- Radioimmunoprecipitation Assay

RNAPII- RNA-polymerase II

SAC- Spindle Assembly Checkpoint

SCF- Skp1–Cullin-1–F-box protein

SDS- Sodium Dodecyl Sulfate

SDS-PAGE- Sodium Dodecyl Sulfate Polyacrylamide Gel Electrophoresis

SEM-Standard Error of the Mean

Ser- Phosphorylation site at the amino acid serine

SIRT1- Sirtuin 1

SIRT2- Sirtuin 2

SM/PBST- Skim Milk in Phosphate Buffered Saline with Tween20

SMURF2- SMAD Ubiquitin Regulatory Factor 2

SNAP29- Synaptosome Associated Protein 29

SUMO- Small Ubiquitin-like Modifier

TGOLN2- Golgi Network integral protein 2

TR- Texas red

UB- Ubiquitin

ULK1- Unc-51 Like Kinase 1

ULMs- Ubiquitin-like modifiers

UPS- Ubiquitin-Proteasome System

WB- Western Blot

ZMPSTE24- zinc metalloprotease related to ste24p

1 LITERATURE REVIEW

1.1. Nuclear structure and the lamina

When discussing eukaryotic cells, it is difficult not to think about their distinctive organelle, the nucleus. The nucleus is one of the biggest organelles in eukaryotic cells and one of the most important. It stores the genetic information to determine cellular identity, function, and responses to exterior stimuli (Lammerding, 2011; Kalukula *et al.*, 2022). In eukaryotes, the nucleus is delimited by the nuclear envelope (NE), which separates the nucleus from the cytoplasm. Two layers of bilipid membranes form the NE termed inner (INM) and outer (ONM) nuclear membrane (Field & Rout, 2019) and a network of undelaying laminas (Gruenbaum *et al.*, 2005). The envelope communicates to the cytoplasm through nuclear pores that selectively transport macromolecules (Wente, 2000; Kalukula *et al.*, 2022).

One of the major components of the NE is the nuclear lamina (Figure 1.1), which is a meshwork of proteins found between the INM and the peripheral heterochromatin (Dechat *et al.*, 2010; Paschal & Kelley, 2013; Casasola *et al.*, 2016; Karoutas & Akhtar, 2021). Among the functions of nuclear lamina are maintenance of the nuclear structure and stability, chromatin organization, anchoring of the nuclear pore complex, mechanical stress resistance, cell cycle regulation, cell differentiation, DNA replication, and gene regulation (Dechat *et al.*, 2010; Paschal & Kelley, 2013; Casasola *et al.*, 2016; Karoutas & Akhtar, 2021).

In animals, the lamina is formed by type V intermediate-filament proteins and lamin-associated proteins (Dobrzynska *et al.*, 2016; Almendáriz-Palacios *et al.*, 2020), where lamins A and B are the major proteins expressed in vertebrates. Lamins undergo alternative splicing to create several isoforms. The major isoforms produced by the *LMNA* gene are lamin A and C (Dittmer & Misteli, 2011). While two genes encode the B-type lamins: *LMNB1* encodes lamin B1 protein, and *LMNB2* gene encodes B2 and B3 protein (Eriksson *et al.*, 2003; Ghosh & Zhou, 2014). Type B lamins are essential for cell survival and are expressed in all cells and during development (Gruenbaum *et al.*, 2005). On the other hand, A-type lamins are primarily expressed in differentiated tissues (Malashicheva & Perepelina, 2021).

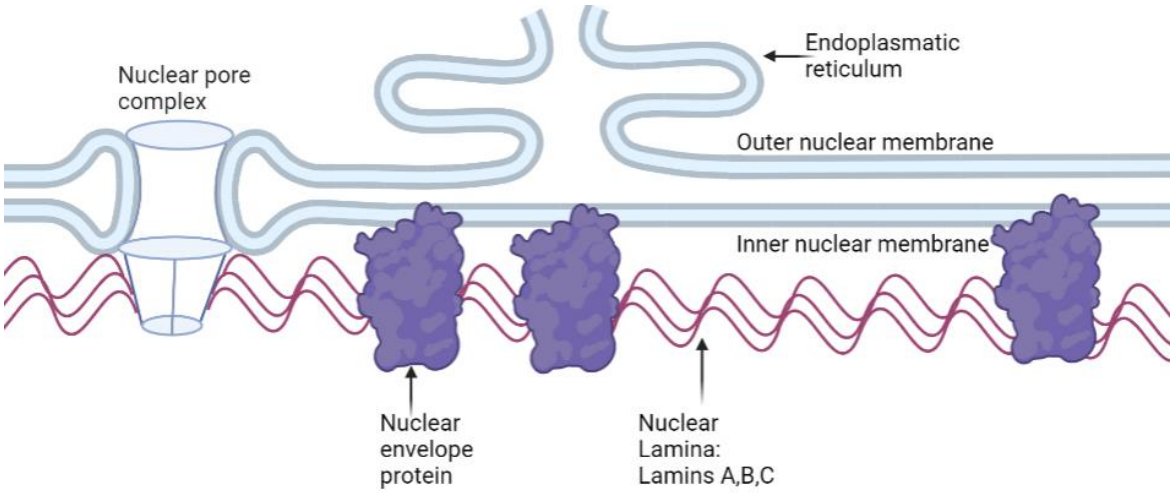

Figure 1.1 Nuclear lamina localization. The nuclear lamina is located between the inner nuclear membrane and peripheral chromatin and it is formed by lamins and lamin-associated proteins. Created in Biorender.

The C-terminal tail domain of lamins is a highly variable region that allows the interaction between lamins and inner nuclear membrane proteins. These lamin-binding proteins include Inner Nuclear Membrane proteins (INM), such as Emerin, MAN1, lamina-associated polypeptides-1 and 2B (LAP1, LAP2B); chromatin proteins; soluble proteins like actin, retinoblastoma protein (RB), barrier-to-autointegration factor (BAF) (Dechat *et al.*, 2008, 2010); and RNA-polymerase II (RNAPII)-dependent transcription complexes and DNA replication complexes (Zastrow *et al.*, 2004; Gruenbaum *et al.*, 2005; Dobrzynska *et al.*, 2016). Likewise, evidence indicates that the nuclear lamina interacts directly with chromatin (Stierlé *et al.*, 2003; Bruston *et al.*, 2010), playing a role in chromatin organization and epigenetic regulation of chromatin (Dechat *et al.*, 2009). In most cases, chromatin association with the nuclear lamina is linked with gene repression (Meuleman *et al.*, 2013). From the examples mentioned above, it can be observed that the broad range of protein interactions with the nuclear lamina reflects the importance and impact that this structure has on the normal functioning of the cell (Casasola *et al.*, 2016; Dechat *et al.*, 2010; Karoutas & Akhtar, 2021).

1.2. Lamina post-translational modifications

Most lamins, apart from lamin C, contain a CaaX motif at the C terminal, comprising a cysteine (C), two aliphatic amino acids (aa), and any of the other amino acids (X). This motif is the target for post-transcriptional modifications (PTM) to produce mature lamins. (Dittmer & Misteli, 2011). These modifications include (1) addition of a farnesyl group in the carboxyl-terminal cysteine, (2) proteolytic cleavage of the aax motif, (3) and methyl esterification of the farnesylated cysteine (Dittmer & Misteli, 2011; Ghosh & Zhou, 2014; Casasola *et al.*, 2016). The addition of the farnesyl group confers hydrophobicity and is thought to facilitate localization to the nuclear envelope (Dittmer & Misteli, 2011). In the case of lamin A, once localized to the NE, Lamin A undergoes a final cleavage of 15 amino acids by the zinc metallopeptidase STE24 (ZMPSTE24), removing the previously added farnesyl group. Hence, only type-B lamins remain farnesylated in their mature form. The presence of this farnesyl group seems to render differences in function and localization of these two types o laminas. Type-B lamins form thin and highly organized filaments that remain closely associated with intracellular membranes, whereas type-A lamins form thicker filaments that add rigidity to the NE (Goldberg *et al.,* 2008). Shimia *et al*. (2015) observed that each lamin type is organized in different meshworks, which shows differences in organization and assembly, suggesting different functional roles in nuclear lamina maintenance. Additionally, B-type and A-type lamins exhibit different mobilities and form various structures (Shimi *et al.,* 2008). Hence, both lamin types, A and B, differ in their biochemical properties, structure, localization, and function.

Phosphorylation (attachment of a phosphate group) is another post-translational modification that lamins undergo during interphase and mitosis, which is catalyzed by several kinases such as CDC2, protein kinase C, and protein Kinase A (Ottaviano & Gerace, 1985; Dittmer & Misteli, 2011). Phosphorylation is higher during mitosis than interphase because it causes the reversible disassembly of lamins during mitosis, suggesting its importance in regulating mitotic reorganization of the lamina (Ottaviano & Gerace, 1985). Lamins contain a conserved site in the head domain that is phosphorylated by the mitotic cyclin-dependent kinase CDK1; in A-type human lamins, this site corresponds to Ser22, where for lamin B1 and B2 it corresponds to Ser 23 and Ser-37 respectively (Simon & Wilson, 2013).

SUMOylation, the addition of a small ubiquitin-like modifier (SUMO), modifies lamins after translation, regulating protein functional properties (Simon & Wilson, 2013). In the case of lamin A, SUMOylation seems important for subcellular localization, where Lamin A interacts with the E2 SUMO enzyme Ubc9 (Zhang & Sarge, 2008). However, even when lamin-SUMOylation has been observed, it occurs less than in any other SUMO substrates (Simon & Wilson, 2013). Yet, decreased SUMOylation levels in Lamin A are associated with diseases like familial dilated cardiomyopathy (Zhang & Sarge, 2008). Additionally, mutations in the *LMNA* gene can cause dysregulation of the SUMOylation process; therefore, it could play an important role in the progression of laminopathies (Boudreau *et al.,* 2012). Interestingly, in cells where DNA damage is induced, Lamin A/C levels decrease; this decrement was mediated through autophagy/nucleophagy initiated by SUMOylation of these proteins (Dou *et al.,* 2015).

Ubiquitination is the covalently attachment of a ubiquitin molecule to a lysine residue. Ubiquitination of target proteins impacts protein function, localization, and fate depending on the type of ubiquitin attachment (Simon & Wilson, 2013). Evidence that lamins can be targeted for degradation by ubiquitination was observed by Khanna *et al.* (2018), where cells expressing lamin A mutations overexpressed the E3 ubiquitin ligase RNF123, which mediated ubiquitination and proteasomal degradation of retinoblastoma protein, lamina associated polypeptide 2α and lamin B1. This could indicate that RNF123-ubiquitination contributes to the mechanisms of laminopathies. Moreover, SMAD Ubiquitin Regulatory Factor 2 (SMURF2), an E3 ligase, physically interacts with lamin A and progerin (a mutant form of lamin A, and targets them for autophagic-lysosomal degradation (Borroni *et al.,* 2018). Lamin B1 was also observed to be turned over by proteasomal degradation mediated by different E3 ligases such as homologous to E6AP C-Terminus (HECT)-type E3 and ligase HECT C2 and WW Domain-Containing Protein 2 (HECW2), which is upregulated in cells expressing Emery-Driefuss muscular dystrophy (EDM) mutation (Khanna *et al.,* 2018). In conclusion, there is evidence that links ubiquitin-mediated degradation and nuclear laminas. However, further research is needed to elucidate the diverse mechanisms of lamins turnover mediated by ubiquitination.

1.3. Lamina and disease

Interactions of the nuclear lamina with a broad range of proteins are implicated in regulating several genes. Therefore, mutations in lamin and lamin-associated protein genes can result in various human diseases (Gerace & Huber, 2012). Mutations in genes encoding components of the nuclear envelope, such as the inner nuclear membranes, outer nuclear membranes, or nuclear lamina, produce a series of genetic disorders named envelopathies. In most cases, these disorders have an autosomal dominant nature (Gaillard & Reddy, 2018) and vary widely from cardiac and skeletal neuromuscular disorders to premature aging (Somech *et al.*, 2005; Chi *et al.*, 2009; Janin *et al.*, 2017). Certain envelopathies even cause developmental pancreatic defects leading to diabetes, such as Hepatic Nuclear Factor 1 Alpha (HNF1A)-diabetes (Schwitzgebel, 2014). However, the most characterized envelopathies are caused by mutations in the *LMNA* gene, which codes for Lamin A and C, leading to multiple diseases termed laminopathies. Laminopathies cause about 15 distinct diseases and are primarily exhibited in mesenchymal tissues such as heart, connective tissue, skeletal muscle, and adipose tissue.

Moreover, laminopathies can either be tissue-specific or affect multiple tissues, mainly characterized by cardiac and skeletal muscle pathologies and progeroid disorders (Deboy *et al.*, 2017; Eissenberg & Gonzalo, 2020). HGPS is one of the most severe examples of laminopathies, characterized by the production of a cytotoxic protein termed progerin (Chi *et al.*, 2009). Table 1.1 summarizes distinct diseases caused by mutations in the *LMNA/C* gene.

Table 1.1 Laminopathies caused by mutations in the LMNA gene.

Disease	Mode of inheritance	*LMNA* defects	Clinical phenotype
Hutchinson-Gilford progeria syndrome	De novo mutations	90% of cases are due to C-to-T change at codon 608 in exon 11 of *LMNA*, activating a cryptic splice donor site	Premature aging including alopecia, loss of subcutaneous fat and premature atherosclerosis; death in early teens
Atypical Werner syndrome	Autosomal dominant	Three reported mutations: A57P, R133L and Ll40R	Premature aging beginning in the second decade; cataracts, sclerodermatous skin, premature atherosclerosis, hair greying
Emery-Dreifuss muscular dystrophy, type 2	Autosomal dominant	Mutations reported in every codon except 12. most are missense	Slowly progressive contractures and muscle weakness; wasting of skeletal muscle and cardiomyopathy with conduction disturbances
Emery-Dreifuss muscular dystrophy, type 3	Autosomal recessive	One reported case: H222Y	Slowly progressive contractures and muscle weakness; wasting of skeletal muscle and cardiomyopathy with conduction disturbances
Limb girdle muscular dystrophy	Autosomal dominant	Six mutations described, three of which are missense	Slowly progressive shoulder and pelvic muscle weakness and wasting; later development of contractures and cardiac disturbances
Dilated cardiomyopathy, type lA	Autosomal dominant	More than 20 mutations described, usually missense mutations in exons 1 or 3	Ventricular dilatation, impaired systolic contractility, arrhythmias, conduction defects
Charcot-Marie-Tooth disease, type 2B1	Autosomal recessive	Single R298C *LMNA* missense mutation in seven Algerian families	Lower-limb motor deficits, walking difficulty, secondary foot deformities and reduced or absent tendon reflexes in the second decade
Familial partial lipodystrophy, Dunnigan type	Autosomal dominant	Missense mutations cluster in exons 8 and 11, -75% of mutations in codon 482 of exon 8	Loss of adipose tissue in the trunk and limbs with concomitant accumulation in the neck and face, often includes insulin-resistant diabetes, hypertraglideridemia and increased susceptibility to atherosclerosis
Mandibulofacial dysplasia	Autosomal recessive usually, one compound heterozygote reported	R527H most common. K542N, A529V and heterozygous R527C/R471C (one case) also reported	Delayed closure of cranial sutures, dental crowding, short stature, lipodystrophy, joint contractures, mandibular and clavicular hypoplasia, acroosteolysis, alopecia and insulin resistance

Disease	Mode of inheritance	*LMNA* defects	Clinical phenotype
Restrictive dermopathy	De novo mutations in LMNA or recessive null mutations in *ZMPSTE24*	Splicing mutations leading to partial or complete loss of exon 11 (two patients). homozygous or compound heterozygous mutations in ZMPSTE24 could also be causative	Intrauterine growth retardation, tight and rigid skin erosions, microstomia, pulmonary hypoplasia; early lethality
Generalized lipoatrophy/ lipodystrophy	Autosomal dominant	Single cases of R133L and Tl0I mutations	Variable phenotypic overlap with other laminopathies with generalized lipodystrophy or lipoatrophy; other features include diabetes, hypertriglyceridemia and progeroid features

Modified from (Capell & Collins, 2006).

1.4. Hutchinson Gilford Progeria Syndrome HGPS

Hutchinson-Gilford progeria syndrome (HGPS) is an extremely rare genetic disorder that affects 1 in 4 million liveborn worldwide. HGPS is characterized by premature aging and development of aging-associated phenotypes such as alopecia, wrinkles, lack of growth, subcutaneous fat loss, progressive cardiovascular disease, thin skin, osteoporosis, and death due to heart attacks and strokes approximately at 14 years old (Gordon *et al.,* 2014; Harhouri *et al.,* 2018). Classic HGPS is caused by a unique *de novo* point mutation in the *LMNA* gene (Ghosh & Zhou, 2014). This activates a cryptic splice site, resulting in a cytotoxic lamin A variant named progerin (Misteli & Scaffidi, 2005; Scaffidi & Misteli, 2007; Gaillard & Reddy, 2018; Serebryannyy & Misteli, 2018).

Progerin builds up in the nuclear lamina; in HGPS patients this results in nuclear aberrations. Eriksson *et al*. (2005) observed that about 70% of fibroblasts present abnormal nuclear shapes, which include wrinkled and lobular nuclear envelope (Eriksson *et al.,* 2003; Misteli & Scaffidi, 2005), thick nuclear lamina, irregular sizes, and interruption of the normal conformation of the nuclear lamina. This causes misplacement and reduced protein levels of several lamin-associated polypeptide (LAP2s) proteins, which is the case of the heterochromatin protein HP1α (Ye *et al.,* 1997; Scaffidi & Misteli, 2005; Orioli & Dellambra, 2018). Additionally, deficient association of

LAP2α with telomeres was observed, preventing cell division and decreasing Lamin B levels (Chojnowski *et al.*, 2015).

Gene regulation is also impacted in HGPS; Lamin A/C regulates chromatin organization, and progerin expression disrupts epigenetic pathways and chromatin organization, resulting in transcriptome changes (McCord *et al.*, 2013). HGPS is characterized by a loss of heterochromatin markers such as H3K27me on the X chromosome (Goldman *et al.*, 2004; Shumaker *et al.*, 2006). Hence, progerin accumulation has a global impact at cellular, genetic, and functional levels, impacting patients' health and quality of life.

Even though HGPS remains incurable, in 2020, the U.S. Food and Drug Administration (FDA) approved the drug lonafarnib as a treatment for HGPS. However, over a 3-year treatment period, the lifespan of treated patients increased by just three months, accompanied by severe side effects such as nausea, vomiting, diarrhea, and fatigue. Therefore, the overall benefit of the current treatment strategies does not outweigh the drawbacks. It is still necessary to understand the mechanisms of the disease regarding protein accumulation in the nuclear lamina and how buildup of proteins can be cleared to improve not just quantity but quality of life. Hence, the present research project intents to bridge this knowledge gap.

1.4.1 Progerin production

As described in Section 1.2, lamins are first expressed as prelamins. To produce their mature form, most lamins undergo three post-translational modifications at the CaaX box of the C-terminal, as shown in Figure 1.2 (except Lamin C). Starting with farnesylation of the cysteine, proteolytic cleavage of the aax motif by either Ras converting enzyme (RCE1) or ZMPSTE24, and carboxyl methylation at the farnesylated cysteine. Lamin A is further processed by the proteolytical cleavage of 15 amino acids that contain the farnesyl group by the ZMPSTE24 enzyme. In HGPS, 90% of cases are caused by a single base substitution C-T in exon 11 at position 1824 of the *LMNA* gene. This mutation activates a cryptic splice site, producing an mRNA missing 150 nucleotides. This mRNA is translated into a mutant protein termed progerin, which has an internal deletion of 50 amino acids near the carboxyl-terminal tail that includes the recognition site for ZMPSTE24 (Capell & Collins, 2006; Ghosh & Zhou, 2014; Gordon *et al.*, 2014; Casasola *et al.*, 2016; Wheaton *et al.*, 2017; Serebryannyy & Misteli, 2018).

Since progerin lacks the ZMPSTEA-recognition site, it remains farnesylated and anchored to the nuclear envelope (Figure 1.2). Accumulation of progerin in the nuclear lamina of HGPS cells disrupts lamin A and B networks, causes aberrant shape and size, signaling dysfunction that leads to genetic instability, alterations in cell division and proliferative rates, as well as cellular stress, including unrepaired DNA (Ghosh & Zhou, 2014; Gordon *et al.*, 2014; Casasola *et al.*, 2016; Wheaton *et al.*, 2017; Serebryannyy & Misteli, 2018).

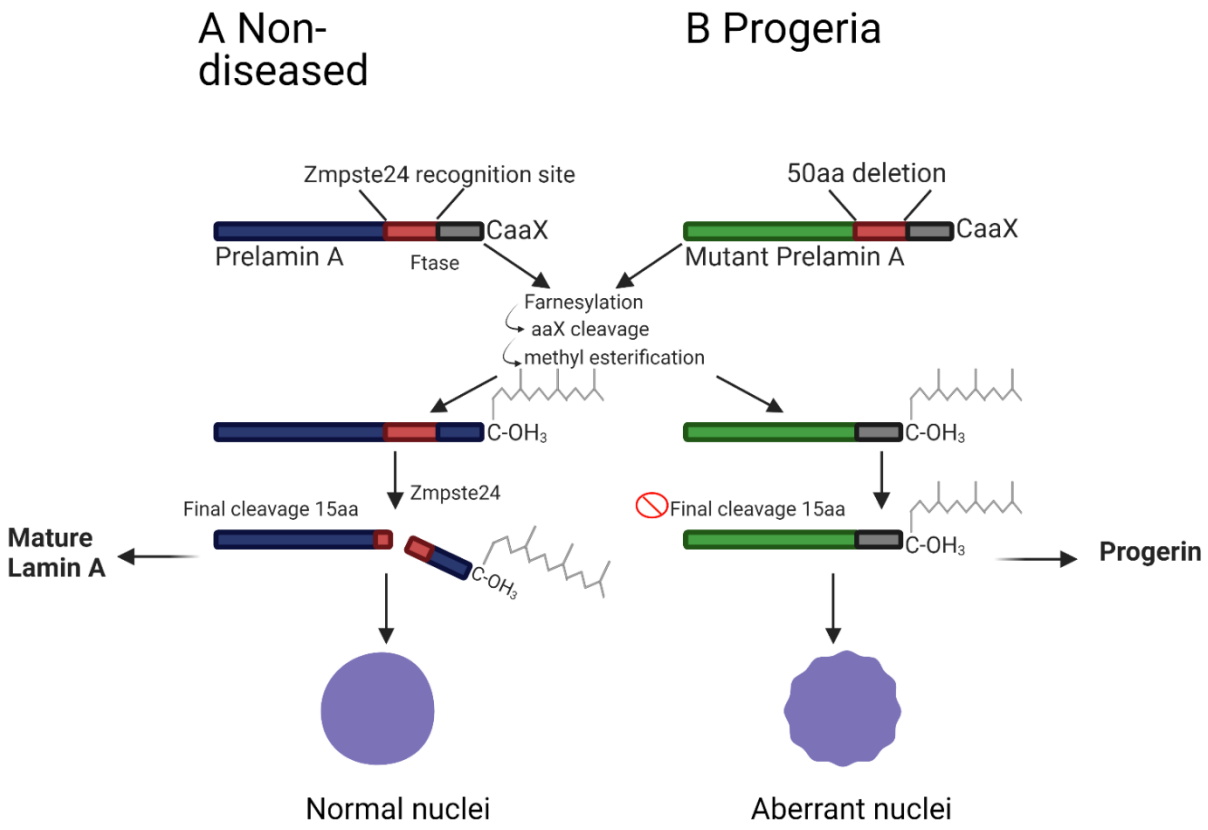

Figure 1.2 Lamin A and progerin processing.
A) Normal lamin A processing: C-terminal cytosine is farnesylated, then the CaaX residue is cleaved, and the now free cytosine is methyl-acetylated. The protease Zmptse24 cleaves 15 aa that include the farnesylated C-terminal. B) In HGPS, a mutation in the *LMNA* gene induces an aberrant splicing site that deletes 50 aa, including the recognition site for Zmptste24. The mutation prevents the cleavage of the farnesyl group. Modified from Coutinho et al. 2009

1.4.2 Link between HGPS and aging

HGPS and the aging process share similarities, including molecular changes and symptomatology. Progerin production results from activating a cryptic or infrequent splicing site (De Sandre-Giovannoli *et al.,* 2003; Eriksson *et al.,* 2003). McClintock and collaborators (2007) observed that a similar splicing event to HGPS occurs at low levels in all ages from skin samples observed from newborn to 97 years. Therefore, the sporadic use of the cryptic splice site in the *LMNA* gene occurs *in vivo* in non-diseased cells. Thus, aging individuals also produce progerin at much lower levels than HGPS patients (Gordon *et al.,* 2014). While progerin mRNA remains low, protein levels accumulate with age (McClintock *et al.,* 2007). This could lead to comparable effects to those observed in HGPS patients. For instance, atherosclerotic plaques in HGPS share features with those found in aging people (Gordon *et al.,* 2014). For example, Scaffidi & Misteli (2007) reported that cellular nuclei from senior patients (81-96 years) share similar morphological defects with those observed in HGPS patients, in addition to down-regulation of nuclear proteins, including HP1 and LAP2.

Furthermore, connections between cellular senescence, generalized calcium dysfunction, vascular calcification, and atherosclerotic plaque formation in both aging and HGPS provide the opportunity to identify the elements involved in aging-related vascular disease (Mackenzie and MacRae, 2011). Given the evidence that links HGPS and the normal aging processes, providing efficient methods to clear progerin and therefore avoid its toxic effects will be valuable to help children suffering from this devastating condition, and can also open the doors for treating seniors suffering from cardiovascular diseases (González Morán, 2014).

1.5 Mechanism of protein clearance

Cell cycle control is governed by changes in the levels of specific proteins. Thus, homeostasis of the proteome keeps cells functional and healthy. The main avenues in charge of maintaining proteostasis (turning over damaged, misfolded, unwanted, or aggregated proteins) are the Ubiquitin-Proteasome System (UPS) and autophagy (Tsakiri & Trougakos, 2015; Zhou *et al.*, 2016; Hommen *et al.*, 2021).

1.5.1 Autophagy

Autophagy is one of the major conserved pathways to maintain proteostasis by degrading proteins with an extensive lifespan and damaged organelles, recycling their building blocks into energy. The process begins with forming double-membrane structures termed autophagosomes that collect cytosolic proteins and organelles. Then, the phagosomes fuse with lysosomes to form structures called autolysosomes, which contain acidic lysosomal hydrolases to destroy their content. Autophagosomes can sequester polyubiquitinated aggregates by specific receptors that recruit ubiquitin to the autophagosome (Wang *et al.*, 2013; Almendáriz-Palacios *et al.*, 2020; Ottens *et al.*, 2021) (see Figure 1.3). The roles of autophagy also include mediating lifespan, where age decreases its function, such is the case in *C.elegans* where knockdown of autophagy genes such as *bec-1*, *atg-7*, and *atg-12* reduce lifespan (Hars *et al.*, 2006).

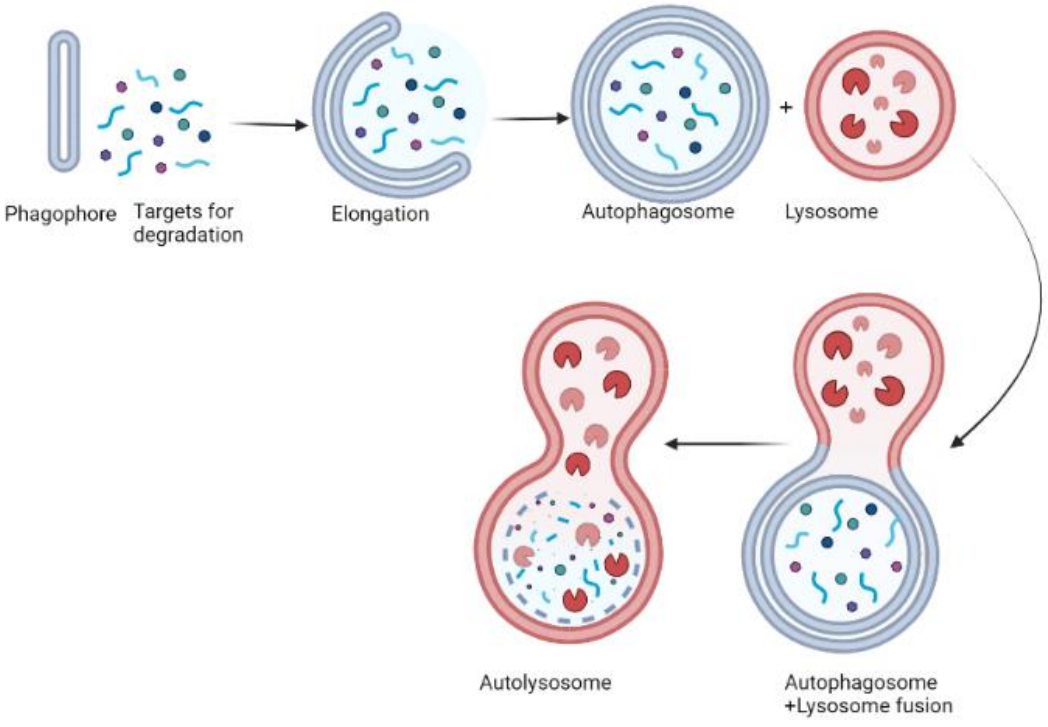

Figure 1.3 Representation of macro autophagy process.
The process begins with the formation of a double membrane structure in the cytoplasm (phagophore). Then this structure increases size around target molecules and forms a closed structure termed autophagosome. Followed by the formation of a hybrid structure product of the fusion of the autophagosome and lysosome. Resulting in an acidified organelle termed autolysosome**.** Created in Biorender.

Although protein turnover by autophagy is generally associated with the cytoplasm, the presence of proteins such as microtubule-associated protein1 light chain 3 (LC3), autophagy-related 5 (Atg5) and autophagy-related 7 (Atg7) in the nuclei points out the role this system plays in the nucleus. Dou and collaborators (2015) identified a direct interaction between the autophagy protein LC3 and the nuclear protein Lamin B1. The researchers found that mutations in the Lamin A/C gene and Emerin triggered autophagy at the nucleus, leading to the creation of autophagosomes that contained nuclear components. They also discovered that inhibiting autophagy made physical nuclear abnormalities worse and reduced cell viability.

Overall, autophagy and the UPS work in a complementary manner; when the proteasome pathway is inhibited, autophagy is induced, and vice versa. For instance, in the central nervous system, under UPS dysregulation, autophagy is activated to prevent neurodegeneration (Pandey *et al.,* 2007). Also, pharmacological inhibition or disruption of autophagy-related genes under nutrient depletion conditions activates proteasomal degradation (Wang *et al.,* 2013). Interestingly, when the proteasome is inhibited with the synthetic compound MG132, it leads to decreased levels of progerin mediated by autophagy (Harhouri *et al.,* 2017).

1.5.2 The Ubiquitin Proteasome System (UPS)

The UPS, one of the major protein clearance regulators, controls proteins whose concentration varies over time (Tsakiri & Trougakos, 2015). To ensure this balance, the UPS primarily uses ubiquitination. Ubiquitination is the covalent attachment of a ubiquitin molecule or ubiquitin molecules (attached to each other forming a chain) to the ε-amino group of lysine residues in a target protein. Depending on the ubiquitin-type molecule, this modification will signal for either protein elimination or subsequent modifications. Nevertheless, cellular stress, metabolic disorders, pathogens, disease-related mutations, and aging can dysregulate this system, which in turn is related to several diseases (von Mikecz, 2006; Varshavsky, 2012; Hommen *et al.,* 2021).

1.5.2.1 Ubiquitin, star player of the UPS

Ubiquitin is a small protein consisting of 76 amino acids (Perez-Hernandez *et al.*, 2020), and it is coded by four different genes (*UBB, UBC, UBA52,* and *RSP27A*) (Blank, 2020). Ubiquitin is expressed in an immature form that can either be fused to a ribosomal protein (when *UBA52* and *RSP27A* are expressed) or fused with six ubiquitin molecules in a head-to-tail manner (in *UBB* and *UBC* expression). These precursors undergo co-translational modifications to produce mature free ubiquitin molecules (Blank, 2020; Perez-Hernandez *et al.*, 2020).

Ubiquitination of a molecule is an ATP-dependent enzymatic reaction that involves three types of enzymes in three hierarchical steps (Figure 1.4). First, an activating enzyme (E1) forms a thioester bond, at the conserved cysteine in its active site, with the C- terminal glycine of ubiquitin (UB). This reaction activates the C terminal of UB for nucleophilic attack. Then, the activated UB is transferred to a conjugating enzyme (E2). Finally, a ubiquitin ligase (E3) facilitates the transfer of UB from the E2 enzyme to the target substrate (Pickart, 2001; Tsakiri & Trougakos, 2015; Zhou *et al.*, 2016). This last group of enzymes (E3) is indeed crucial since they confer specificity to the reaction (Pickart, 2001), interacting with the substrate either directly or using an adaptor molecule (Hershko & Ciechanover, 1998).

Ligation will differ depending on the type of E3 involved in the reaction. The mammalian genome codes approximately 377 different E3 ligases (Medvar *et al.*, 2016); the most studied are Skp1–Cullin-1–F-box protein (SCF) and the Anaphase Promoting Complex APC. These E3s are involved in many cellular processes, including cell cycle regulation (Vodermaier, 2004; Skaar & Pagano, 2009; Zhou et al., 2016; Quek et al., 2018; T. Harkness, 2018). E3 enzymes can belong either to homologous to the E6AP carboxyl terminus (HECT) domain family, really interesting new gene domain family (RING) that contains the majority of E3 enzymes, or ring between ring (RBR). HECT and RBR enzymes bind ubiquitin by an obligate thioester intermediate between the substrate and its active site. RING enzymes work as a scaffold to bring together the substrate and E2 (Metzger *et al.*, 2012; Perez-Hernandez *et al.*, 2020).

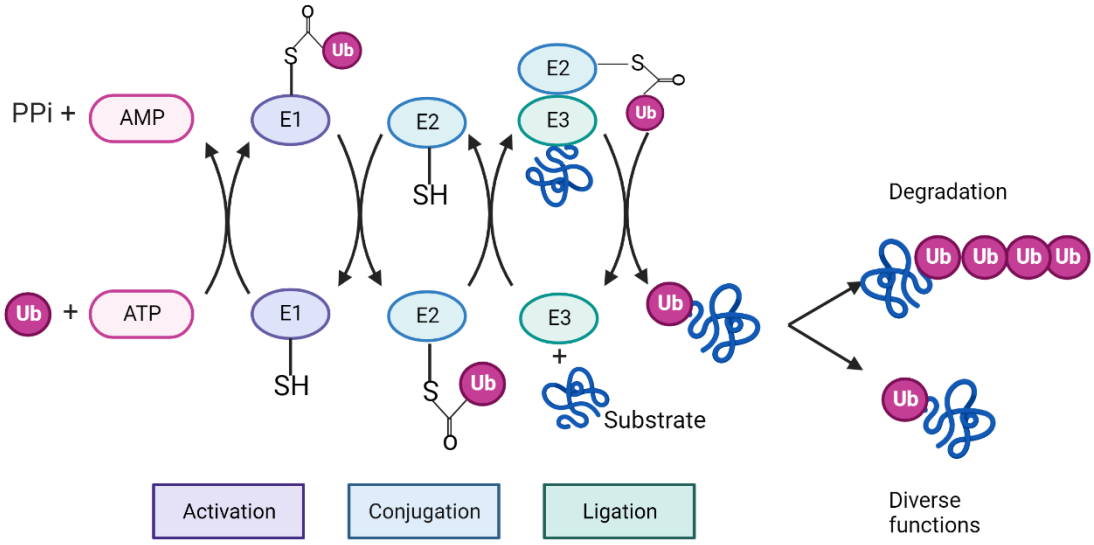

Figure 1.4 Ubiquitination cascade of target molecule.
Ubiquitination is an ATP-depended reaction. It starts when the ubiquitin molecule is activated at the active site of a E1 ubiquitin-activating- enzyme, forming a thioester bond between the E1 and the C-terminal carboxyl group of the ubiquitin molecule. The next step is conjugation by the E2 ubiquitin-conjugating-enzyme that transfer the active ubiquitin molecule to the active site of the E2 enzyme. Finally, the E3 ligase catalizes the creation of an isopeptide bond between a lysine from the substrate and the C-terminal glycine of the ubiquitin molecule**.** Creted in Biorender.

Substrates can be modified by one or multiple ubiquitin molecules resulting in mono ubiquitination, multi-mono ubiquitination, or polyubiquitination (Figure 1.5). Different polyubiquitin chains can be built by using one of 7 different lysines within ubiquitin (Lys6, Lys11, Lys 27, Lys 29, Lys33, Lys 48, and Lys 63). Depending on the type of ubiquitination, the modified substrate will be targeted for proteolysis or non-proteolytic and reversible events (Strieter & Korasick,

2011). Mono-ubiquitination plays a regulatory role in transcription, endocytosis, membrane trafficking, and histone function (Passmore & Barford, 2004) and regulates gene expression and DNA repair (Sadowski & Sarcevic, 2010). For instance, the polycomb group proteins (PcGs) PRC1 and PRC2 maintain cellular identity by transcriptional repression. While PRC1 monoubiquitinates histone H2A lysine 119- ($H2A^{K119ub1}$) which is essential for repression of Cytosine-phosphate-Guanine (CpG) rich promoters, PRC2 catalyzes the tri-methylation of histone H3 lysine 27($H3^{K27}$). Depletion of $H2A^{K119ub1}$ destabilizes PRC1 activity, resulting in the loss of the epigenetic marker $H3^{K27}$ (Tamburri *et al.*, 2020). On the other hand, to form polymers or chains, ubiquitin molecules form links between the lysine side chain of one molecule to the C-terminal carboxyl end of the next Ub molecule (Hochstrasser, 2009). The attachment of poly-ubiquitin chains using the canonical Lys^{48} to a substrate is irreversible and targets proteins for degradation by the proteasome, while attachment of ubiquitin chains built through the Lys^{63} residue regulate kinase activation (Sadowski & Sarcevic, 2010), DNA repair and immune responses (Wu & Karin, 2015; Romo-Tena *et al*., 2018). Another type of chain is produced by Lys^{11}, which was shown to play important roles in cell cycle regulation and proteasomal degradation. For instance, the APC assembles Lys^{11} chains on proteins like securin or cyclin B1 to target them for proteasomal degradation, enabling the transition from metaphase to anaphase (Perez-Hernandez *et al.*, 2020). Furthermore, ubiquitin chains can be heterotrophic. This means ubiquitin molecules are attached through distinct lysine or N-terminal methionine residues. As a result, these links can produce either mixed chains (each ubiquitin is modified once by another ubiquitin) or branched (each ubiquitin is modified by more than one ubiquitin molecule). For instance, during mitosis, the APC

links branched Lys^{11}/Lys^{48} chains in the protein kinase NeK2A kinase (involved in mitotic regulation) to increase proteasomal recognition (Meyer & Rape, 2014).

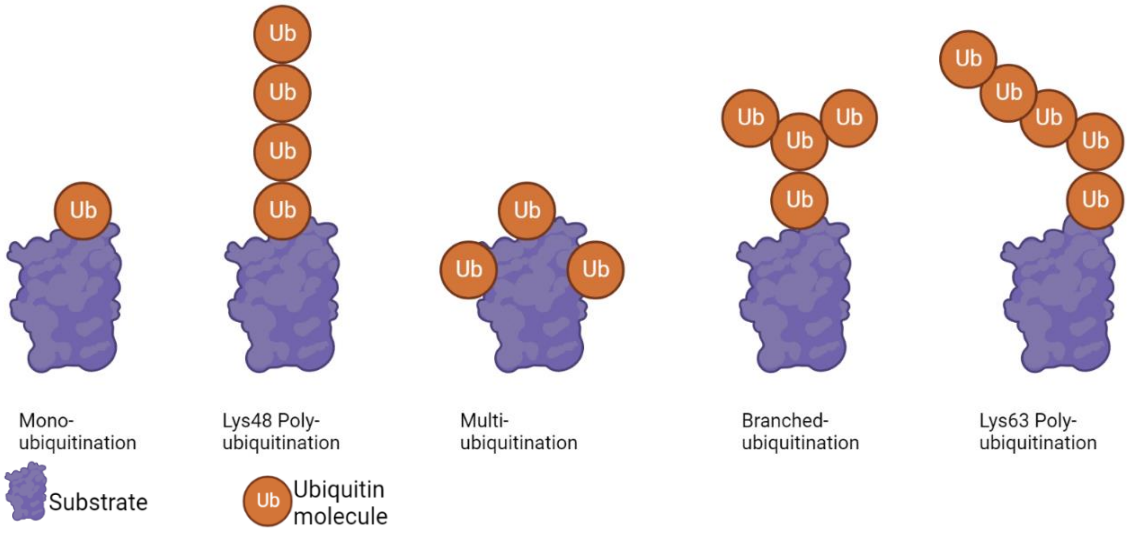

Figure 1.5 Types of ubiquitin modifications in a substrate.
A substrate can be modified by one ubiquitin molecule (mono ubiquitination) or various ubiquitin molecules attached to each other (polyubiquitination). Ubiquitin recognizes the ε-amino group of lysine residues in a target protein. Canonical polyubiquitination uses Lys^{48} and Ly^{63}. Lys^{48} mediates the targeting of proteasomal degradation recognized by the proteasome. Lys^{63} linked chains have non-proteolytic functions. Created in Biorender.

1.5.2.2 Ubiquitin-like molecules

Ubiquitin-like modifiers (ULMs) are pos-transcriptional modifiers, like ubiquitin, critical in diverse biological processes regulating protein stability, interactions, and functions. This group encompasses eight families in humans: SUMO, NEDD8, ATG8, ATG12, URM1, UFM1, FAT10, and ISG15. Like ubiquitination, incorporation ULMs requires an enzymatic cascade mediated by E1, E2, and E3 enzymes. In this reaction, most ULMs are covalently attached to target proteins by their C-terminal diglycine motif (Blank, 2020).

Small-ubiquitin-like modifier (SUMO), one of the most studied ULMs, is a small protein of ~10 KDa; in humans, the genome codes for four distinct SUMO (SUMO1-4) proteins expressed by at least four genes (SUMO1-4) (Hochstrasser, 2009). The targets of this modifier are mostly nuclear and necessary for most organisms (Geiss-Friedlander & Melchior, 2007). For instance, in mice, disruption of SUMO1 caused embryonic lethality and developmental defects in SUMO1

haploinsufficiency (Alkuraya *et al.,* 2006). Additionally, it was observed that nuclear lamins get SUMOylated; Zhang and Sarge pointed out that lamin A is SUMOylated at Lys201 (Y. Q. Zhang & Sarge, 2008). Additionally, upon DNA damage Lamin A/C are SUMOylated to interact with the autophagy-related ubiquitin-like protein ATG8/LC3 (Blank, 2020).

1.5.3 Anaphase Promoting Complex (APC), an important player in the UPS

Cell division events are controlled by cyclical accumulation, modification, and destruction of regulatory proteins. Two kinds of proteins are involved in the biochemical control of cell cycle progression. First, cyclin-dependent protein kinases or CDKs, are proteins that control protein phosphorylation, which in most cases, has an activator effect. The proteins phosphorylated by CDKs are involved in processes that trigger mitosis, such as lamina beak down or spindle formation (Cook, 2001). The second kind of regulatory proteins, termed cyclins, are required by CDKs for their catalytic activity (e.g., Cyclin B1, Cyclin A). Cyclins accumulate in a cyclic way, and their degradation is important to exit mitosis; this process is largely mediated by the APC (Cook, 2001; T. D. Pollard et al., 2017).

The APC is a conserved ubiquitin ligase; in mammals it is composed of 14 subunits where APC2 and APC11 are critical for its catalytic activity, APC10 is necessary for interactions with the coactivators cell division cycle 20 (CDC20) and CDC20 homolog 1 (CDH1) for substrate recognition, and CDC27 forms part of a scaffold unit for coactivator binding (Kataria & Yamano, 2019). The APC targets for degradation (through the 26S proteasome) regulatory proteins that inhibit cell cycle progression, building polyubiquitin chains on lysine residues that are recognized by the proteasome. Thus, the APC controls anaphase entry and progression, exit of mitosis, and G1 maintenance (Castro *et al.,* 2005; Peters, 2006). For this purpose, the APC can either *inactivate* certain processes when the substrates (catalytic proteins or essential activators in the cell cycle) are degraded or *activate* pathways when their inhibitors are destroyed by the proteasome (Peters, 2006). The APC's primary role is recognized by initiating chromosomal segregation and anaphase. However, the activity of the APC is not limited to regulating mitosis (Wei *et al.,* 2004); it plays important roles in processes dysregulated in HGPS, including maintenance of genomic stability (Zhou *et al.,* 2016), controlling lifespan, stress response (Harkness, 2018), apoptosis, and senescence (Zhou *et al.,* 2016). It was noted, based on preliminary work in the Harkness lab, that the APC loses function over time in aging cells and cancer cells (Postnikoff *et al.,* 2012; Mackenzie

et al., 2016; Arnason *et al.,* 2022), providing a possible reason for why cells age and develop worsened cancers.

APC activity is regulated during the cell cycle by the co-activator proteins CDC20 and CDH1, and the Spindle Assembly Checkpoint (SAC). CDC20 and CDH1 interact with APC substrates to promote its ubiquitination and control mitotic progress and G1. In contrast, the SAC prevents premature chromosomal segregation and anaphase onset by inhibiting the APC^{CDC20} complex (Castro et al., 2005; Zhou et al., 2016; Harkness, 2018). The activity of APC can also be modulated by synthetic inhibitors like apcin (APC inhibitor) that inhibits the APC^{CDC20} complex, or pharmacological agents that activate the APC such as MAD2 inhibitor 1 (M2I-1) that inhibits the activity of the SAC (Kastl *et al.*, 2015).

1.5.3.1 Functions of APC during cell cycle

CDKs, cyclins, and the APC are key in controlling cell cycle progression during mitosis. During the late S phase and G2, cyclin B1 levels increase and bind to Cdk1, which is necessary to promote mitosis and chromosomal alignment (Pollard *et al.,* 2017). Then, the Cdk1/cyclin B1complex phosphorylates and fully activates the APC, facilitating the binding with CDC20 (primary regulator of mitosis) and inhibiting CDH1 (Peters, 2006; Pollard *et al.*, 2017). Acetylation of CDC20 and CDH1 governs these coactivator's availability to bind the APC; their hyperacetylation inhibits APC activity, while deacetylation has the opposite effect (Zhou *et al.,* 2016). In yeast, Sirtuin2 (Sir2), the homolog of the human SIRT1, deacetylates CDC20, enhancing APC activation and protein degradation (Harkness, 2018). While SIRT2 deacetylates APC coactivators in mice, deficiency in the Sirt2 gene increases the levels of APC substrates (Li *et al.,* 2008). The activated APC^{CDC20} complex will target securin, resulting in the activation of separase. Separase cleaves the cohesin multiprotein complex that holds sister chromatids together, initiating anaphase (Uhlmann *et al.,* 2000). Cyclin A and B degradation is also necessary for the initiation of anaphase because mitotic exit requires inactivation of CDK. Therefore, APC^{CDC20} targets type A and B cyclins for proteasomal degradation to enable mitotic exit (Castro *et al.,* 2005).

The degradation of cyclin B1 leads to the cessation of CDH1 inhibition, which in turn promotes the formation of the APC^{CDH1} complex (Harkness, 2006; Harkness, 2018). Between anaphase and G1 phase, APC^{CDH1} recognizes substrates such as CDC20, Polo and Aurora kinases, UBE2C, and

gemini (Sivakumar & Gorbsky, 2015), avoiding the premature onset of S phase (Alexandru *et al.,* 1999). Aurora A kinase is exclusively degraded by APC^{CDH1}; keeping low levels of this protein prevents aberrant mitosis and tetraploid cells (LE & JV, 2002; Meraldi *et al.,* 2002). The activity of APC^{CDH1} will continue from the end of the mitotic exit until the beginning of S1 phase (Zhou *et al.,* 2016). During G1/S phase, the inhibitory protein EMI1 inactivates APC^{CDH1}, leading to the accumulation of cyclins amid S/G2. In consequence, CDH1 is targeted for degradation by the SKP-F-box complex (SCF) (Harkness, 2018).

1.5.3.2 Functions of the APC in nutrient sensing and stress response

The APC is regulated differently depending on nutrient availability and stress conditions. When nutrients are present, AKT inhibits the APC by modulating cellular functions such as cell growth, metabolism, cell cycle progression, and survival (Simons *et al.,* 2012). However, when cells are under stress, SIRT2 activates FOXO proteins, which transcribe stress response genes, including adenosine monophosphate kinase (AMPK) (Harkness, 2018). AMPK senses low energy status (López-Otín *et al.,* 2013) and prevents APC inhibition, enabling the cell response to stress. As a result, APC activity is lower in the presence of nutrients and higher under stress (Harkness, 2018). The relationship between the cell cycle and metabolism provides additional insights into the connection between changes in APC activity and nutrient availability/stress response.

Dysregulation of metabolic pathways drives cellular aging and aging-associated diseases (AADs) (Kubben & Misteli, 2017a, 2017b). Given that the APC controls protein degradation and essential cellular processes and is linked to nutrient sensing and lifespan, it is possible that this complex might impact progerin accumulation in both normal and HGPS-mediated aging. Thus, activating this complex may lead to progerin clearance, improvements in nuclear morphology, and increased lifespan.

1.5.3.3 Abnormalities in the APC

Given the importance of the UPS and especially the APC in normal cellular processes, it is not surprising that malfunction in the APC leads to protein accumulation, toxicity, and disease. Thus,

the question remains; is protein accumulation a consequence of APC dysregulation, or is protein accumulation the reason the APC stops working properly in progeria?

Evidence indicates that a correct protein balance in the organism is related to lifespan, where Ub ligases are essential (Jana, 2012; Tsakiri & Trougakos, 2015). Therefore, proteostasis malfunctioning can cause toxicity and be one of the major players in age and age-related disorders (Pérez *et al.,* 2009; Labbadia & Morimoto, 2014). As a result, APC dysregulation causes buildup of its target proteins, affecting the aging process since protein accumulation causes toxicity and protein oxidation and mislocation in aging individuals (David *et al.,* 2010). This is why embryonic fibroblasts of APC-Cdh1-deficient mice undergo early embryonic death, and replicative senescence due to the accumulation of APC substrates (Li *et al.,* 2008).

Another consequence of protein aggregation is observed during neurodegenerative diseases such as Alzheimer's disease, which presents as protein aggregates and cell death when cyclin B1 (APC substrate) accumulates, leading to aberrant cell cycle entry and promoting cell death (Almeida *et al.,* 2005). Interestingly, there is evidence suggesting a role for the APC^{CDC20} complex in premature aging. A *de novo* germline mutation c.856C>A in CDC20 was identified in a patient showing a premature aging phenotype, including chromosomal instability and SAC dysregulation. This mutation caused aberrant activation of APC^{CDC20}, resulting in chromosome instability (Fujita *et al.,* 2020). Therefore, it is necessary to elucidate the relationship between protein accumulation during diseases such HGPS and aging-related diseases.

1.6 Understanding aging for a better quality of life: Link between APC aging and HGPS

The previous sections show that aging and the APC are tightly related, and dysregulation of proteostasis can exacerbate damaging cellular defects like HGPS. The present section looks to infer the link between aging and the APC and the impact that the reactivation of the APC activity has on progeroid syndromes.

Worldwide the elderly human population is increasing. In Canada for instance, one in five persons is 65 years and older (Statistics Canada, 2021); by the year 2050, this population will double from 12% to 22% (World Health Organization, 2021). However, even when lifespan has increased, health-span has not, since age is the leading risk factor for prevalent diseases such as

cancer, neurodegeneration, and cardiovascular diseases (Niccoli & Partridge, 2012; Longo *et al.*, 2015). These age-related diseases are a rising financial burden developed countries face (Longo *et al.*, 2015). Therefore, it is imperative to understand the aging process to enhance quality of life for the elderly population.

The first step to understanding the aging process begins with questioning what aging is. Aging is defined as the progressive deterioration of the biological functions needed by all living organisms to survive and reproduce (Gilbert, 2000). Thus, it is caused by the natural decay and usage of the cellular machinery and its components. As a result, it continuously triggers the buildup of free radicals, proteins, and cellular damage (Harkness, 2018). Therefore, we can identify aging by a set of certain hallmarks, which include accumulation of genetic damage, alterations in the localization and number and structure of the chromosomes due to the accumulation of somatic mutations, telomere shortening, alterations in the epigenome, loss of protein homeostasis, dysregulation of the nutrient-sensing pathway, impaired mitochondrial function and integrity, cell cycle arrest, defects in the generation of stem and progenitor cells (Lopez-Otin *et al.*, 2013; Guerville *et al.*, 2019; Chakravarti *et al.*, 2021).

Even when aging seems to be a process driven by entropy, a key to extend a healthy lifespan relies on the genome. Evidence that age is in part controlled by the genome was first provided while searching for mutants in *Caenorhabditis elegans (C. elegans*), where some mutations either extended lifespan or accelerated aging (Klass, 1983; Johnson, 1990; Niccoli & Partridge, 2012; Leidal *et al.*, 2018). Later, it was observed in several model organisms, such *Saccharomyces cerevisiae*, *C. elegans*, *Drosophila melanogaster*, and mice, that mutations decreasing the activity of components in the nutrient-sensing pathway increased lifespan (Niccoli & Partridge, 2012), including the Insulin-like growth factor (IgF)/ target of rapamycin TOR forkhead FOX O (FOXO) (Fontana *et al.*, 2010; Niccoli & Partridge, 2012). Moreover, aging involves an intricate interaction with other components of the cellular machinery, such as the Anaphase Promoting Complex APC. Postnikoff and colleagues (2012) demonstrated that in yeast, the APC interacts genetically with the Fkh pathway (FOXO in mammals) to extend lifespan, indicating that this complex connects stress sensing and nutrient sensing pathways (Harkness et al., 2004; Mackenzie et al., 2016; Harkness, 2018). Hence, it can be modulated even when longevity depends on nutrient and stress-sensing pathways. Modulation of longevity can be achieved by genomic and epigenomic

alterations through changes in lifestyle, such as diet (Gilbert, 2000; Longo et al., 2015; Harkness, 2018; Kane & Sinclair, 2019).

The APC is strongly linked with the aging process and other diseases. The APC is typically recognized for promoting cell cycle progression and G1 maintenance (Malo *et al.,* 2016). It is also involved in other processes like genome stability, cell growth, and apoptosis, and is a key factor involved in proteostasis. However, as we age, proteome maintenance declines, leading to the accumulation of cytotoxic aggregates and changes in protein abundance (Hipp *et al.,* 2019). Accumulation of proteins is particularly deleterious; this is evidenced when the APC activity is impaired, leading to the accumulation of its target proteins. These abnormalities are associated with the onset of cancers such as ovarian cell clear cell carcinoma (Gütgemann *et al.,* 2008), poor prognosis, and development of multiple drug resistance MDR (Arnason *et al.,* 2020).

Another cellular structure highly affected by age and protein acculturation is the nuclear lamina. In HGPS, progerin toxicity accumulates, impairing various cellular mechanisms resembling aging, like genome stability, cellular senescence toxicity, and nuclear structure. As such, is it possible that one of the master regulators of protein clearance, which is involved in stress response and mechanisms that extend lifespan, may be impaired in progeroid syndromes? If so, re-establishing APC activity could prolong lifespan by clearing progerin from cells. Furthermore, this implication could help understand the mechanism of aging and diseases.

2. HYPOTHESIS AND OBJECTIVES

Given the importance of the APC in mediating cell cycle progression, cellular stress, aging, and its role in maintaining protesostasis, we hypothesized that APC activation decrease progerin levels. We further hypothesize that this may improve cellular morphology and increase cell lifespan in culture. Therefore, increased APC activity in HGPS patient cells may promote progerin clearance from the cell membrane, re-establishing normal cellular function and health.

I have targeted three main objectives to provide evidence supporting this hypothesis.

Objective 1: Determine the interaction between the APC and progerin by:

a) Proximity ligation assays of APC units and activators and progerin
b) Co-immunoprecipitation and western blot analysis
c) Colocalization

Objective 2: Determine if reactivation of APC with M2I1-1 can decrease levels of progerin in HGPS cells by monitoring:

a) Progerin level changes upon APC activation or inhibition evaluated by immunoblotting.

Objective 3: Determine if increased activity of the APC leads to improved nuclear morphology and increased cellular lifespan by monitoring:

a) Cell growth, evaluated as doubling times.
b) Cellular morphology changes
c) Progerin levels in the nuclear lamina

HGPS serves as a valuable model for understanding both the normal process of aging and age-related diseases, as progerin accumulation is present in both HGPS patients and normal aging individuals, suggesting its potential contribution to age-related diseases. Studying the impact of APC activation on HGPS will shed light on the cellular pathways governing both cellular aging and progeria, paving the way for improved treatment options for HGPS children and enhancing the prognosis of age-related diseases. Ultimately, this research will benefit the growing senior population by promoting healthy aging and improving overall quality of life.

3. MATERIALS AND METHODS

3.1 Cell culture

The study used the following cell lines for the experiments: Healthy human foreskin fibroblasts named 2DD, immortalized fibroblasts termed NB1 hTERT, and human primary dermal fibroblasts isolated from skin biopsies of HGPS patients (HGADFN271, HGADFN167, and HGADFN169 from Corriell Repositories). Fibroblasts were cultured in 1X Dulbeccos's Modified Eagle Medium (pH 7.7, Corning, USA, Cat# ca45000-304), containing high glucose (4.5 mg/mL), sodium pyruvate and glutamine. The media was supplemented with fetal bovine serum (FBS) (10% for Nb1-hTER cells and 20% for 2DD and progeria cells) (Gibco, Thermo Fisher Scientific, USA, Cat#: 12483-020) and 1.0% penicillin-streptomycin (Ge Healthcare Life Sciences, USA, Cat#: SV30010). Cultures were maintained under standard culture conditions: 37^{o}C with 5% CO_2 in a humidity-controlled incubator. All cells were plated at 3,000 cells/cm^2 in culture dishes to allow cells to produce growth factors but prevent them from reaching confluence. The media was changed every 3-4 days to provide fresh nutrients and ensure drug presence when treatments are applied.

Table 3.1 Description of cell line, gender, and age of cells used for tissue culture

Cell line	Male/Female	Age at donation (yr. /mos.)
HGADFN271	Male	1yr 3 mos.
HGADFN167	Male	8yr 5 mos.
HGADFN169	Male	8yr 6 mos.

Source: Progeria research foundation, ExPASY bioinformatics resource Portal.

3.2 Cell passage

Cells were passaged when they reached 70% density to avoid contact inhibition. For this purpose, the cells were incubated with 3 ml of Tryple Express (Life Technologies, USA, Cat#: 12604013) for 3 to 5 minutes or until entirely disassociated from the plate surface. Then, using 7 mL of media, the cells were rinsed from the plate and collected into a 15 mL conical tube, followed by centrifugation at 300 ´*g* for 5 minutes (Eppendorf, Hamburg, Germany). The supernatant was

discarded, and the resulting pellet was gently resuspended in 10 mL of media. 10µL of the previous suspension were mixed with 10µL of Trypan Blue Solution 0.4% (Life Technologies, Canada, Cat# 15250061) and transferred to a Countess reusable slide; cell concentration was calculated using Countess™ (Invitrogen) automated cell counter. Finally, cells were seeded at a density of 4500 cells/cm$^{2.}$. Cells were plated onto 22 mm^2 glass coverslips in 6 well dishes for microscopy analyses.

To determine the population doubling times, the following equation was used:

$$\boldsymbol{PDT} = \frac{\Delta t}{log_{2\left(\frac{\Delta N}{N_0}+1\right)}}$$

Where PDT is the population doubling time, Δ*N* is the difference between the final number of cells and the initial count, representing the number of cells grown during the time interval Δ*t*.

3.3 Cell treatments

All treatment compounds, except for MG132 (Sigma, Canada, Cat#1211877-36-9), were reconstituted in dimethyl sulfoxide (DMSO). To induce the stress response of APC, progerin clearance, population doublings, and nuclear morphology enhancement, the APC activator drug M2I-1 was evaluated at concentrations ranging from 1-10 µM for 24-72 h. To achieve APC inhibition, we used APCIN (Thermo Scientific, Cat#50-205-3972) at concentrations ranging from 5-10 µM. Additionally, MG132 was used at concentrations of 5-10 µM to inhibit the proteasome response. Before use, MG132 was reconstituted in molecular-grade water and filtered sterilized. The cells were then incubated with the indicated concentrations and treatment times.

The effects of APC activation on cellular health were assessed using population doubling times. Cell counts were recorded at each passage, and doubling times were calculated using the formula provided in the cell counting section. To evaluate the impact of the treatment on lifespan, cells were cultured for several weeks with a total of four passages, and the total number of days in culture was recorded. The effects of treatment with M2I-1 and vehicle (DMSO) were compared to determine the impact of APC activation on cells. The total number of days in culture was reported.

To investigate the effect of autophagy inhibition, we used chloroquine (Sigma Aldrich, cat# 50-63-5) at a final concentration of 5 µM in culture media for a 48 h period, either in combination with the vehicle control (DMSO same volume as treatment) or with 5 µM of M2I-1. Western blot analyses and densitometry were used to evaluate protein abundance, as well as colocalization analysis of cells grown in 22 mm^2 coverslips.

NOTE: All measurements and assays were performed on 3 biological replicates to ensure the validity and reproducibility of the data/observations.

3.4 Western Blotting (WB)

To obtain whole protein lysates, cells grown in tissue culture were scraped and collected with Laemmlli buffer (62.5 mM Tris HCl pH 6.8, 2% SDS, 10% glycerol (v:v), 100 mM 2-mercaptoethanol, 1x protease inhibitor cocktail (ThermoFisher Scientific, P187785), 1x phosphatase inhibitor cocktail (Millipore Sigma, p5726)). Lysates were preapred on ice to prevent protein denaturation. Protein concentration was determined using a Nanodrop 2000TM (Invitrogen), and lysates were diluted to a common concentration using laemmlli buffer containing bromophenol blue to verify protein migration. Lysates were loaded on sodium dodecyl sulphate polyacrylamide gel electrophoresis (SDS-PAGE) gels (5.0% polyacrylamide stacking gel and 8-12% polyacrylamide resolving gel) to denature proteins and allow their migration from the negative pole, based on their size. The gels were run in 1x running buffer (25 mM Tris, 190 mM glycine, 0.1% SDS (pH 8.3) at 125 V for 1.5 h, followed by transfer to nitrocellulose membranes in transfer buffer (25 mM Tris, 190 mM glycine, 20% methanol (pH 8.3)). Wet transfer was performed at 0.23 mA for 1.5 h at 4°C with constant agitation. After transfer, membranes were stained with Ponceau S (0.1% (w/v) Ponceau S, in 1% v/v acetic acid, Thermo Fisher) to document the relative loads, washed in PBST (1x PBS with 1% Tween20), and blocked at room temperature for 1 h 5% (w:v) skim milk powder in phosphate buffered saline containing 0.05% Tween20 (SMP/PBST), with constant agitation. The membranes were then incubated overnight at 4°C with appropriate antibodies diluted in 2.5% 2.5% SMP in PBST, followed by three 5 min washes in 5% SMP/PBST. The samples were incubated for 1 h with the secondary antibody diluted 2.5% SM/TBST. After the secondary incubation, the membranes were washed three times in 5% SM/PBST for 5 min each, followed by one wash in 0.5% PBST and one wash in 1x PBS. Finally, the immunoblots were developed using enhanced chemiluminescence (ECL).

The following primary antibodies were used in a 1:1000 dilution: mouse anti progerin (Santa Cruz, cat#SC-81611), mouse anti Lamin A/C (Santa Cruz, cat#sc-376248) rabbit anti cyclin B1 (Sigma, C8831), mouse anti Lamin A/C (Santa Cruz, cat# sc-376248), rabbit anti CDC20 (Sigma, cat#, sc-5296).The secondary antibodies used were goat anti rabbit HRP (dilution 1:2500, Jackson Scientific, cat#, 115-035-003), goat anti mouse HRP (dilution 1:1500, Jackson Scientific115-035-144).

Western blot bands were analyses by densitometry using ImageJ. To determine fold changes each band was normalize to the load control, the resulting values of each target protein were then compared to the normalized vehicle control.

Fold change= (Normalized sigal $_{\text{Sample}}$) / (Normalized signal $_{\text{Vehicle control}}$)

Note: Experiments were run in triplicate since HGPS samples are scarce and grow over a limited number of passages that can be used for all experiments.

3.5 Immunofluorescence

Cells were grown on sterilized 22 mm^2 coverslips to 70% confluence and fixed with 4% formaldehyde (FA) in 1x phosphate saline buffer solution PBS (137 mM NaCl, 10 mM sodium phosphate dibasic, 2.7 mM KCl, pH 7) for 10 min at RT, permeabilized (0.5% Triton X-100 in PSB) for 10 min at RT and washed three times for 5 min in PBS. Cells were incubated at RT with 25-50 µL of 1:200 primary antibody dilutions in 1% bovine serum albumin (BSA) for 1 h in a humidity chamber. Cells were washed for 5 min in PBS/0.05% Triton X-100. Successively, coverslips were incubated at RT for 1 h with 25-50 µL of 1:200 dilutions of the appropriate secondary fluorescent antibodies. Cells were then washed with PBS/0.05% Triton X-100 5 min. The coverslips were mounted in photo protective mounting media (VectaShield^{TM}) containing DAPI to counterstain chromatin and allow nucleus visualization.

Images were collected on a Ziess X61 epifluorescence microscope equipped with a range of objectives. Images were processed using the software Image J and Photoshop. Cells were counted for irregular nuclear morphology. Improvements in nuclear morphology were evaluated by immuno-fluorescence (IF) microscopy following labeling with both anti-Progerin and anti-LMNA antibodies.

The following primary antibodies were used for immunofluorescence: mouse anti progerin (dilution 1:200, Santa Cruz, cat#SC-81611), mouse anti Lamin A/C (dilution 1:200, Santa Cruz, cat#sc-376248), rabbit anti CDC20 (Sigma, sc-5296), rabbit anti ubiquitin (Proteintech, cat#10201-2-AP).

3.6 Proximity ligation assay

The proximity ligation assay (PLA) is a technology that enables the detection of native protein-protein interactions at endogenous protein levels. For this purpose, the proteins of interest are targeted by specific primary antibodies, which will covalently link to DNA primers. Then, if the proteins or protein epitopes are in proximity, connector oligos will interact with the PLA probes. Then, circular DNA amplification and hybridization with fluorescent probes enable the visualization of fluorescent spots. The main aim of this assay was to determine interaction of progerin, and the APC subunit termed APC2 in progeria cells. Furthermore, if an interaction of these proteins was detected, we aimed to determine whether these interactions are affected by the APC activator M2I-1.

Before conducting and optimizing the Proximity Ligation Assay (PLA) reaction, it was crucial to assess whether the microscope being used had the capability to detect fluorescence from the PLA fluorescent dye (with an excitation wavelength of 644 nm and an emission wavelength of 669 nm), which falls within the same range as Texas red fluorescent dye. To determine this, a sandwich immunofluorescence assay was performed on 2DD cells cultured on 1 cm2 cover slides. The protocol for the sandwich immunofluorescence involved fixation, permeabilization, antibody incubation, and washes as described in Section 3.5. First, a mouse anti-progerin antibody was used as the primary antibody at a dilution of 1:200, followed a 5 min wash in PBST. Then, the cells were incubated with a secondary antibody, Texas Red (TR), at a dilution of 1:200 in 1% BSA for 1 hour at room temperature. Subsequently, the slides were washed again and further incubated with a third antibody, a rabbit anti-sheep antibody labeled with a green fluorescent dye (λex 488 nm), as there was no availability of a secondary antibody against goat. However, since the goat genome shares approximately 98% homology with sheep, the rabbit anti-sheep antibody was expected to recognize the goat antibody. Detection of fluorescence from the Texas Red-labeled anti-sheep antibody with this method would indicate that our microscope is capable of detecting the red fluorescent dye used in the PLA kit.

Then, the PLA reaction was performed using Doulink PLA from Sigma (cat# DUO92202-1KT). To set this experiment and establish controls, antibodies performance was evaluated, followed by an optimization of the dilution necessary to carry on the reaction. The experiment was tested first in healthy fibroblast lines (2DD) using SUN1 antibody to evaluate the performance of the PLA reaction. Images were obtained using a Ziess X61 epifluorescence microscope at a magnification of 100 times.

To assess the ideal concentration of the antibodies that will be used in PLA, the performance of the antibodies was evaluated in individual IF reactions. This was done to understand the performance of each antibody individually. As determined in previous IF experiments, the APC2 antibody produces strong fluorescence in a dilution of 1:200. Therefore, this dilution was selected for the PLA reaction. However, the other antibodies of interest were tested in different concentrations (1:50, 1:100 and 1:200) and combinations, as shown in Table 3.2.

Table 3.2 Antibodies combinations for PLA reaction standardization

Antibody to test	Interacts with
Progerin	APC2
CDC27	APC2
CDC20	APC2
CDC20	Progerin

After visualization of the images, the ideal antibody concentrations selected were rabbit anti APC2 1:200 (Atlas, cat# HPA066539), rabbit anti CDC20 1:50 (Invitrogen, cat# WH3351044), mouse anti progerin 1:50 (Abcam, cat# ab66587), mouse anti CDC27 1:50 (Santa Cruz, cat# sc-9972), and rabbit anti ubiquitin 1:50 (Proteintech, cat# 10201-2-AP). Once the reaction was optimized, the PLA reaction was performed over the samples of interest following the protocol from the manufacturer.

Briefly, cells that grew in 1 cm^2 sterilized cover slides at 70% confluency were fixed and permeabilized, as stated in Section 3.5. The reaction was optimized at 15µM for a more efficient use of resources and materials, the coverslips were cut into 4 pieces using a diamond-tip pen after placing them in a well with PBS. Subsequently, a blocking step was performed using

approximately 1 drop of Duolink® Blocking solution for each sample. The samples were incubated upside down in a heated humidity chamber for 60 min at 37°C. Next, the antibody dilutions were prepared as stated in Table 3.2 and incubated with the primary antibodies in a humidity chamber for 1h at RT. After this period, the samples were washed in buffer A (prepared according to the manufacturer's instructions) and incubated with the PLUS and MINUS PLA probes in a humidity chamber for 1 h at 37°C. Then, after 2 washes with buffer A, the samples were incubated with ligase for 30 min at 37°C. Samples were incubated with Polymerase diluted in the correspondent buffer for amplification. The incubation was performed at 37°C for 100 min. After the final washes in buffer B (Resuspended according to manufacturer instructions), the slides were mounted with Mounting Medium with DAPI. The slides were visualized in the Ziess X61 microscope; Gain and exposure times were optimized for each channel, and the number of foci of 30 cells per treatment was determined.

3.7 Immunoprecipitation.

After cells reached 70% confluency, they were scraped on their media (DMEM) at RT, collected in conical tubes, and centrifugated at 300 ´*g* for 5 min at RT. After this, the pellet was collected in 1 mL tubes and washed with PBS, followed by a 2 min centrifugation. Then, 200 µL of 1X RIPA buffer (Cell signaling technology, cat#9806) were added to each tube. Lysates were vortexed vigorously and sonicated. Protein concentrations were measured by the Lowry assay according to the manufacturer's instructions (Sigma, Total Protein kit, Micro-Lowry, Peterson's Modification, TP0300).

Immunoprecipitation was performed using Protein G Sepharose beads (Sigma, cat#17-0618-02). To preclear, 200 µg of protein were incubated with 50 µL of 50% slurry of the beads, 4 µg of mouse IgG antibody (EMD Millipore, cat# NI03-100UG), and brought to 500 µL with RIPA buffer containing protease inhibitor cocktail (Sigma, cat#P8340). The tubes were rocked for 1 hour at 4°C and centrifugated at 12000 RFC for 10 min at 4°C. The supernatant was collected and precleared again as described before. Then, the tubes were centrifugated at 12000 RFC at 4°C for 10 min, and the supernatant was collected in a new 1mL tube where 4 µg of the primary antibody of interest were added (Lamin A/C, Santa Cruz, cat#sc-376248) and incubated overnight with continuous rotation at 4°C. The tubes were centrifugated for 10 min at 4°C, and the supernatant was collected into a new 1 mL tube; 30 µL of this fraction were mixed with 4x Loading buffer and

used as “unbound fraction “control. The remaining beads were washed twice with 500 µL of wash buffer (HNTG buffer filtered: 1% Triton X-100, 10% glycerol, 20 mM 4-(2-hydroxyethyl)-1-piperazine ethane sulfonic acid (HEPES), 150mM NaCl), vortexed for 20 sec and spun down for 2 min at 5000´*g*. Wash buffer was discarded from the tubes, and the excess was collected with a 0.3 mm needle until the beads were dry. Protein was eluted with 30 µL of 1x loading buffer and boiled for 5 min at 100°C; then they were spun down at 5000 ´*g* for 2 min at RT. SDS-PAGE and immunoblotting were performed as described above.

3.8 Colocalization

Line scans were used to determine if the probes targeting progerin and ubiquitin colocalized. To do so, HGPS primary fibroblasts were treated with or without 5 µM of chloroquine in combination with the vehicle control DMSO or the APC activator M2I-1. Then, double protein staining was performed, incubating the cells simultaneously with primary antibodies: mouse progerin (dilution 1:200, Santa Cruz, cat#SC-81611) and rabbit ubiquitin (Proteintech, cat#10201-2-AP). Following by secondary antibodies Alexa Fluor 488 anti-mouse and donkey anti-rabbit cy3 (Jackson Immuno Research, cat#711-165-152) as detailed in Immunofluorescence. Images of cells were collected at 100x magnification with constant exposure times. Gray-scale images were imported into Photoshop and converted to RGB files. Then images were imported into ImageJ (NIH, USA), and line scan analysis of the images were obtained.

3.9 NB1hTert-Δ50 stable cell line

The plasmids used for transfection, pEGFP-C2 (addgene, USA) and pEGFP-Δ50, were previously designed, constructed, and verified through sequencing by Dr. Z. Belak, a previous member of the Eskiw lab. For this, the coding sequences from the plasmid pdDNA3.1-D50 obtained from addgene were amplified by PCR with primers recognizing the multiple cloning sites EcoRI (at 5’ end) and BglII (at 3’ end). For the cloning step, the PCR products were purified, digested, and then ligated to the plasmid pEGFP-C1. To ensure that the amplified DNA and receiving vector have compatible ends, pEGFP-C1 plasmid was digested with the same restriction enzymes as the PCR products. Before transfection, the plasmids were linearized according to the manufacturer’s instructions by the restriction enzyme ApaI1 (New England BioLabs, USA, Cat#R0507S); linearization was confirmed by electrophoresis using a 1.5% agarose gel.

NB1hTert fibroblast growing in 6-well dishes (80% of confluency) produced a non-clonal population that stably expresses progerin-GFP or GFP. On the transfection day, cells were incubated for 3 h on Opti-MEM (ThermoFisher Scientific, cat#31985062). Then, the transfection was carried out using lipofectamine™300 (ThermoFisher Scientific, cat#L3000001) according to the manufacturer's instructions after the following adjustments per well: 5 µg of DNA (linearized plasmid) and 5 µL of P3000™ reagent and 7.5 µL of Lipofectamine™3000 reagent. Cells were incubated with the transfection mix for 6 h. After this period, 2 mL of regular media were added to each well (DMEM with 10% FBS and 1% P/S Opti-MEM), followed by a 24 h incubation. Later, normal media was replaced with selection media consisting of 500 µg/mL of G418 sulfate (Thermo Fisher Scientific, USA, cat#: 11811031) in DMEM. Cell growth and survival was monitored visually. The expected selection time under full selection pressure was 5 days. If cell death was too high before this period, cells were returned to normal media for 24 h or until proliferation resumed. Then, cells were returned to the selection media. Cells were fixed and monitored to confirm plasmid insertion by immunofluorescence and western blot.

3.10 Statistics

For each treatment (control, M2I-1, or APCIN), 30 cells were chosen randomly, and the number of foci or PLA fluorescent dots were counted. To achieve this, the images were processed in the software image J to detect just the nuclei of each cell and manually count the number of foci in each cell. The data was registered in a CSV file and analyzed in the statistical software R. We ran a Kruskal test to examine differences in each treatment, followed by a Wilcox test to establish significant differences between the control cells and the treatments applied. Finally, the data was graphed in a box plot with error bars. For western blot analyses, data is presented as mean ± standard error of the mean SEM.

4. RESULTS

4.1 Progerin levels decrease upon APC activation. Western blot levels are dose dependent

The main hypothesis of this thesis stated that activation of the APC would decrease progerin levels in primary HGPS fibroblasts. To test this hypothesis, we treated primary progeria fibroblasts with three concentrations of M2I-1 (1, 2.5, and 5 µM) for 72 hours. We evaluated APC activity by assessing changes in the relative levels of its substrates, such as Cyclin B1 . These concentrations were based on previous assays in cancer cells, where 5 µM was the optimal dose to activate the APC without causing toxicity (Arnason *et al.*, 2022). However, because HGPS cells are more sensitive to stress than cancer cells, it was necessary to evaluate lower concentrations of the APC activator and determine the dose and time that shows a reduction in progerin levels without inducing cellular toxicity (Figure 4.1). Reduction in APC substrate levels, such as Cyclin B1 in response to M2I-1 in progeria cells, indicates APC activation, Figure 4.1 demonstrates that progerin levels decrease in response to different concentrations of M2I-1, with the most effective concentration being 5 µM. At this concentration, we also observed a reduction in Lamin A/C and cyclin B1. The reduction in Cyclin B1 is considered a proxy for APC activity and may be linked to the decrease in progerin levels.

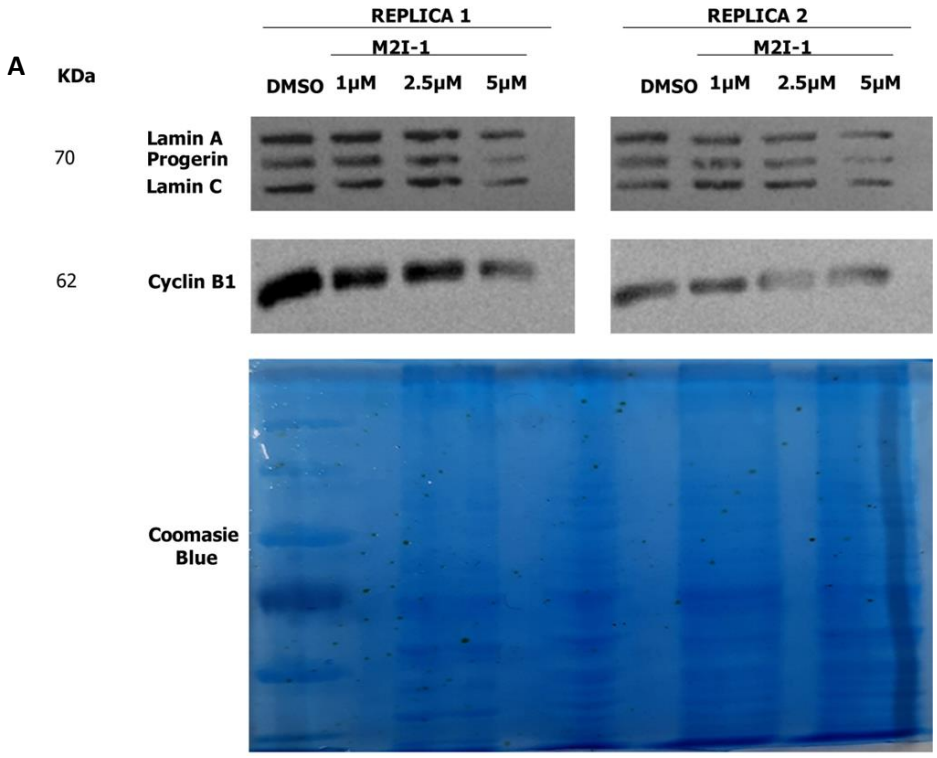
A
KDa
REPLICA 1
M2I-1
DMSO 1μM 2.5μM 5μM
REPLICA 2
M2I-1
DMSO 1μM 2.5μM 5μM
70
Lamin A
Progerin
Lamin C
62
Cyclin B1
Coomasie Blue

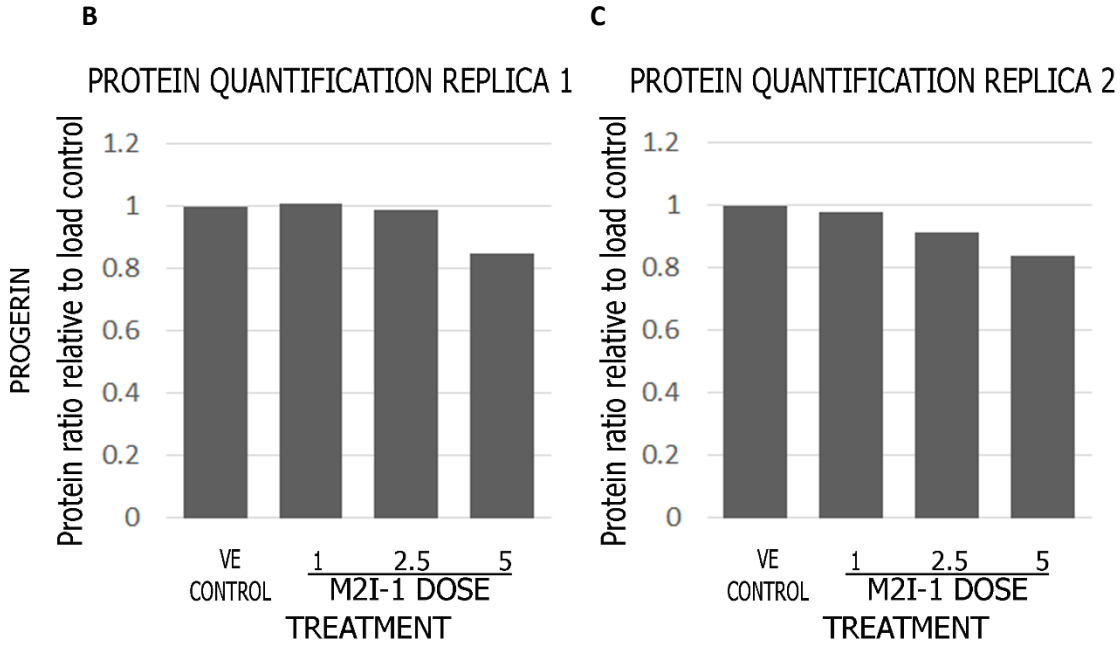
B
PROTEIN QUANTIFICATION REPLICA 1
PROGERIN
Protein ratio relative to load control
1.2
1
0.8
0.6
0.4
0.2
0
VE CONTROL
1
2.5
5
M2I-1 DOSE TREATMENT
C
PROTEIN QUANTIFICATION REPLICA 2
Protein ratio relative to load control
1.2
1
0.8
0.6
0.4
0.2
0
VE CONTROL
1
2.5
5
M2I-1 DOSE TREATMENT

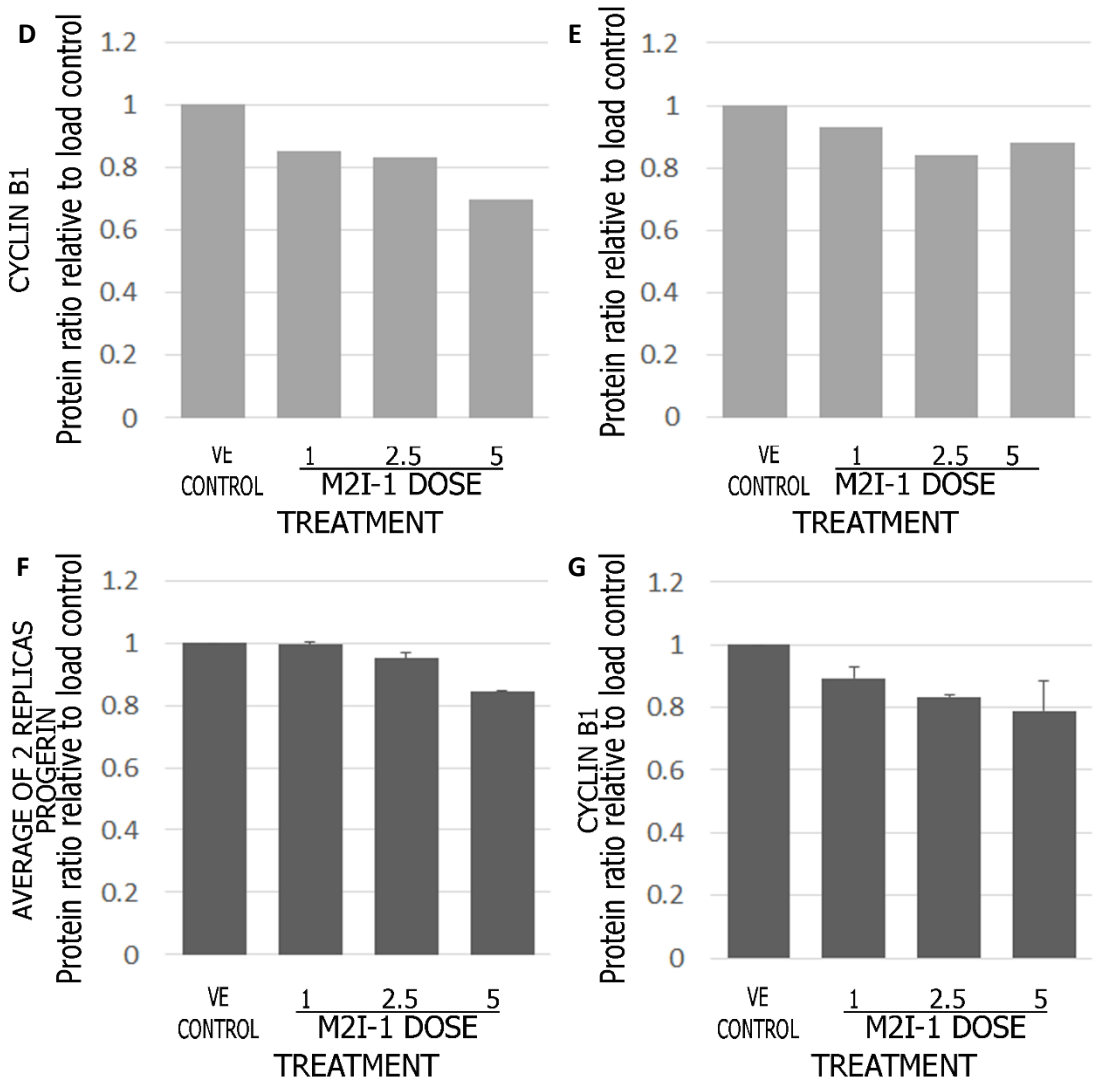

Figure 4.1 Progerin levels decrease when APC is activated with 5 µM of M2I-1.
Primary fibroblasts from HGPS patients were treated with 1, 2.5, and 5 µM of M2I-1 for 72 h.
A) Western blot of the protein lysates corresponding with each treatment showing bands for Lamin A/C, progerin, cyclin B1, and Coomassie blue staining for protein visualization. Protein extracts from the different treatments were loaded in 8% SDS-PAGE gel. Cell line HGADF169.
B) Histogram representing the ratio of relative protein abundance of progerin in replica 1 C) Histogram representing the ratio of relative protein abundance of cyclin B1 in replica 1.
D) Histogram representing the ratio of relative protein abundance of progerin in replica 2 E) Histogram representing the ratio of relative protein abundance of cyclin B1 in replica 2.
F) Representing the average ratio of relative protein abundance in two replicas G) Bar graphic representing the average ratio of relative protein abundance of cyclin B1 in two replicas**.**
For the WB mouse anti-Lamin A/C was used, which recognizes lamin A, Lamin C, and progerin.

4.2 Activation of APC with M2I-1 has an impact on progerin levels and cellular morphology.

To investigate the effects of APC activation on nuclear morphology, we treated HGPS primary fibroblasts (HGADFN169) growing on coverslips with M2I-1 or vehicle control DMSO for 72 hours. Based on our previous western blot results showing a decrease in progerin levels with M2I-1 treatment, we hypothesized this would lead to improvements in nuclear morphology. After treatment, cells were fixed and labeled with a primary antibody against progerin, and 100 cells were counted per treatment to assess changes in cellular morphology. Although this initial assessment was qualitative, it provided insights that motivated us to pursue further evaluations of APC activation using quantitative techniques.

Fluorescence intensity of progerin was assessed per each cell observed under a fluorescent microscope (Figure 4.2), and classified into three categories: 1) Strong signal, for bright and robust signal (detected by visual evaluation); 2) Faint signal, for weaker signal than category 1; and 3) Hard to detect, for signals that were difficult or not detected. Figure 4.3 demonstrates the fluorescence intensities used to categorize the cells. Morphological changes were assessed on a scale of 1 to 3 (Figure 4.4) using Figure 4.5 to classify the cells. The categories were established as follows: 1) “Normal-like,” resembling non-diseased cells 2) “Blebbing,” defined as bulges in the nuclear lamina and typical of diseased cells, and 3) “Other, presenting unusual shapes. The number of cells corresponding to each category was noted. After treatment with M2I-1, there was an increase in the number of cells with a morphology resembling that of non-diseased cells compared to cells treated with the vehicle control.

After activating APC with M2I-1, we observed a decrease in progerin fluorescence intensity (Figure 4.2), indicating an average reduction in progerin levels and an improvement in cellular morphology (Figure 4.4). To assess the impact of APC activation on overall cellular lifespan, we analyzed the effect of M2I-1 on population doubling times, as described in Section 3.

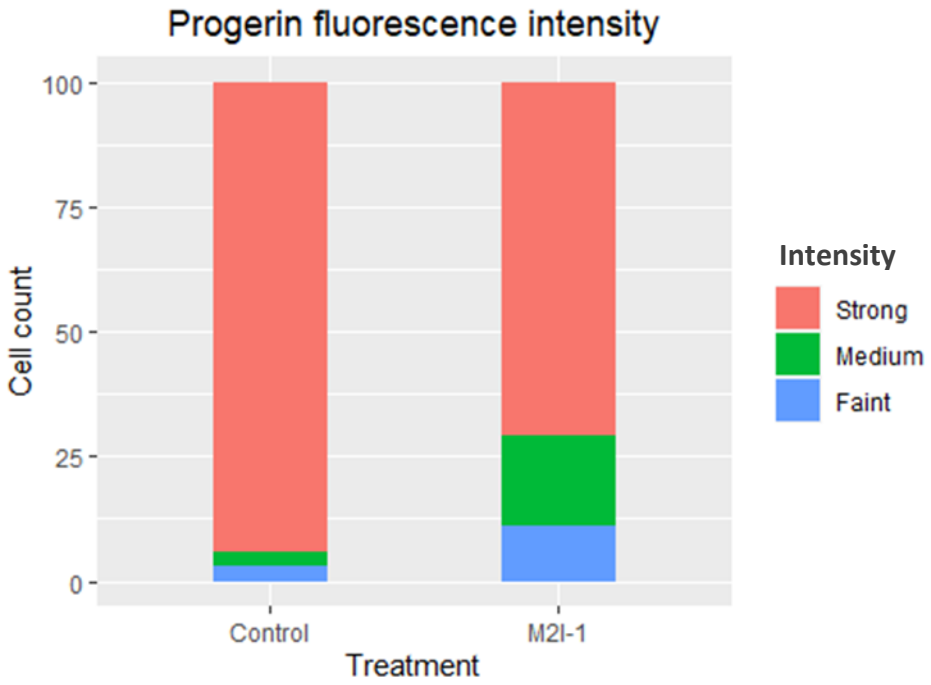

Figure 4.2 Impact on progerin fluorescent intensity in HGPS cells after APC activation with M2I-1. Evaluation of progerin intensity in HGPS cells treated with/without M2I-1 using fluorescence microscopy. HGPS primary fibroblasts were labeled with the primary antibody against progerin, fluorescence intensity levels were classified as 1) Strong signal, for bright and strong signal detected by visual evaluation; 20 Faint signal, for weaker signal than 1 and 3) Hard to detect, for signal that was difficult or not detected compared to 1 and 2**.**

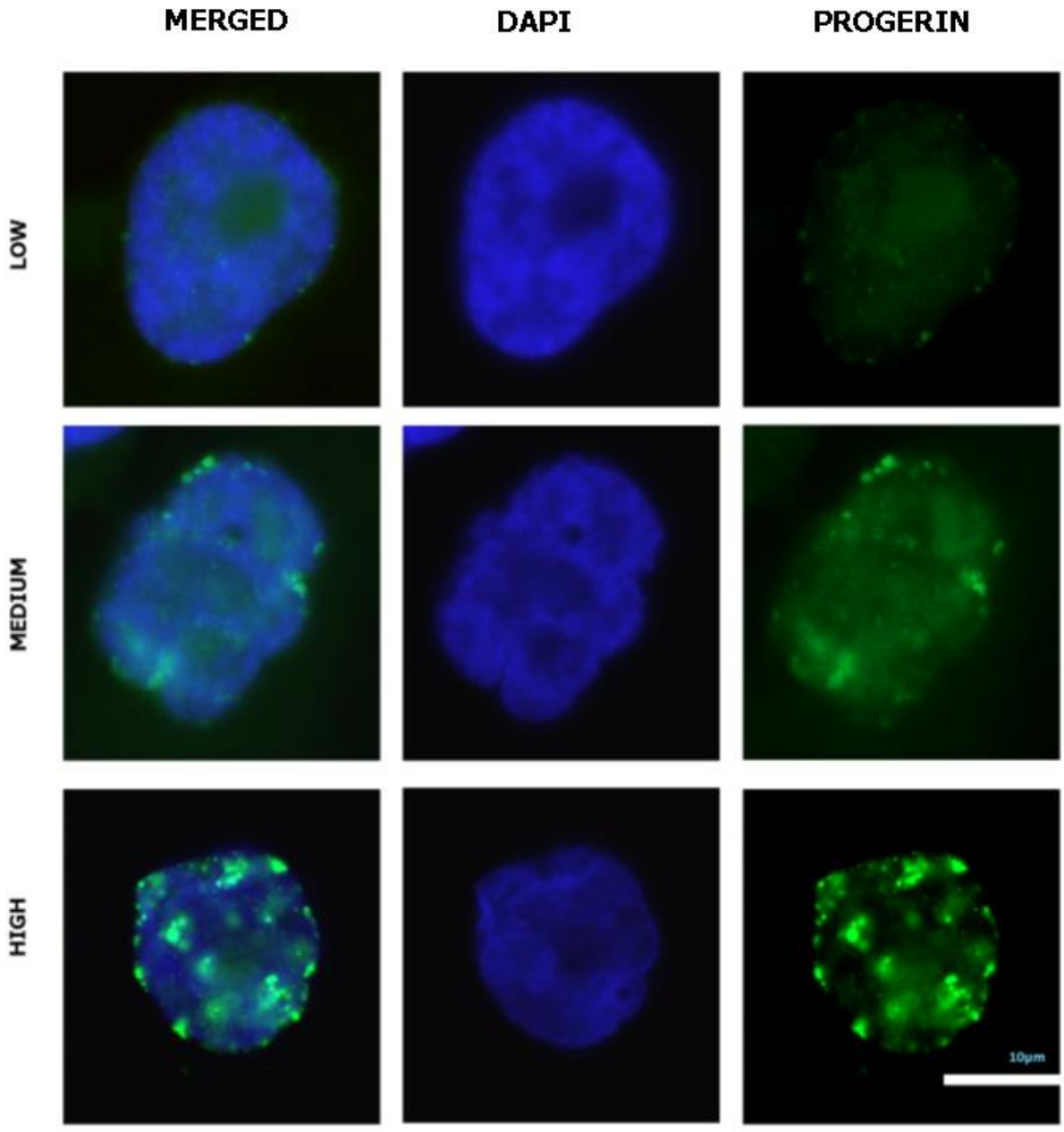

Figure 4.3 Example of progerin fluorescence of HGPS cells considered for the analysis of progerin fluorescence intensity treated with/without M2I-1.
Low indicates low intensities of fluorescence detected by eye or cells that were hardly detected. Medium represents cells with a higher intensity than in the low category but not as intense as cells in the high category which presented bright intensity and foci. Blue: Dapi, Green Progerin.

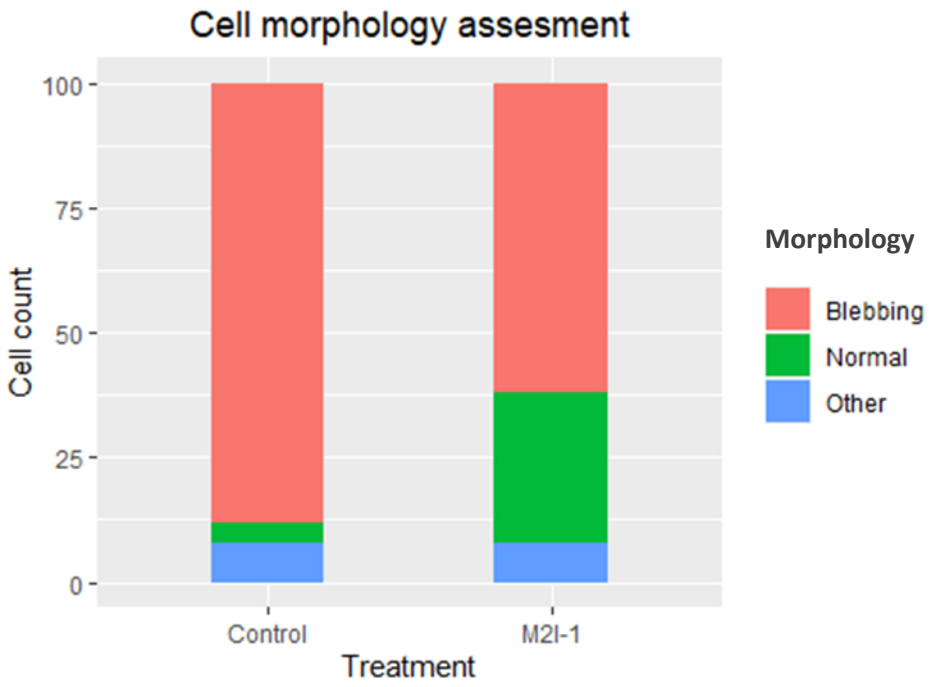

Figure 4.4 Morphology assessment after APC activation.
Three categories of cell morphology were established by observation at the microscope. First category is represented by pink: Classic HGPS cells phenotype represents cells with irregular periphery and blebbing structure. Green: Represents HGPS cells with a "normal-like" nuclear. The second category is represented by green: cells exhibiting a "normal-like" nuclear structure, resembling non-diseased cells. The third category, represented by blue, includes other aberrant nuclear structures such as heath-shaped and donut-like forms**.**

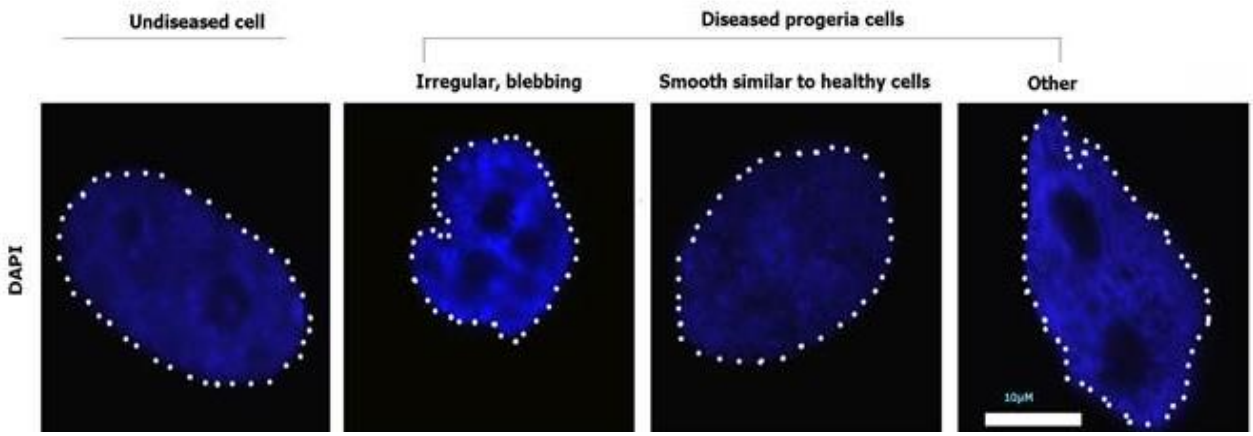

Figure 4.5 Example of cellular shapes corresponding to each category assessed for morphology changes on HGPS cells treated with/without M2I-1.

Non-diseased: untreated 2DD fibroblasts. Diseased progeria cells: HGADFN169 primary fibroblasts

4.3 Impact of APC on population doubling times

This project hypothesizes that activating APC with M2I-1 will improve cellular phenotypes, as assessed in Section 3.2, and impact cellular senescence. Proliferative rates and cellular growth changes have been shown to indicate improvement of the HGPS phenotype in previous studies by Gillespie *et al*. (2015). To evaluate this hypothesis, HGPS fibroblasts were treated with either DMSO (vehicle control) or M2I-1, and PDT was measured by counting the cultures every 4 to 5 days. Results from Figure 4.6 indicate that HGPS cells treated with M2I-1 exhibited slower PDT and fewer doublings than those treated with DMSO.

On average, HGADFN169 fibroblasts under vehicle control had a population doubling time of 3.5 days (84 h) (SEM ± 0.118 days) resulting in an average of 8 doublings. In contrast, M2I-1 cells had an average doubling time of 4.9 days (118 h) (SEM ± 0.863 days) and 6 doublings on average (Figure 4.6 A and B). Similarly, HGADFN167 fibroblasts under vehicle control had an average doubling time of 3.5 days (84 h) (SEM ± 0.549 days) and 4 doublings. Conversely, those treated with M2I-1 had an average doubling time of 6 days (144 h) (SEM ± 0.897 days), resulting in an average of 3 doublings over four passages (Figure 4.6 C and D).

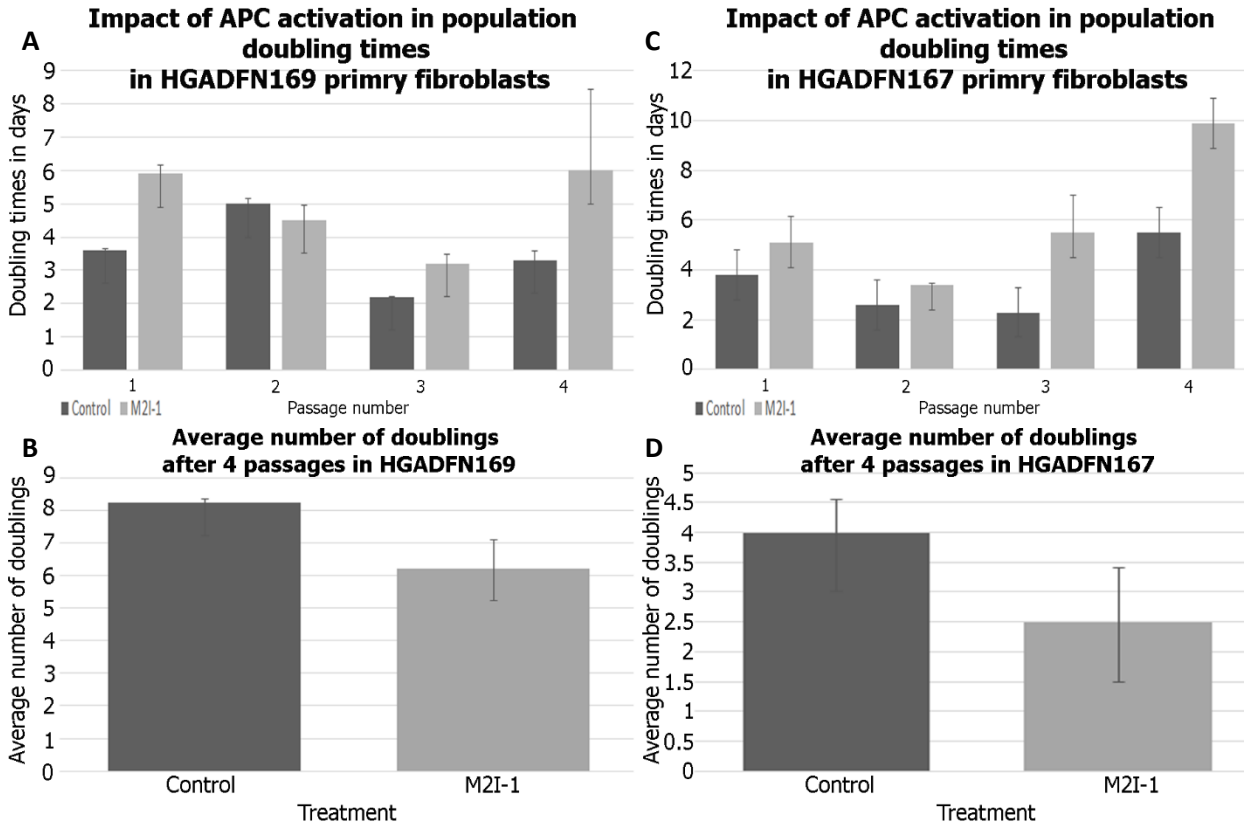

Figure 4.6 Doubling times differences between control group and treatment in HGADFN169 and HGADFN167 fibroblasts.

Control: HGPS primary fibroblasts treated with the vehicle DMSO, M2I-1: cells treated with 5µM of the APC activator M2I-1. Doubling times are shown in hours.

A: The difference in doubling times in HGPS cells was evaluated from passage 13 to passage 16 in HGADFN169 primary fibroblasts.

B: Average number of doublings of 4 passages in cells treated with the vehicle control compared with cells treated with the APC activator M2I-1in HGADFN169 primary fibroblasts.

C: The difference in doubling times in HGPS cells was evaluated from passage 13 to passage 16 in HGADFN167 primary fibroblasts.

D: Average number of doublings of 4 passages in cells treated with the vehicle control compared with cells treated with the APC activator M2I-1in HGADFN167 primary fibroblasts**.**

4.4 Activation of APC with 5 µM of M2I-1 is involved in progerin removal in HGPS primary fibroblasts

We observed that activation APC activation decreases progerin abundance. Previous research has also demonstrated that Metformin and Everolimus have therapeutic potential in reducing progerin expression and improving aberrant phenotypes in HGPS cells by inducind autophagy (Egesipe *et al*., 2016; Gabriel *et al*., 2016). We theorized that combining APC activation with either Metformin or Everolimus would synergize clearing progerin and enhancing cellular morphology in HGADFN169 primary fibroblast. To test this, we treated the cells with DMSO, M2I-1 alone, or M2I-1 in combination with either Metformin or Everolimus. We also added MG132 to evaluate if proteasome inhibitors would increase progerin (Figure 4.7). We determined a working dose of MG132 that does not produce toxicity at 5 µM. We performed western blotting on whole-cell protein lysates to determine the impact of these treatments on progerin levels. We found that M2I-1 alone reduced progerin abundance; however, we did not observe strong evidence of synergistic effects with Everolimus. Since APC catalyzes protein degradation via the proteasome, we hypothesized that inhibition of the proteasome with MG132 would increase progerin abundance.

To investigate whether the APC is involved in progerin removal through a pathway other than the proteasome, we conducted a repeat experiment in HGADFN169 HGPS fibroblasts. This time, we added a combination of MG132 and M2I-1 to the treatments (Figure 4.8). The combination of MG132 with M2I-1 had the most significant impact on LMNA/C and progerin levels. Based on these results, we hypothesize that APC activation may function independently of the proteasome to mediate progerin degradation. Furthermore, progerin removal upon APC activation may be mediated by autophagy. Our findings were consistent with those of Harhouri *et al*. (2017), where inhibition of the proteasome induces progerin degradation through macro autophagy; these findings could be ground-breaking since the APC has not been previously shown to function independently of the proteasome.

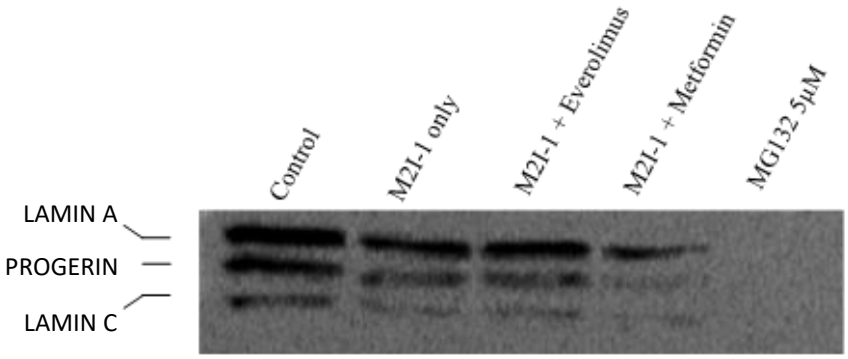

Figure 4.7 Evaluation of possible synergetic effects of the APC activator and repurposed drugs Everolimus or Metformin and proteasomal inhibition.
Western blot from HGADFN169 primary fibroblasts treated for 48 h with (left row to right): DMSO as vehicle control, APC activator M2I-1, Everolimus in combination with M2I-1, Metformin in combination with M2I-1, MG132 as proteasomal inhibitor and MG132 in combination with M2I-1.

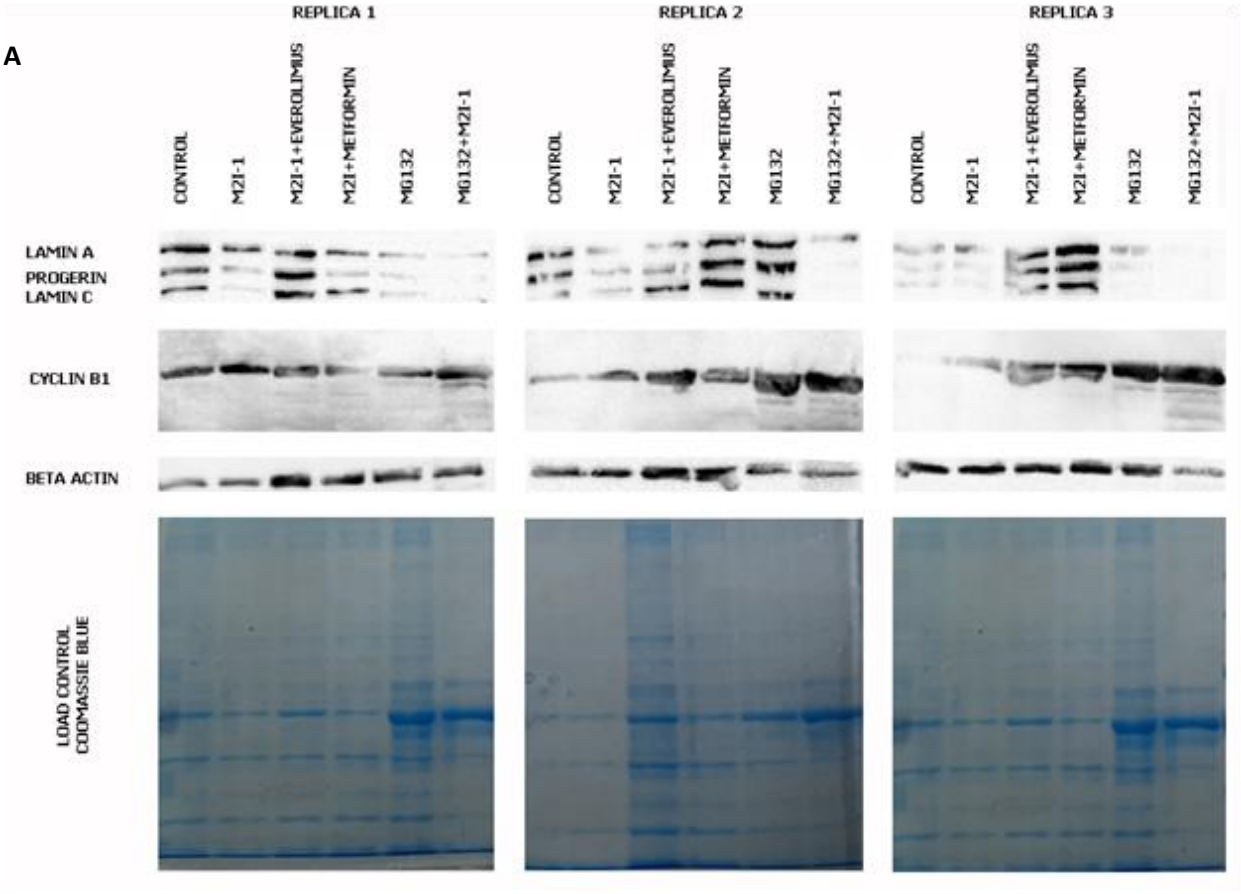
A
REPLICA 1
REPLICA 2
REPLICA 3
CONTROL
M2I-1
M2I-1+EVEROLIMUS
M2I+METFORMIN
MG132
MG132+M2I-1
LAMIN A
PROGERIN
LAMIN C
CYCLIN B1
BETA ACTIN
LOAD CONTROL
COOMASSIE BLUE

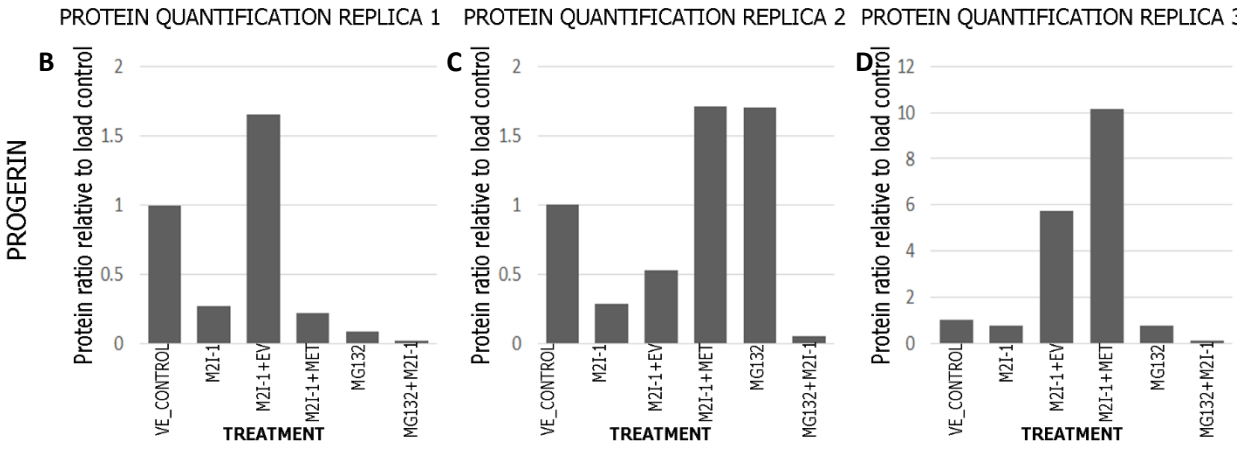
PROTEIN QUANTIFICATION REPLICA 1
PROTEIN QUANTIFICATION REPLICA 2
PROTEIN QUANTIFICATION REPLICA 3
PROGERIN
B
C
D
Protein ratio relative to load control
VE_CONTROL
M2I-1
M2I-1+EV
M2I-1+MET
MG132
MG132+M2I-1
TREATMENT

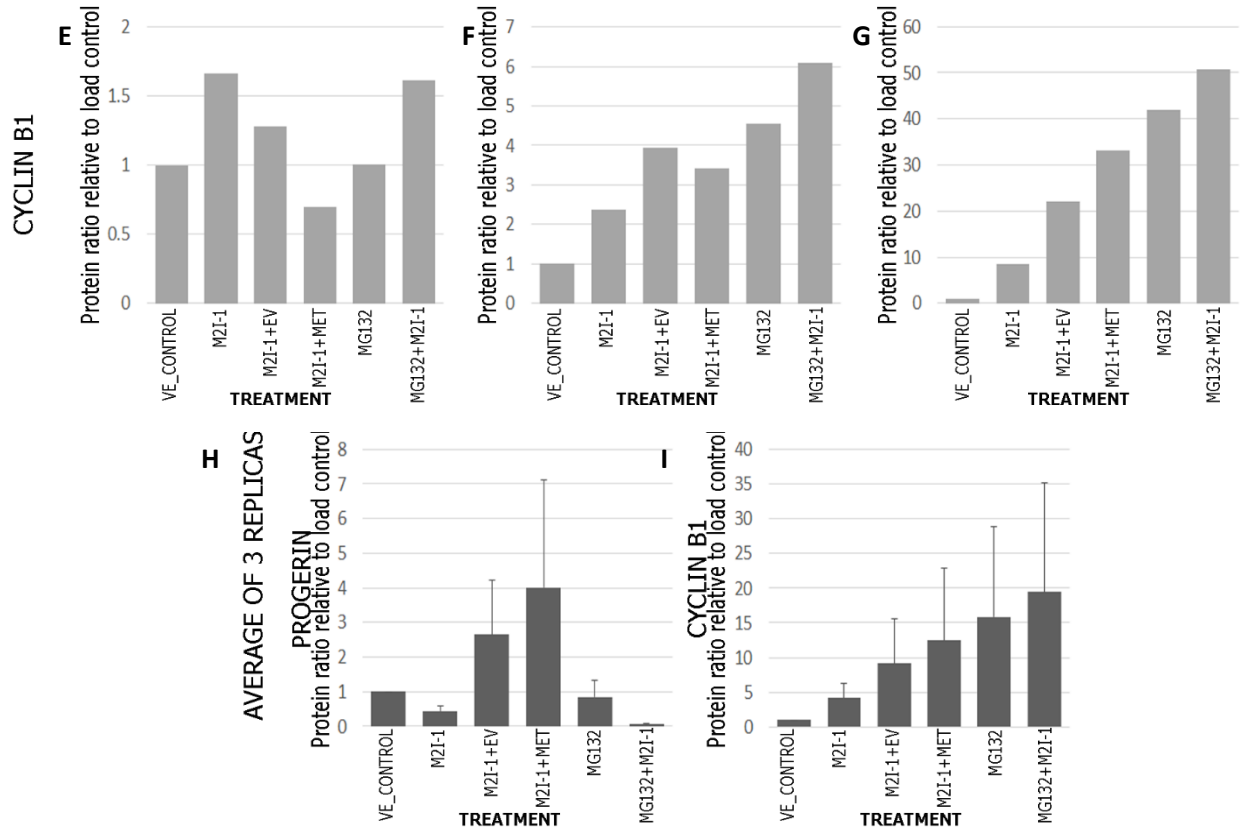

Figure 4.8 Evaluation of synergistic effects of Everolimus and Metformin and M2I-1, and assessment of proteasome inhibition.

Untreated cells growing at the same conditions as cells treated were used as control, as well as cells treated with the vehicle only. Cells were treated with 5µM of M2I-1 alone, or 5µM M2I-1 in combination with either 100nM of Everolimus or 500µM of Metformin. To determine the effect of proteasome inhibition, two concentrations of MG132 were evaluated: 5 and 10µM. Lamin A/C antibody was used to assess progerin abundance, whereas Cyclin B1 to determine changes in APC activity.

A) Western blot of the protein lysates corresponding with each treatment showing bands for Lamin A/C and progerin, cyclin B1, beta-actin, and Coomassie staining for protein visualization. Protein extracts from the different treatments loaded in 8% SDS-PAGE gel to ensure protein abundance prior to Western blots. Cell line HGADF169.

Bar graphic representing the ratio of relative protein abundance of progerin in: B replica 1, C replica 2, D replica 3.

Bar graphic representing the ratio of relative protein abundance of cyclin B1 in: E in replica 1, F replica 2, G replica 3.

H) Bar graphic representing the average ratio of relative progerin abundance in three replicas

I) Bar graphic representing the average ratio of relative cyclin B1 abundance in three replicas.

The observations presented indicate that APC activation impacts progerin levels in HGPS cells. To confirm the role of this protein complex in progerin clearance, we inhibited the APC using Apcin (Figure 4.9). We hypothesized that inhibiting the APC could increase progerin levels compared to the vehicle control and lead to buildup of APC substrates like cyclin B1 (Figure 4.9).

We determined that a final concentration of 5 μM APCIN and an incubation time of 72 hours were required to inhibit the APC, with no observed cellular toxicity. The experiment was conducted in triplicate, and two out of three replicas showed a decrease in progerin levels upon APC activation and proteasome inhibition, as quantified by western blot. In addition, we assessed differences in progerin levels by immunofluorescence (Figure 4.10), comparing fluorescence signals among all treatments after imaging at least 50 cells per treatment. Results were analyzed using the Kruskal Wallis test followed by a Pairwise Wilcoxon test with a Bonferroni correction of P value, with outliers removed using interquantile range in R (Zehfus *et al.*, 2021). Compared to the vehicle control, we observed a reduction of progerin levels after the addition of M2I-1 (*p*-value $\geq$ 0.00047), MG132 (*p*-value $\geq$ 00680), M2I-1 combined with Metformin (*p*-value $\geq$0.00044), and MG132 combined with M2I-1 (*p*-value $\geq 2.4X10^{-6.}$). After quantifyng progerin fluorescent levels, we observed that M2I-1 and M2I-1 combined with MG132 decreased progerin levels, supporting our theory that progerin removal is caused by autophagy induction.

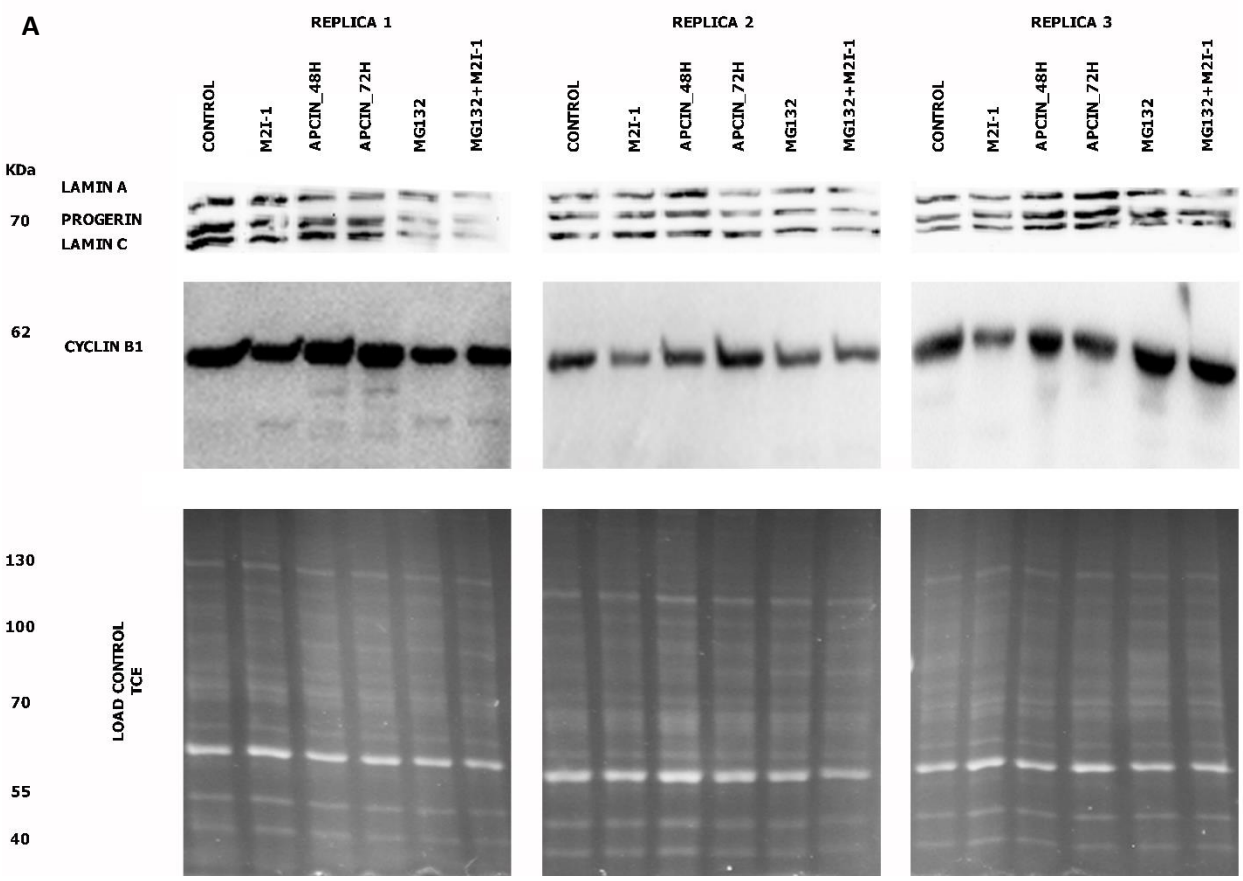
A
REPLICA 1
REPLICA 2
REPLICA 3
CONTROL
M2I-1
APCIN_48H
APCIN_72H
MG132
MG132+M2I-1
KDa
LAMIN A
70
PROGERIN
LAMIN C
62
CYCLIN B1
130
100
70
55
40
LOAD CONTROL TCE

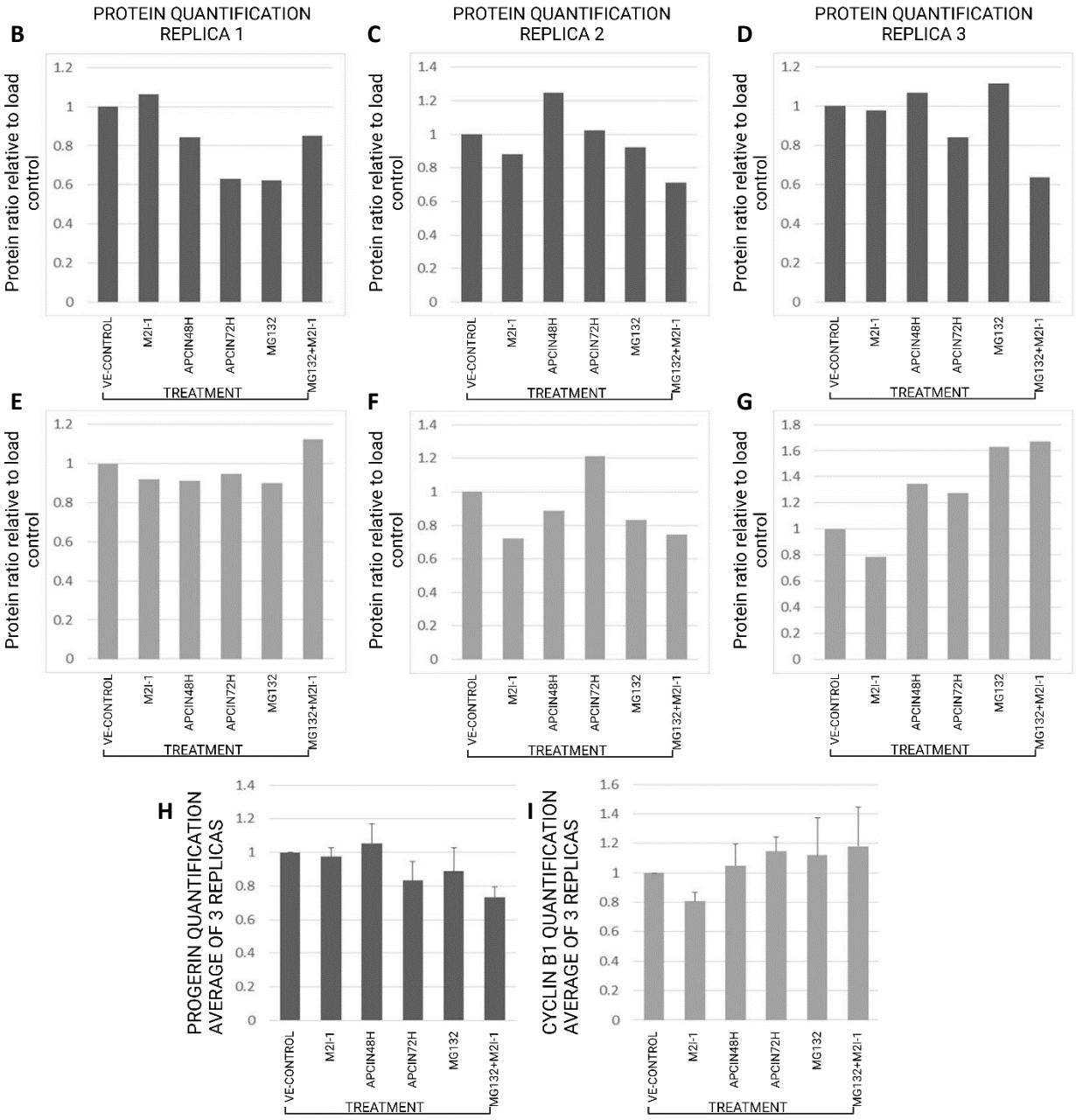

Figure 4.9 Impact of APC activity modulation on progerin levels in the cell line HGADFN169.
A: Western blot of protein lysates extracted from HGPS primary fibroblasts.
From left to right lane treatments are as follows: control cells treated with the vehicle DMSO; this is not what you show in the western. , corresponding to cells treated with 5µM of apcin for 48 hours; APCIN72 representing cells treated with 5µM of apcin for 72 hours; MG132 for cells treated with 5µM of the proteasomal inhibitor MG132 for 48 hours and MG132+M2I corresponding to cells treated for 48 hours with MG132 in combination with M2I-1.

The image shows protein levels for Lamin A/C with three bands at a molecular weight around 70KDa with progerin being the middle band observed. The membrane above represents the protein levels for cyclin B1 to assess APC activity and the last image shows the loading control of total protein visualized with Trichloro ethanol TCE to assure protein abundance prior Western blots.
Protein extracts from the different treatments loaded in 8% SDS-PAGE gel. Cell line HGADF169.
Bar graphic representing the ratio of relative protein abundance of progerin: B in replica 1, C in replica, and D in replica 3.
Bar graphic represents the relative protein abundance ratio of cyclin B1 in: E replica 1, F replica 2 and G replica 3.
H) Bar graphic representing the average ratio of relative protein abundance in three replicas I) Bar graphic representing the average ratio of relative protein abundance of cyclin B1 in three replicas.

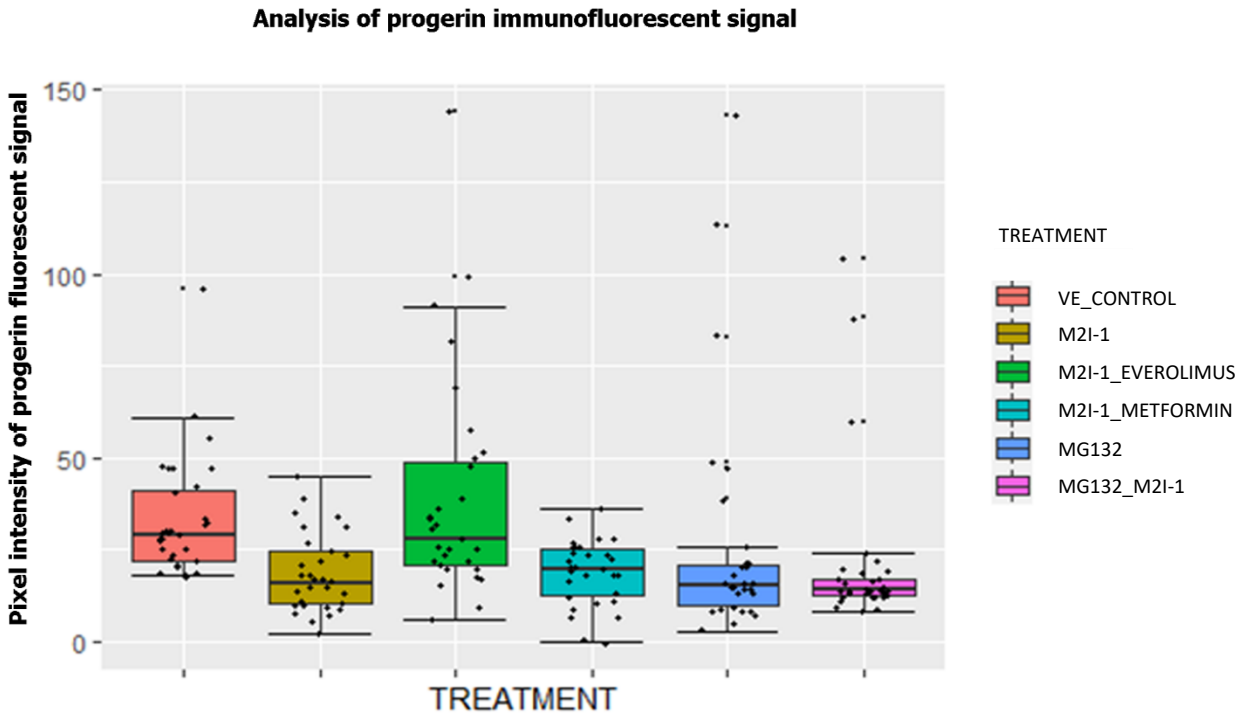

Figure 4.10 Analysis of synergetic effects of M2I-1 and Everolimus/Metformin and proteasomal inhibition by immunofluorescence.
Quantification of progerin immunofluorescence signal of HGPS fibroblasts treated with either DMSO, M2I-1, M2I-1 with Everolimus, M2I-1 in combination with Metformin, MG132 and MG132 in combination with M2I-1, over a period of 48 h.
DMSO: Vehicle control
M2I-1: APC activator
Everolimus: mTOR inhibitor
Metformin: AMPK activation
MG132: Proteasome inhibitor

4.5 Detection of protein-protein interactions between APC proteins and progerin.

4.5.1 Progerin and the APC are in proximity.

Through western blot analysis, we observed a decrease in progerin abundance in HGPS cells following APC activation. This led us to question whether the APC physically interacts with progerin to facilitate protein clearance. As the APC primarily mediates protein ubiquitination to remove proteins, we hypothesized that progerin clearance might involve ubiquitination. To provide evidence for this, we performed PLA analyses to detect protein-protein interactions between progerin and constitutive structures of the APC. We used two cell lines: NB1 primary human fibroblasts, a cell line immortalized with hTERT as non-diseased control, and HGPS primary fibroblasts HGADFN169. HGPS cells were treated with either the vehicle DMSO, M2I-1, or APCIN for 72 hours. The interaction between the APC subunits APC2 and CDC27 was used as positive control for the reaction, Figure 4.11 to.4.15 show the results of these analyses.

Antibodies directed either to APC2 (part of the APC catalytic unit) or CDC20 (APC coactivator involved in substrate recognition) were used to detect interactions between the APC and progerin. NB1-Htert cells were used as a negative control for the reactions that involve progerin since these cells do not produce the mutant protein. After the PLA reaction, a minimum of 30 cells per condition were randomly selected for analysis, and the images were collected and processed with the software ImageJ. The number of fluorescent dots (foci) in each nucleus was counted, and the data were collected and analyzed with the statistical software R. A Kruskal Wallis test was used to determine significant differences between treatments with adjustment of Bonferroni. We used the Wilkinson pairwise to determine differences between treatments, and statistical values were obtained. The data was summarized with a box plot, to compare the distribution of fluorescence intensity among all the treatments.

We found differences in the number of foci between normal fibroblasts and progeria cells, as well as differences between cells treated with M2I-1 or APCIN. Interactions between the two APC subunits, APC2 and CDC27, were lower in progeria cells compared with non-diseased control cells (Figure 4.11, Figure 4.12, Figure 4.15 A). Furthermore, we identified that M2I-1 increases the number of foci in the interaction for APC2-CDC27 when compared with the vehicle control. On the other hand, when APCIN is applied, no differences were found with the vehicle control

progeria cells. These findings suggest that upon activation with M2I-1, higher levels of the complex can be detected; this also suggests that the APC is impaired or less expressed in progeria cells (Figure 4.15 A), and it can be rescued with the application of M2I-1. M2I-1 vs. Control (*p*-value ≥0.203 and M2I-1 vs. apcin *p*-value ≥ 0.024).

The presence of foci or fluorescent dots for both APC2-progerin (Figure 4.13, Figure 4.15 B) and CDC20-progerin (Figure 4.14, Figure 4.15 C) suggests that the APC interacts with progerin, or that at least are in close enough physical proximity to produce a positive signal. Furthermore, their interactions increase when cells are treated with M2I-1, indicating that APC activation is involved in progerin turnover (*p*=0.0042). Detectable fluorescent signal between the APC coactivator, CDC20, and progerin, also increased when progeria cells were treated with M2I-1(*p*=0.0042) and decreased when APCIN was applied (*p*=0.4109 compared with the control group). However, APCIN had a more evident effect in the APC2-progerin intreraction, where foci numbers decreased the number of foci almost to cero (Figure 4.13, Figure 4.15 B), which was not the case for CDC20-progerin. Therefore, is possible that progeria interacts first with CDC20, and APCIN interfere in the interaction with CDC20 and the APC.

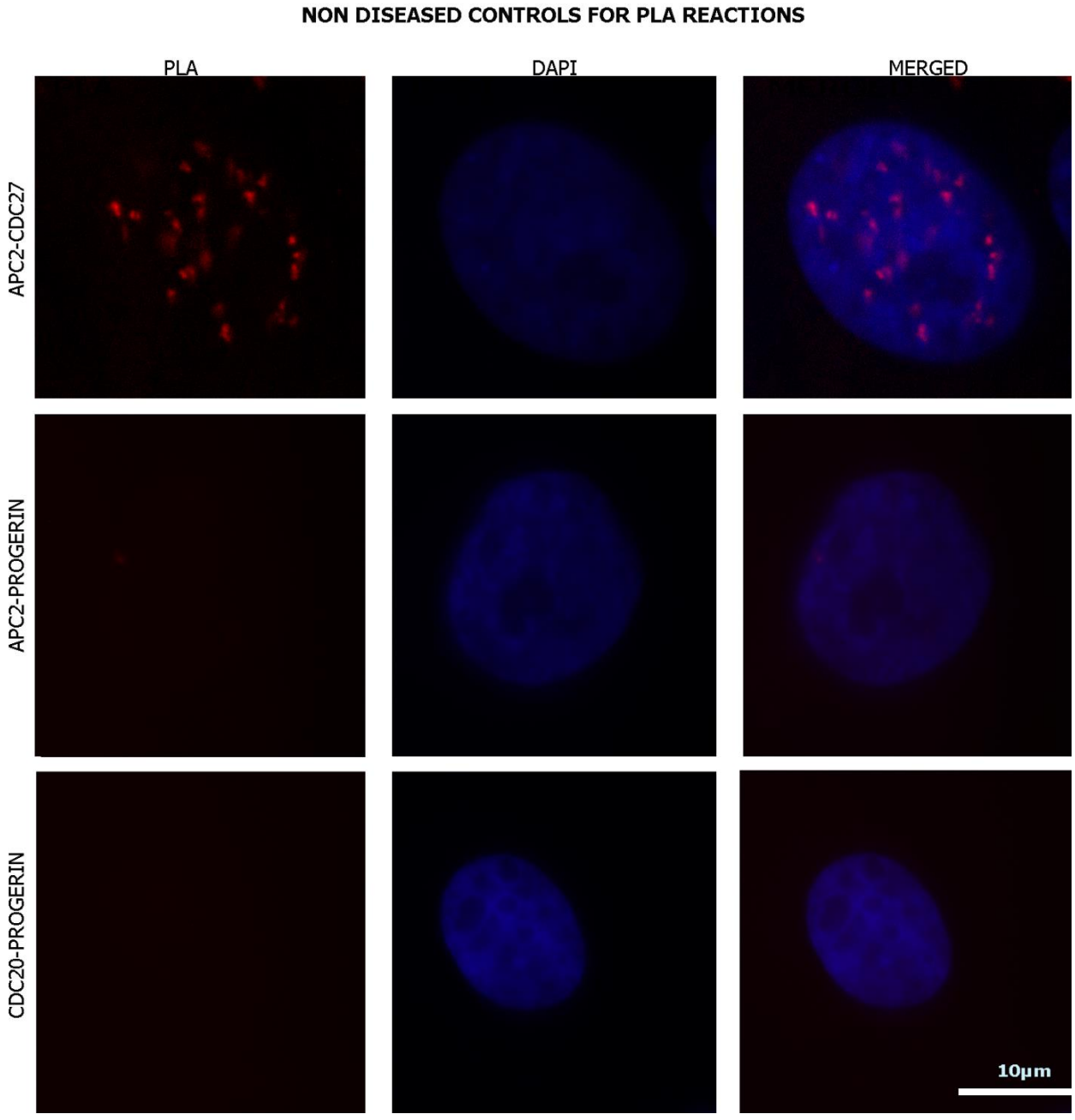

Figure 4.11 PLA interactions in the control non-diseased cells.
NB1-hTert without treatment and grown in coverslips for 72 h. PLA interactions in non-diseased cells were compared against HGPS progeria cells. APC2-CDC27 is the positive control reaction between two units of the APC complex. APC2-progerin and CDC20-progerin were used to determine reaction specificity since NB1 cells do not produce progerin. CDC20-progerin reaction was used. This figure only addresses APC2 and CDC27. Bar 10 µm.

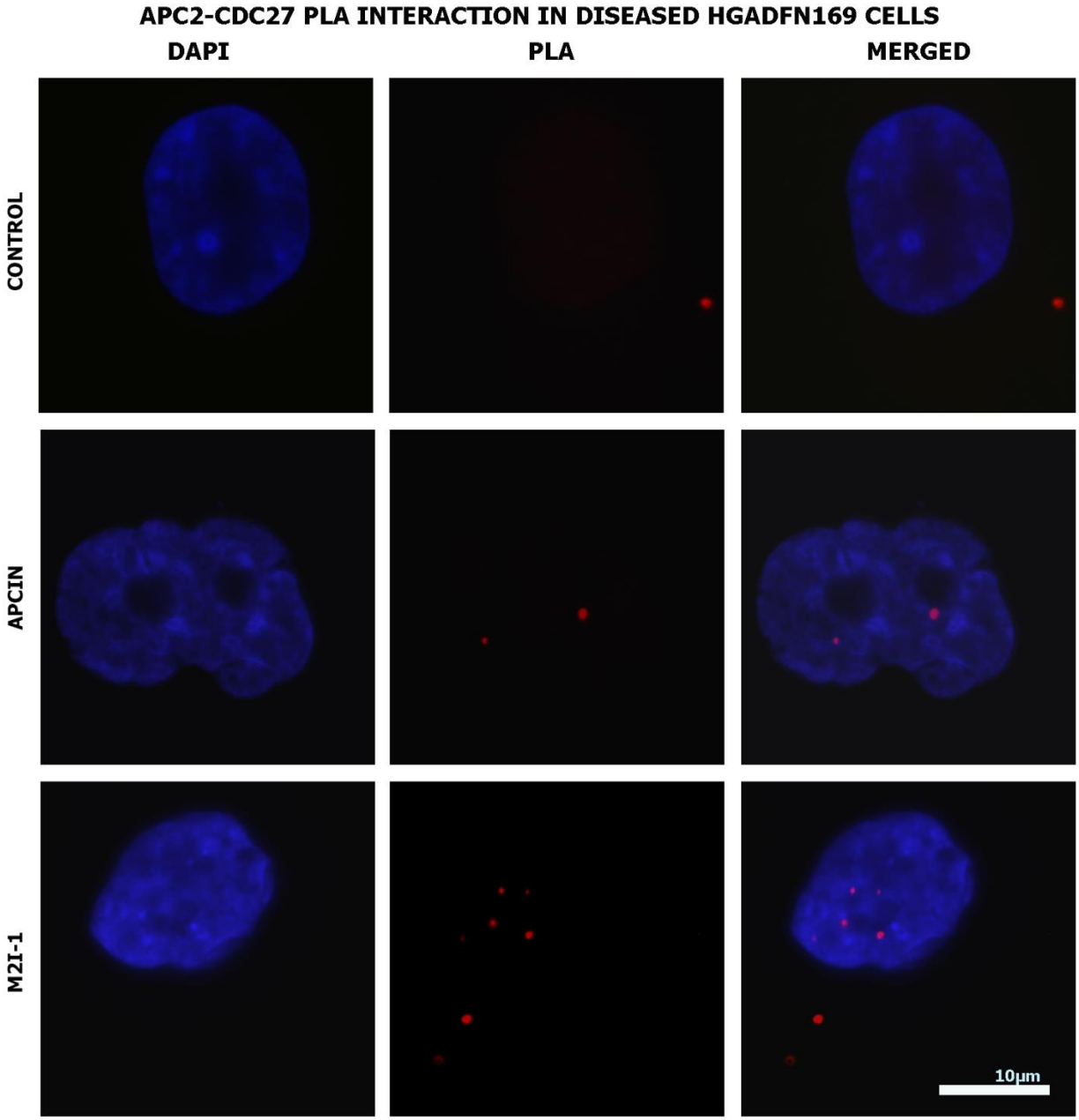

Figure 4.12 PLA interaction between APC2 and CDC27 in HGPS HGADFN169 cells after being treated with the APC activator M2I-1 or APC inhibitor APCIN.

Red dots indicate foci where proteins are in proximity. APC2-CDC27 is the positive control for the reaction between two units of the APC complex.

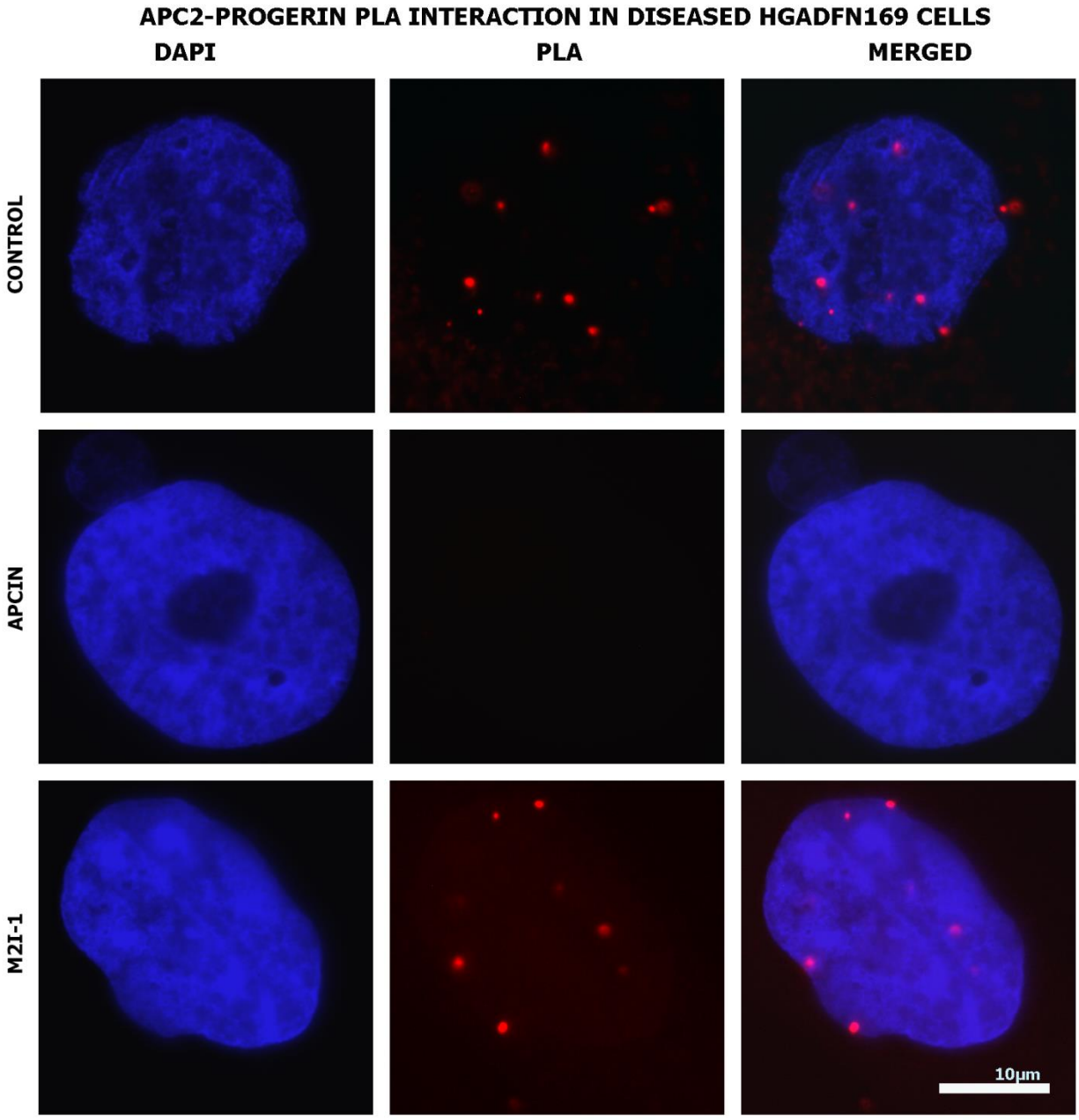

Figure 4.13 PLA interactions between APC2 and progerin in HGPS HGADFN169 cells after being treated with the APC activator M2I-1 or APC inhibitor APCIN.
Red dots indicate foci where proteins are in proximity.

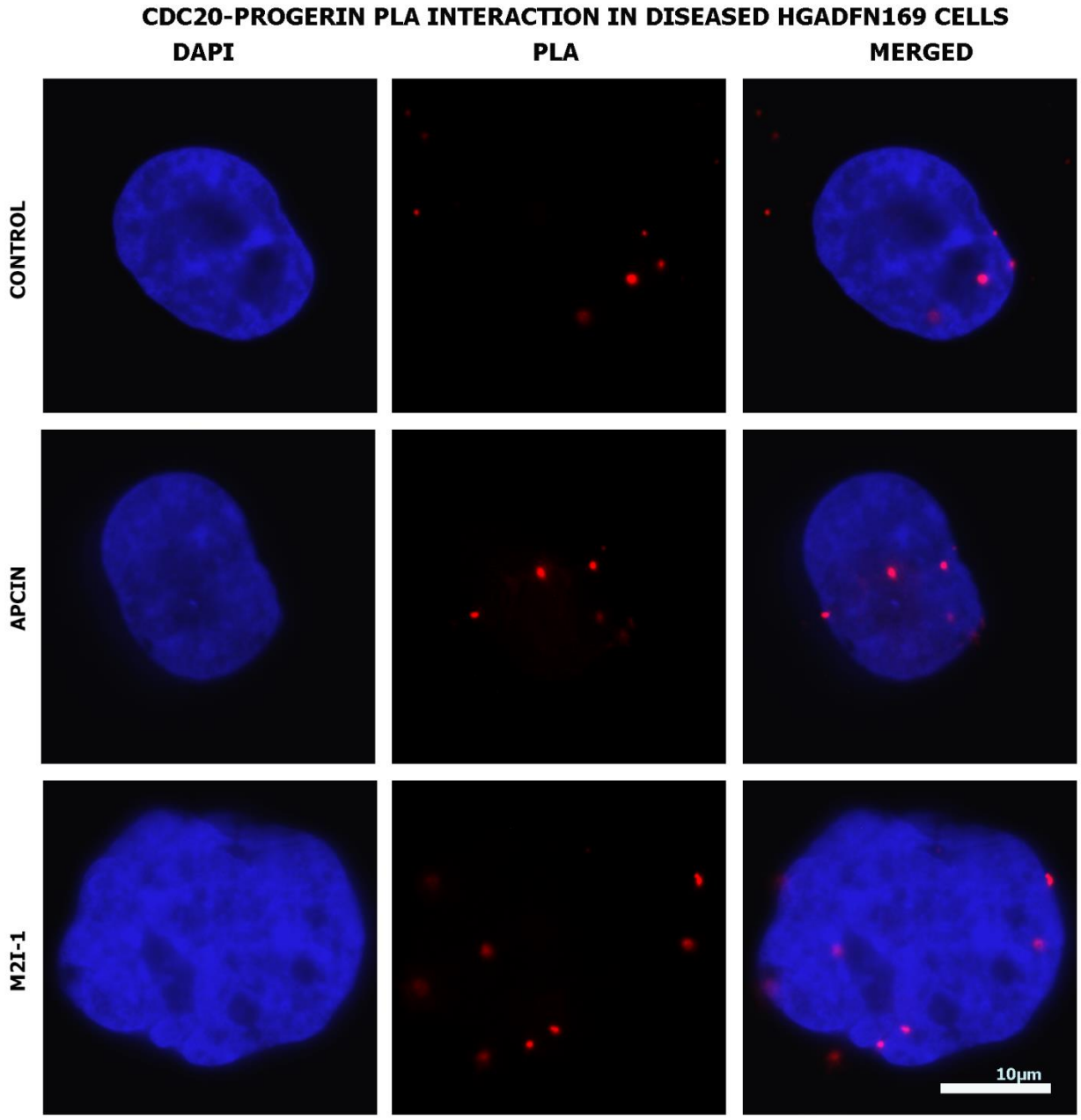

Figure 4.14 PLA interactions between CDC20 and progerin in HGPS HGADFN169fibroblasts after being treated with the APC activator M2I-1 or APC inhibitor apcin.
Red dots indicate foci where proteins are in proximity.

A

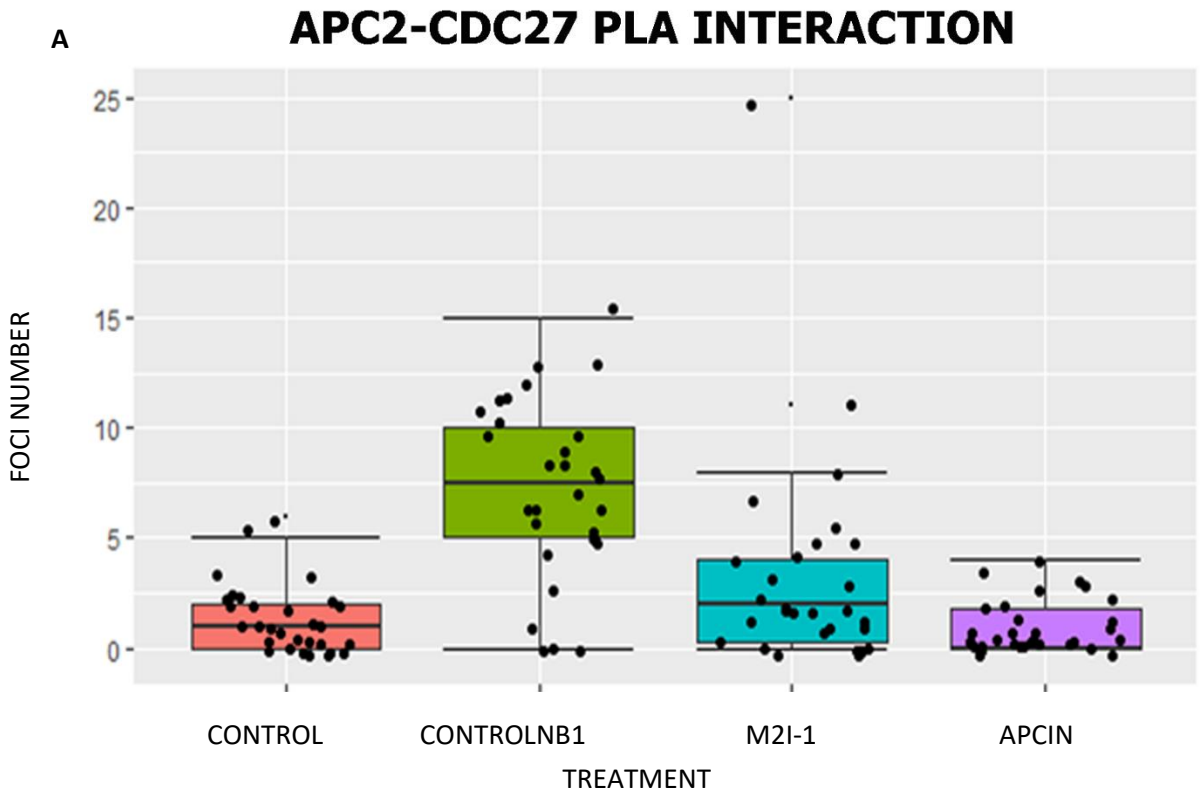
APC2-CDC27 PLA INTERACTION
FOCI NUMBER
25
20
15
10
5
0
CONTROL
CONTROLNB1
M2I-1
APCIN
TREATMENT

B

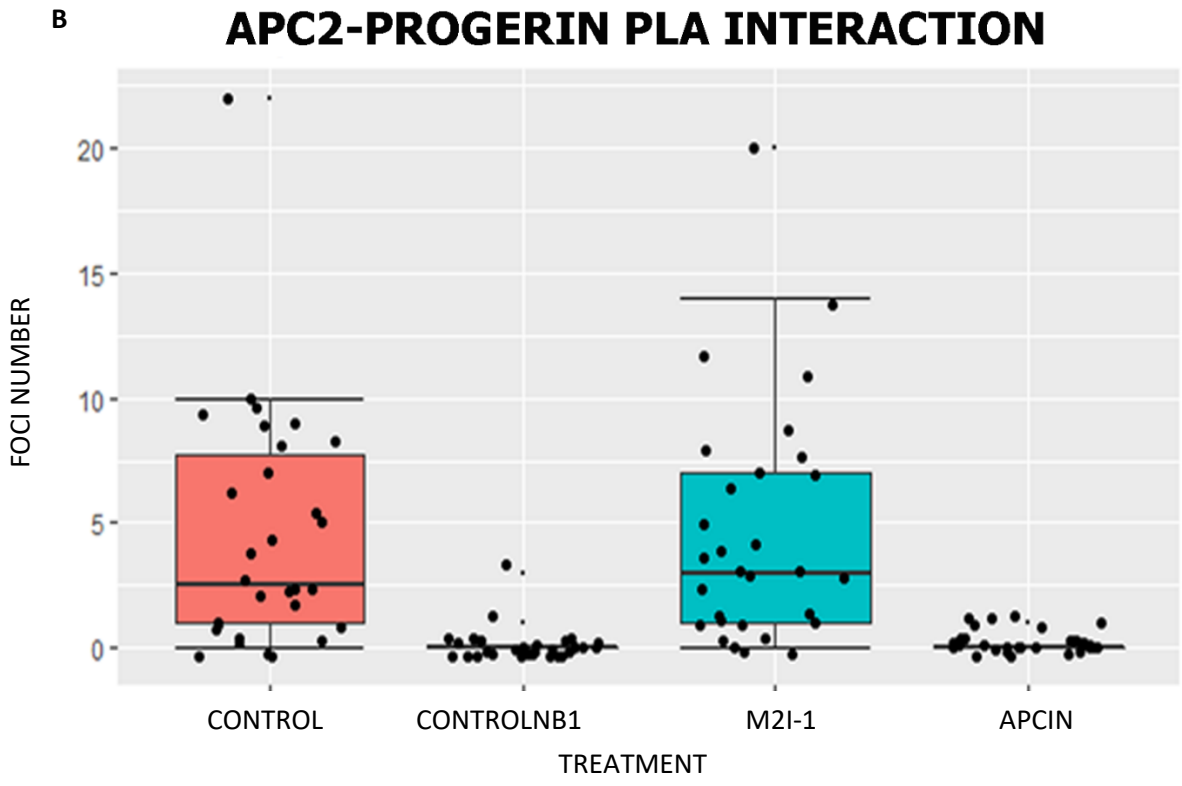
APC2-PROGERIN PLA INTERACTION
FOCI NUMBER
20
15
10
5
0
CONTROL
CONTROLNB1
M2I-1
APCIN
TREATMENT

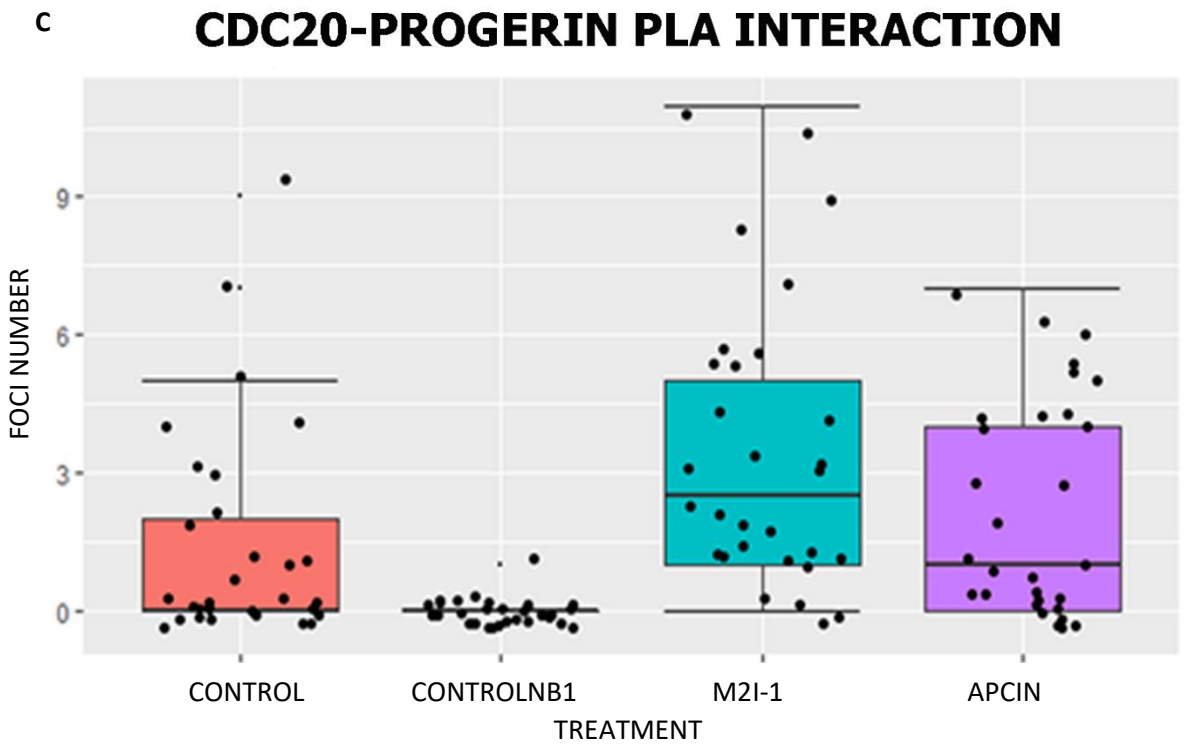

Figure 4.15 Quantification on the number of foci for PLA assay with NB1-hTert as non diseased control cells and HGADFN169 primary fibroblasts.

A) Positive control of the reaction corresponding to APC subunits that conform the APC complex APC2, which forms part of the complex catalytic unit, and CDC27 which forms part of the scaffold unit. B) PLA interaction between progerin and the APC coactivator CDC20. C) PLA interaction between APC2 and progerin.

Control: HGPS cells treated with the vehicle control, Control NB1: control for non-diseased cells, M2I-1: APC activator tested in HGPS cells in a concentration of 5µM, apcin: APC inhibitor used at µM in HGPS cells. All treatments were carried out for 72 h.

After conducting PLA interactions, we observed that the APC complex is in proximity with progerin, leading us to hypothesize that progerin may undergo ubiquitination. To test this hypothesis, we performed PLA analysis on HGPS primary fibroblasts by probing for progerin and ubiquitin and treated the cells with either vehicle control DMSO, APC activator M2I-1, or APCIN to observe changes in the number of red fluorescent dots, or foci in response to activation or inhibition of the APC (Figure 4.16 and 4.17).

Our findings indicated an increase in the number of foci when the APC was activated, suggesting that interactions between progerin and ubiquitin are enhanced after M2I-1 is added to the cells or when the APC comes in close proximity to progerin enough to be detected by PLA. In contrast, when the APC was inhibited with APCIN, the number of foci decreased dramatically. These results support the hypothesis that PLA interacts with progerin when the APC is activated.

Based on these findings, we sought to further investigate the mechanism of progerin clearance, specifically whether autophagy plays a role in this process and what effect the progerin-ubiquitin interaction has when autophagy is inhibited as shown in Section 4.5.2.

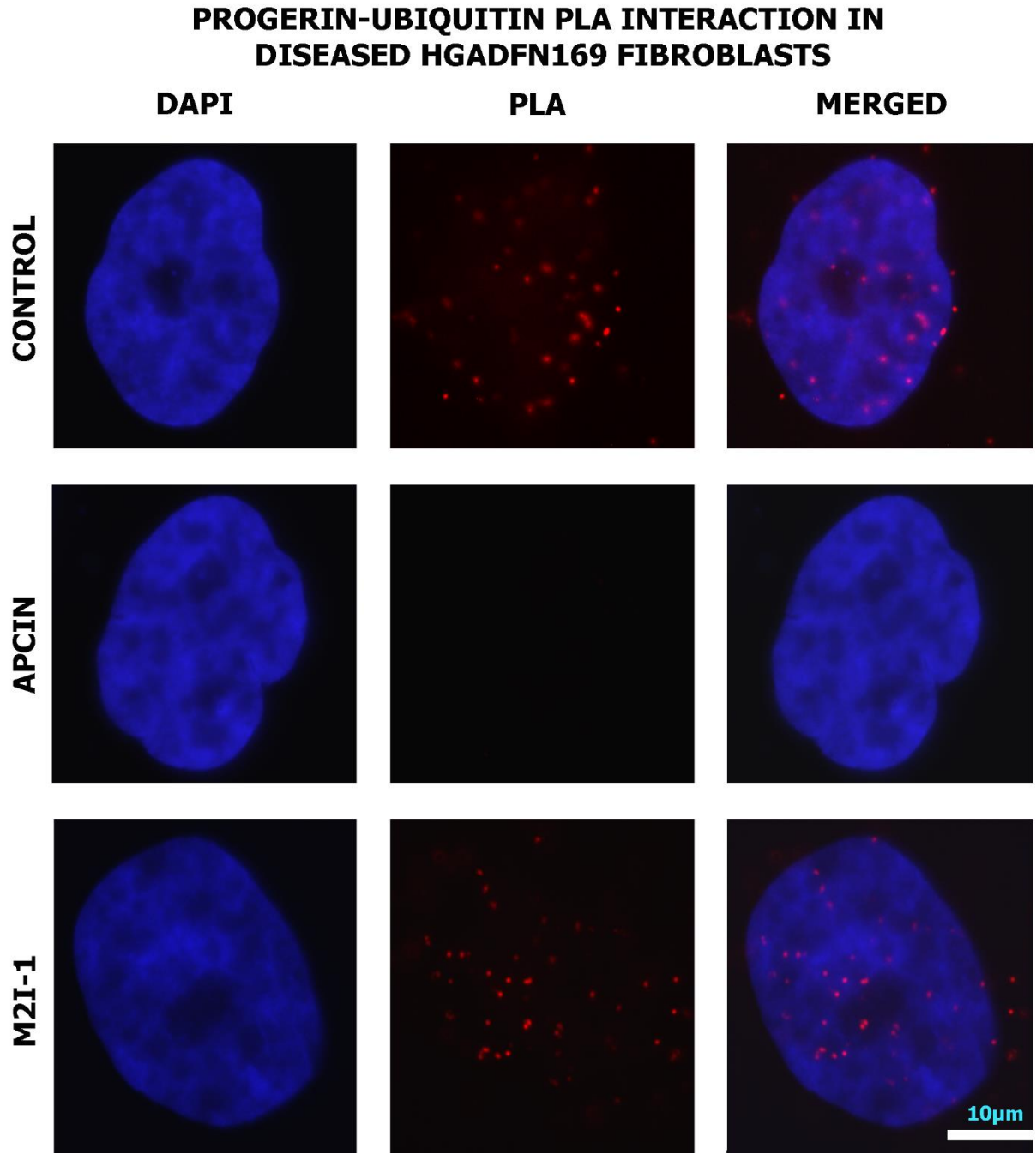

Figure 4.16 PLA interaction in HGADFN169 primary fibroblasts between progerin and ubiquitin. Changes in number of foci after APC activation with M2I-1 or inhibition with apcin, DMSO is utilized as the vehicle control, 72 h. Scale bar 10 µm.

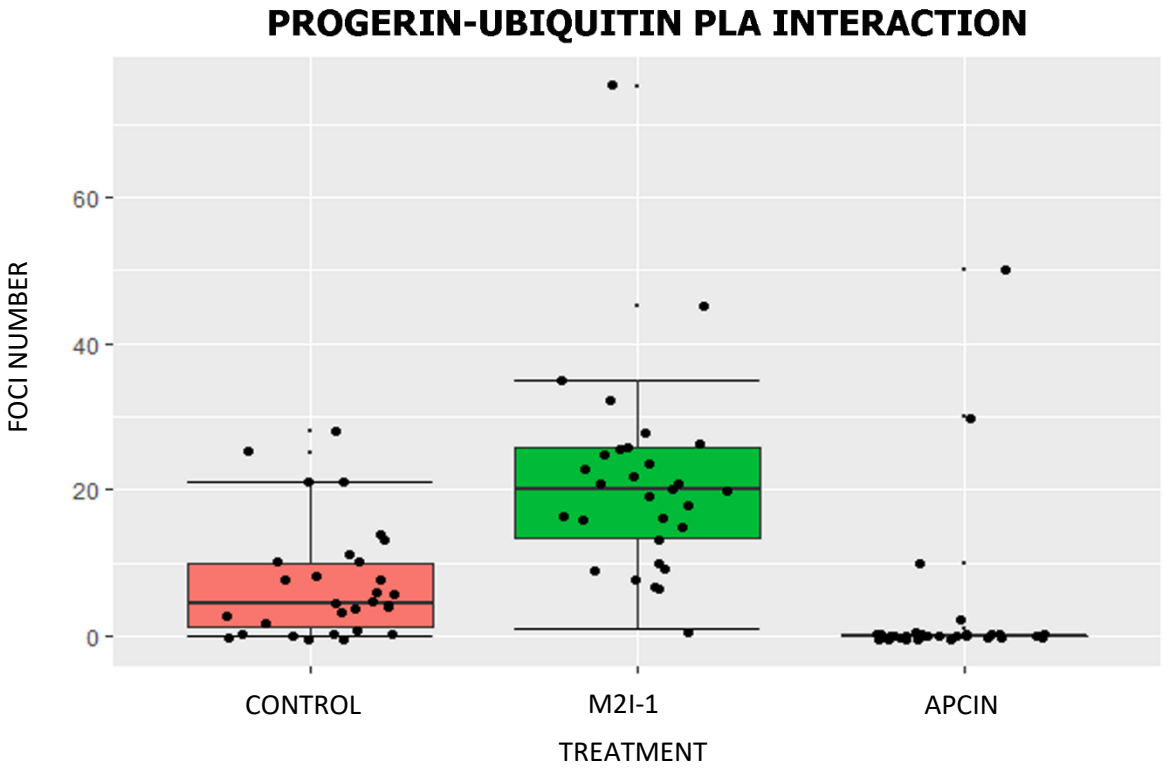

Figure 4.17 Quantification of foci per cell in the PLA reaction progerin-ubiquitin.
HGADF169 primary fibroblasts were treated with either DMSO (Vehicle control represented in pink), APC activator M2I-1 represented by the green box and the APC inhibitor apcin in black.

4.5.2 Determine interaction between progerin, APC and ubiquitin.

Upon activation of the APC, a reduction in progerin levels was observed by western blot, suggesting a possible interaction between progerin and the APC. PLA assays also revealed close proximity between progerin and the APC, further supporting this hypothesis. To investigate this interaction, co-immunoprecipitation (Co-IP) was performed by pulling down Lamin A/C and progerin and detecting possible interacting proteins. The insoluble nature of Lamin A/C and progerin proteins was considered, with a small percentage expected to remain in the unbound fraction. The majority of the protein complexes interacting with Lamin A/C and progerin were expected to be found in the bound fraction. Western blot analysis showed that Lamin A/C and progerin were present in both the bound and unbound fractions but were more abundant in the bound fraction (Figure 4.18). The presence of CDC20 (APC coactivator) and the bait proteins indicated a direct interaction between the APC through its coactivator and either Lamin A/C or progerin (Figure 4.18 B).

In contrast, western blot analysis did not confirm the ubiquitination of progerin (Figure 4.18 C). Although different molecular size ubiquitin bands were detected, none confirmed the ubiquitination of progerin (~100 KDa). Exposure times were increased to detect low intensity bands, resulting in a saturated band around ~180 kDa, shown in blue Figure 4.18 C. To investigate progerin-ubiquitin interactions further, colocalization assays were performed.

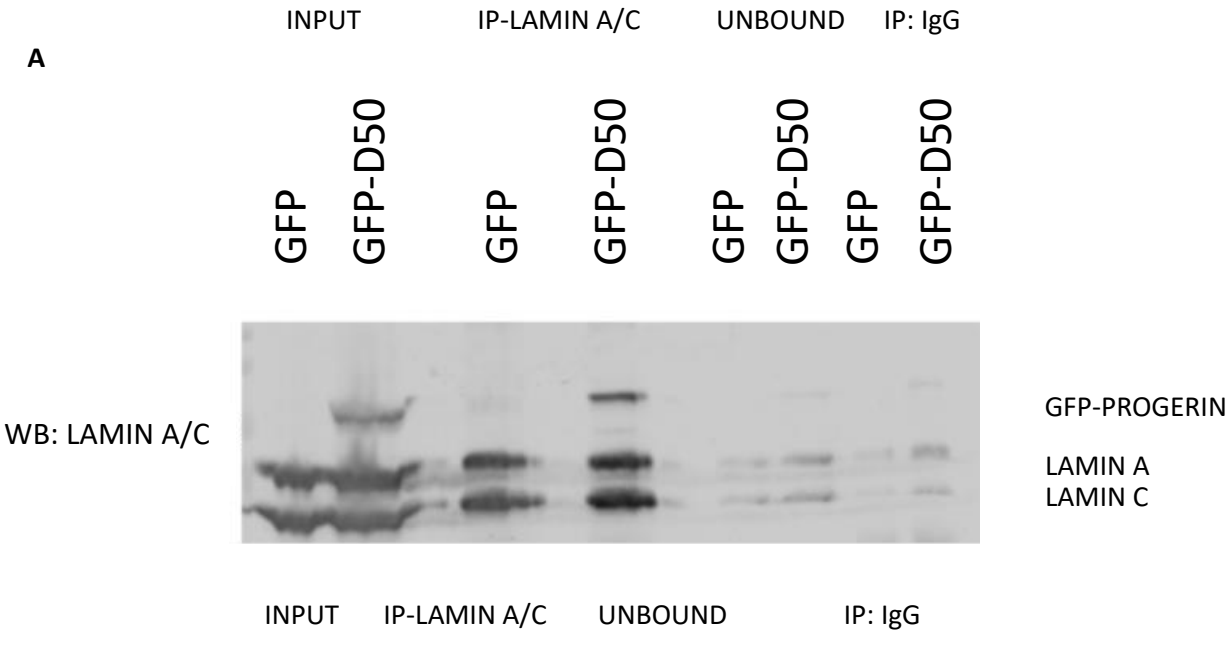
INPUT
IP-LAMIN A/C
UNBOUND
IP: IgG
A
GFP
GFP-D50
GFP
GFP-D50
GFP
GFP-D50
GFP
GFP-D50
WB: LAMIN A/C
GFP-PROGERIN
LAMIN A
LAMIN C
INPUT
IP-LAMIN A/C
UNBOUND
IP: IgG
B
GFP
GFP-D50
GFP
GFP-D50
GFP
GFP-D50
GFP
GFP-D50
WB: CDC20

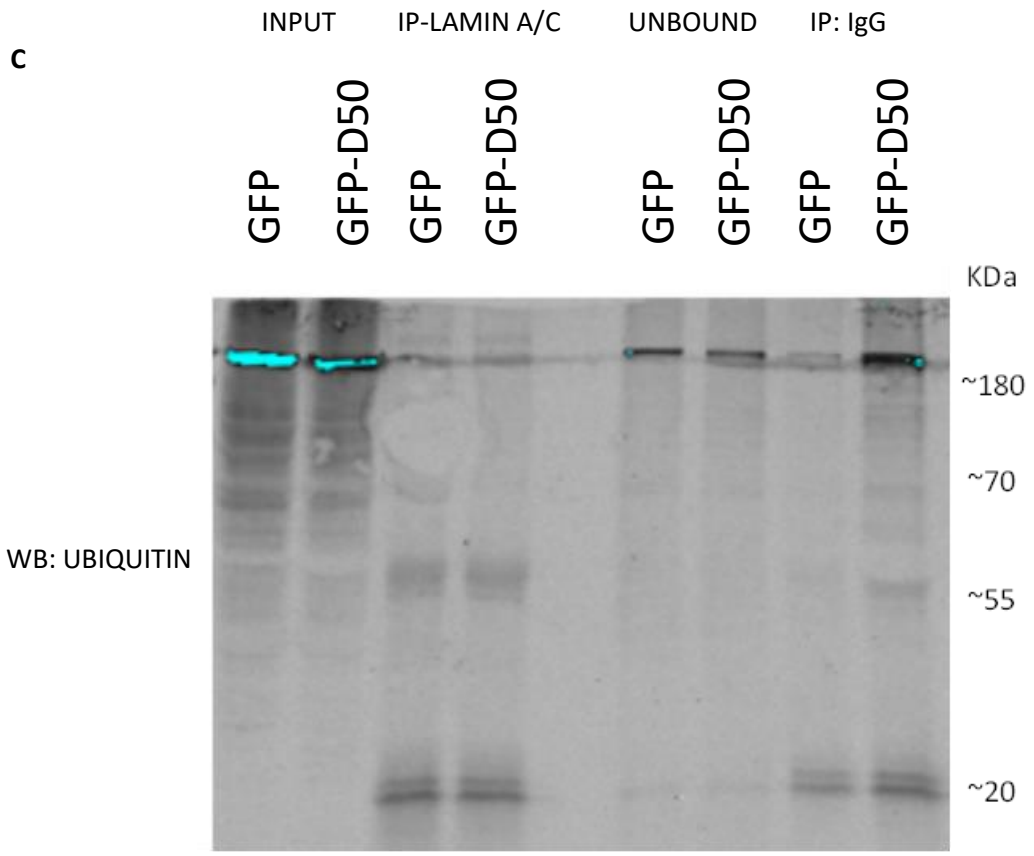

Figure 4.18 Western blots indicating protein levels of Lamin A/C endogenous interactors.
Western blots using primary antibodies for Lamin A/C (A), CDC20 (B), or ubiquitin (C). Cells used for immunoprecipitation were NB1 hTERT- immortalized fibroblasts expressing just GFP or the D50 mutation expressing progerin-GFP. Non-specific mouse IgG was used as an immunoprecipitation control as well as the unbound fraction of immune precipitation.

4.6 Autophagy plays a role in progerin removal

In previous experiments, we observed reduced progerin levels upon APC activation. This decrease was further enhanced when MG132, a proteasome inhibitor, was added to the media of HGPS169 cells. These findings are consistent with Harhouri et al. (2017), who demonstrated that treating progeria cells with MG132 leads to a decrease in progerin levels partially mediated by autophagy. Therefore, we hypothesized that inhibiting autophagy would lead to an increase in progerin levels that could be detected by immunoblotting. To test this hypothesis, we treated HGADFN169 and HGADFN167 cells with M2I-1 alone and observed a 20% decrease in progerin levels in HGADFN169 and a 61% decrease in HGADFN167 (Figure 4.19, Figure 4.20). Interestingly, when cells were treated with chloroquine and vehicle control, progerin levels increased by 15% and 177% in HGADFN169 and HGADFN167 fibroblasts respectively. When M2I-1 and chloroquine were combined, progerin levels increased by 13% in HGADFN169 and 24% in HGADFN167. However, treatments with chloroquine in combination with either MG132 or MG132 with M2I-1 did not increase progerin levels in either cell line.

Overall, these results suggest that autophagy contributes to progerin turnover. When autophagy is inhibited, progerin levels increase as it can no longer be cleared. These findings offer insight into progerin clearance mechanisms and suggest potential therapeutic targets for treating progeria.

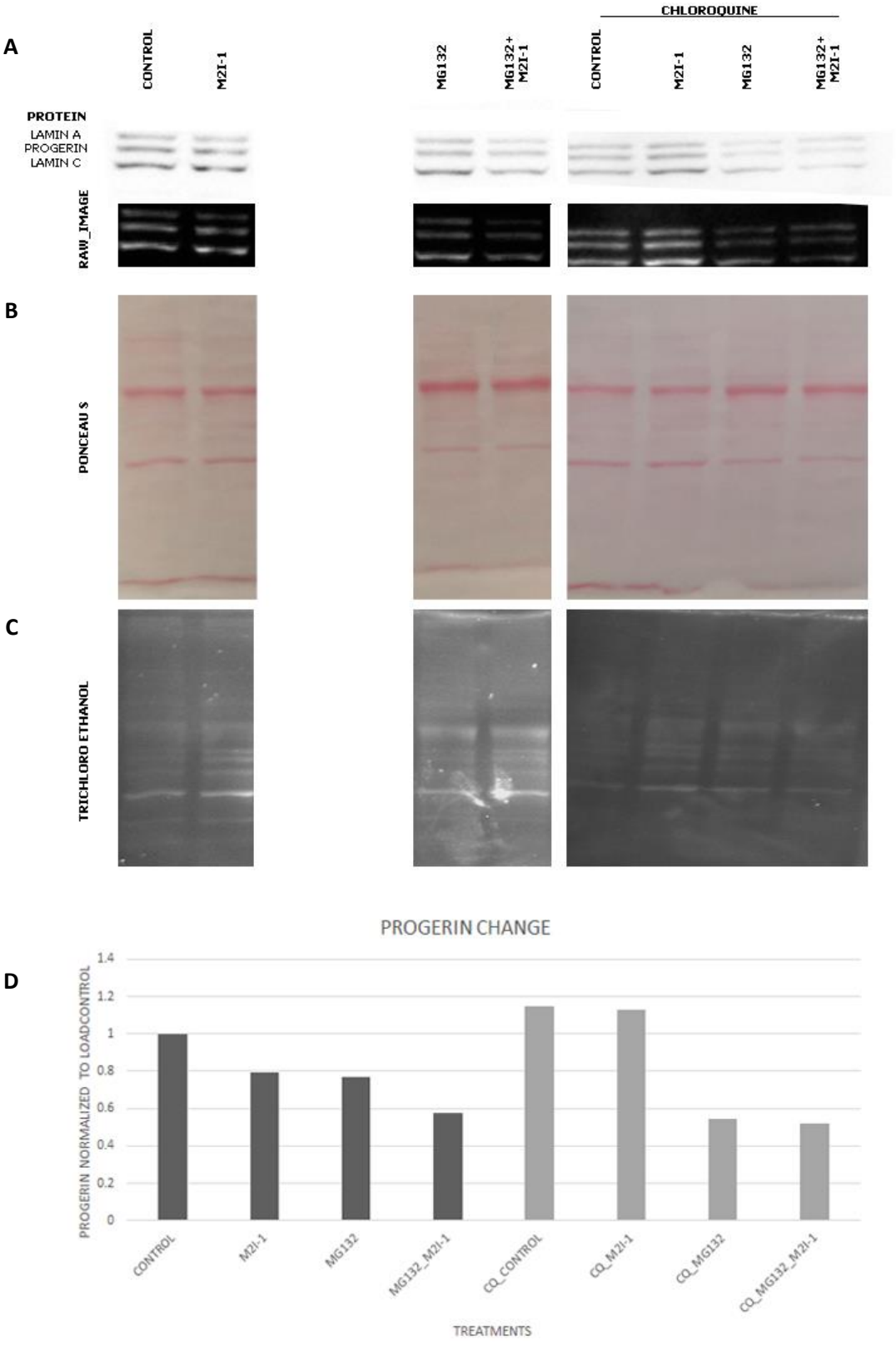
A
CONTROL
M2I-1
MG132
MG132+ M2I-1
CHLOROQUINE
CONTROL
M2I-1
MG132
MG132+ M2I-1
PROTEIN
LAMIN A
PROGERIN
LAMIN C
RAW_IMAGE
B
PONCEAU S
C
TRICHLORO ETHANOL
D
PROGERIN CHANGE
PROGERIN NORMALIZED TO LOADCONTROL
1.4
1.2
1
0.8
0.6
0.4
0.2
0
CONTROL
M2I-1
MG132
MG132_M2I-1
CQ_CONTROL
CQ_M2I-1
CQ_MG132
CQ_MG132_M2I-1
TREATMENTS

Figure 4.19 Western blot analysis of protein lysates in HGADFN169 HGPS primary fibroblasts.
Increased levels of progerin are associated with autophagy inhibition with 5 µM of chloroquine after 48 h. Levels of progerin increase when compared with HGPS primary fibroblasts not treated with chloroquine. Treatment is as follows: Control: DMSO as vehicle control, M2I-1: APC activator, MG132: proteasome inhibitor, and MG132_M2I-1: MG132 in combination with M2I.CQ_CONTROL: DMSO (vehicle control) in combination with chloroquine, CQ_ M2I-1: 5µM of APC activator M2I-1 with 5µM of chloroquine, CQ_MG132: 5µM of proteasome inhibitor MG132 in combination with 5µM of Chloroquine, CQ_MG132_M2I-1: 5µM of proteasome inhibitor MG132 in combination of 5µM of M2I-1 and 5µM of Chloroquine.
A) Shows the western blot image for Lamin A/C; it also shows below the raw image acquired from the imager.
B) Ponceau S staining for total loaded proteins and verification of transfer efficiency.
C) Trichloroethanol staining as load control.
D) Bar graph representing progerin quantification normalized to load control in response to different treatments.

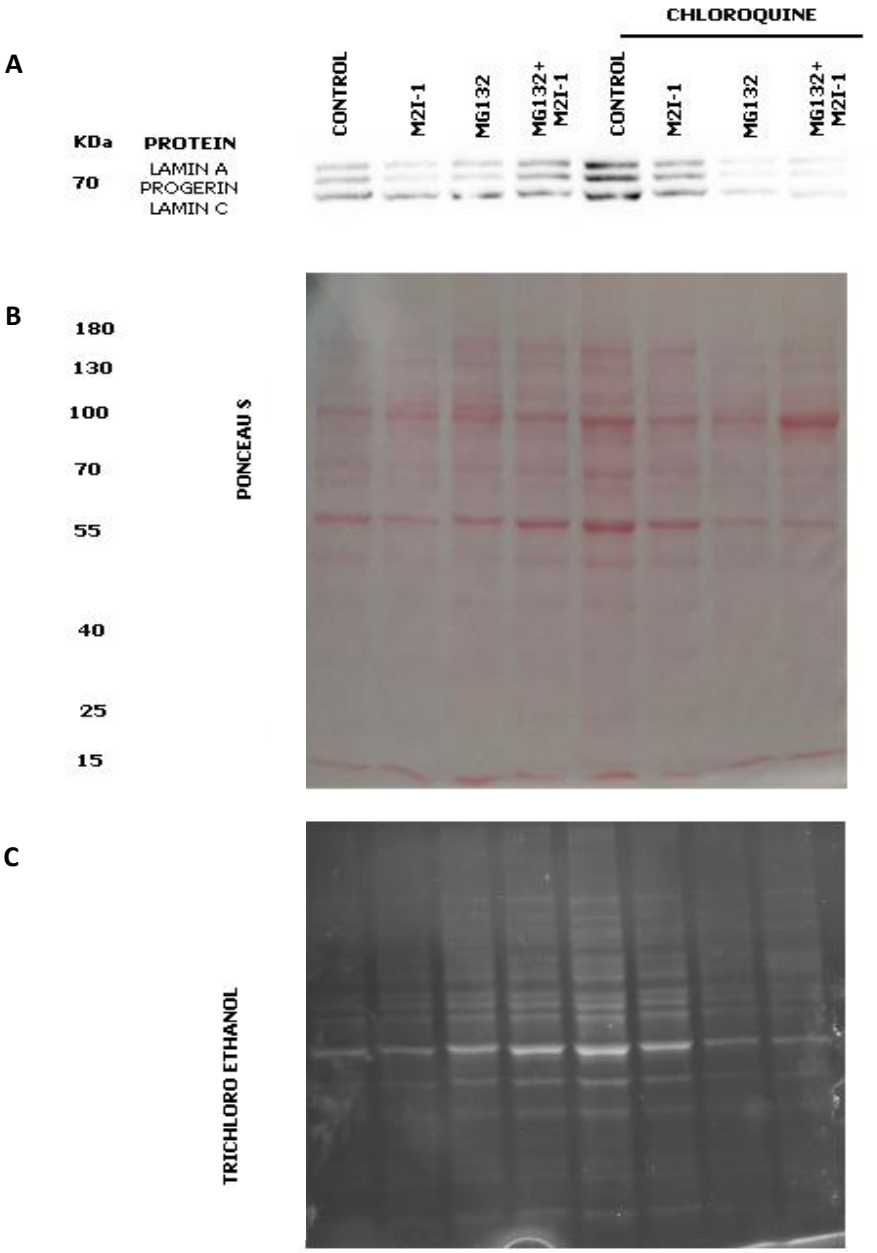
A
CHLOROQUINE
CONTROL
M2I-1
MG132
MG132+ M2I-1
CONTROL
M2I-1
MG132
MG132+ M2I-1
KDa
PROTEIN
70
LAMIN A
PROGERIN
LAMIN C
B
180
130
100
70
55
40
25
15
PONCEAU S
C
TRICHLORO ETHANOL
D
PROGERIN CHANGE in 167
Ratio normalized to load control
3
2.5
2
1.5
1
0.5
0
CONTROL
M2I-1
MG132
MG132_M2I-1
CQ_C
CQ_M2I-1
CQ_MG132
CQ_MG132_M2I-1
Treatments

Figure 4.20 Western blot analysis of protein lysates in HGADFN167 HGPS primary fibroblasts. A) Western blot from hole protein lysates from fibroblasts under different treatments. Control DMSO as vehicle control, M2I-1: APC activator, MG132: proteasome inhibitor, and MG132_M2I-1: MG132 in combination with M2I.CQ_CONTROL: DMSO (vehicle control) in combination with chloroquine, CQ_ M2I-1: 5µM of APC activator M2I-1 with 5µM of chloroquine, CQ_MG132: 5µM of proteasome inhibitor MG132 in combination with 5µM of Chloroquine, CQ_MG132_M2I-1: 5µM of proteasome inhibitor MG132 combined with M2I-1 (5µM) and Chloroquines (5µM) Increased levels of progerin are associated with autophagy inhibition with 5 µM of chloroquine after 48h. Levels of progerin increase when compared with HGPS primary fibroblasts not treated with chloroquine. B) Ponceaus staining and C) Trichloro ethanol were used as controls to monitor the total amounts of loaded proteins.
D) Protein quantification of progerin levels after treatments**.**

We hypothesized that the APC might mediate the mobilization of progerin to the cytoplasm, as autophagy primarily occurs there. Therefore, we reasoned that inhibiting autophagy could result in the accumulation of progerin in the cytoplasm or a change in its localization, which could be detected by immunofluorescence microscopy. To test this hypothesis, we imaged primary fibroblasts from HGPS patients (HGADFN169) and measured changes in progerin intensity or localization after adding 5 μM of chloroquine to the culture media for 48 hours to inhibit autophagy (Figure 4.21). We compared chloroquine treatment with DMSO, M2I-1, MG132, or a combination of MG132 and M2I-1, and we compared these drug combinations against cells not treated with chloroquine. Consistent with previous experiments, we observed a reduction in progerin fluorescence intensity in cells treated with M2I-1 (Figure 4.21). Furthermore, we found that when autophagy was inhibited, progerin levels increased compared to cells not treated with chloroquine.

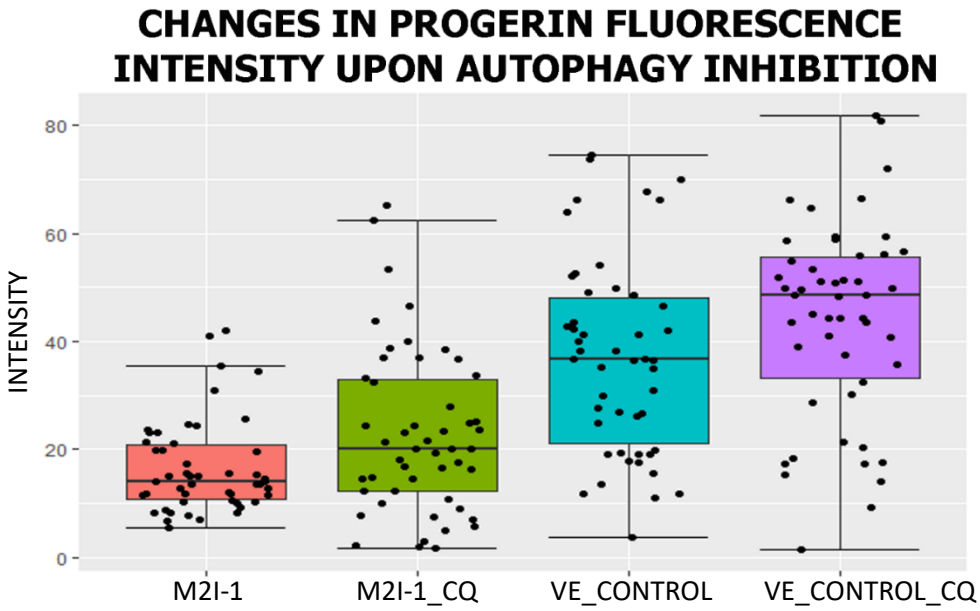

Figure 4.21 Quantification of progerin immunofluorescence levels in HGADFN169 primary fibroblasts with/without autophagy inhibition.

Cells were treated with/ without chloroquine (5 µM) as an autophagy inhibitor in combination with DMSO (same volume as treatments) as vehicle control or M2I-1 (5 µM). Fibroblasts were grown on coverslips, for 48 h cells, then were treated as described above, fixed, permeabilized and immunolabeled with the primary antibody against progerin. At least 30 cells were counted, and fluorescence was quantified with the software IMAGEJ.

To better understand the roles of autophagy and APC activation, we investigated the distribution of fluorescently labeled progerin and ubiquitin. We compared changes in the localization of these two probes after treating HGPS primary fibroblasts with or without chloroquine. As shown in Figure 4.22 A, a stronger colocalization signal (yellow signal) was observed after treatment with chloroquine. Cells treated with the vehicle control, with or without chloroquine, exhibited a higher colocalization signal of progerin and ubiquitin in the nuclei. Conversely, lower to no signal was detected in cells treated with M2I-1, even when chloroquine was added. Figure 4.22 A shows the fluorescent signal for ubiquitin and progerin captured under the standard conditions used in previous experiments. We captured images of ubiquitin at low exposure to prevent overexposure and high exposure to detect signals in the cytoplasm (Figure 4.22 B).

It is important to note that the strong ubiquitin signal can cause overexposure of the image in the nuclei. To address this, we re-imaged the cells using lower exposure times for progerin and ubiquitin (Figure 4.22 B). Once again, we observed overlapping signals of both probes in specific cells, particularly in cells treated with the vehicle control. However, we observed less frequent and lower colocalization signals when APC was activated. To quantify the colocalization, we used RGB linear scans that determined overlapping pixels in the image. Overlapping peaks of the red (ubiquitin) and green (progerin) channels indicated colocalization of the two fluorescent probes. Figure 4.23 demonstrates the results of the colocalization analysis.

Taken together, our results suggest that when autophagy is inhibited, and APC is not activated, progerin targeted with ubiquitin accumulates in the nuclei. APC may be involved in mobilizing or solubilizing progerin out of the nuclei. Therefore, when APC is active, progerin is within proximity of ubiquitin or is tagged for degradation. However, the rate of this process may be too slow to be detected in our experiments.

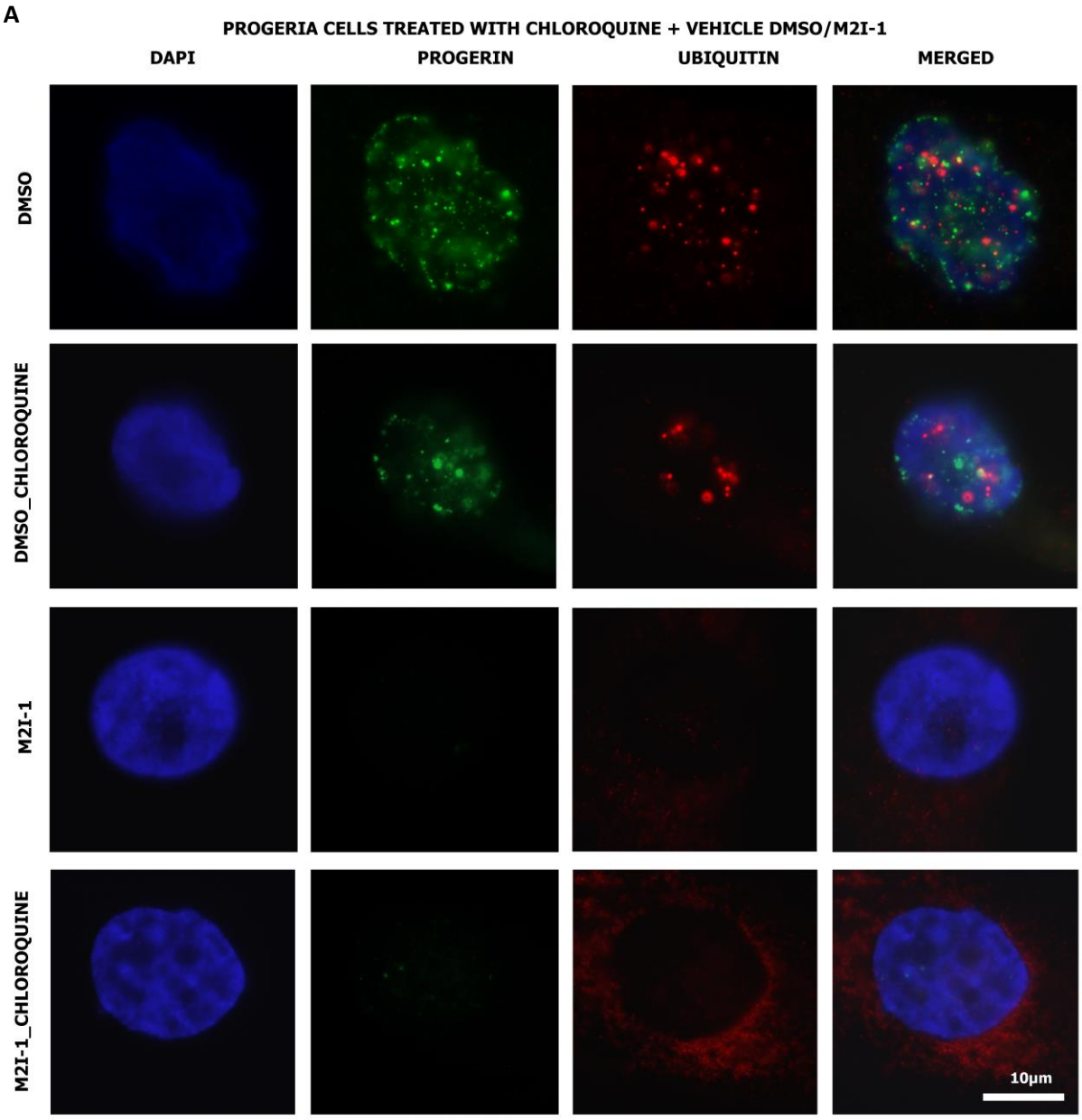
A
PROGERIA CELLS TREATED WITH CHLOROQUINE + VEHICLE DMSO/M2I-1
DAPI
PROGERIN
UBIQUITIN
MERGED
DMSO
DMSO_CHLOROQUINE
M2I-1
M2I-1_CHLOROQUINE
10µm

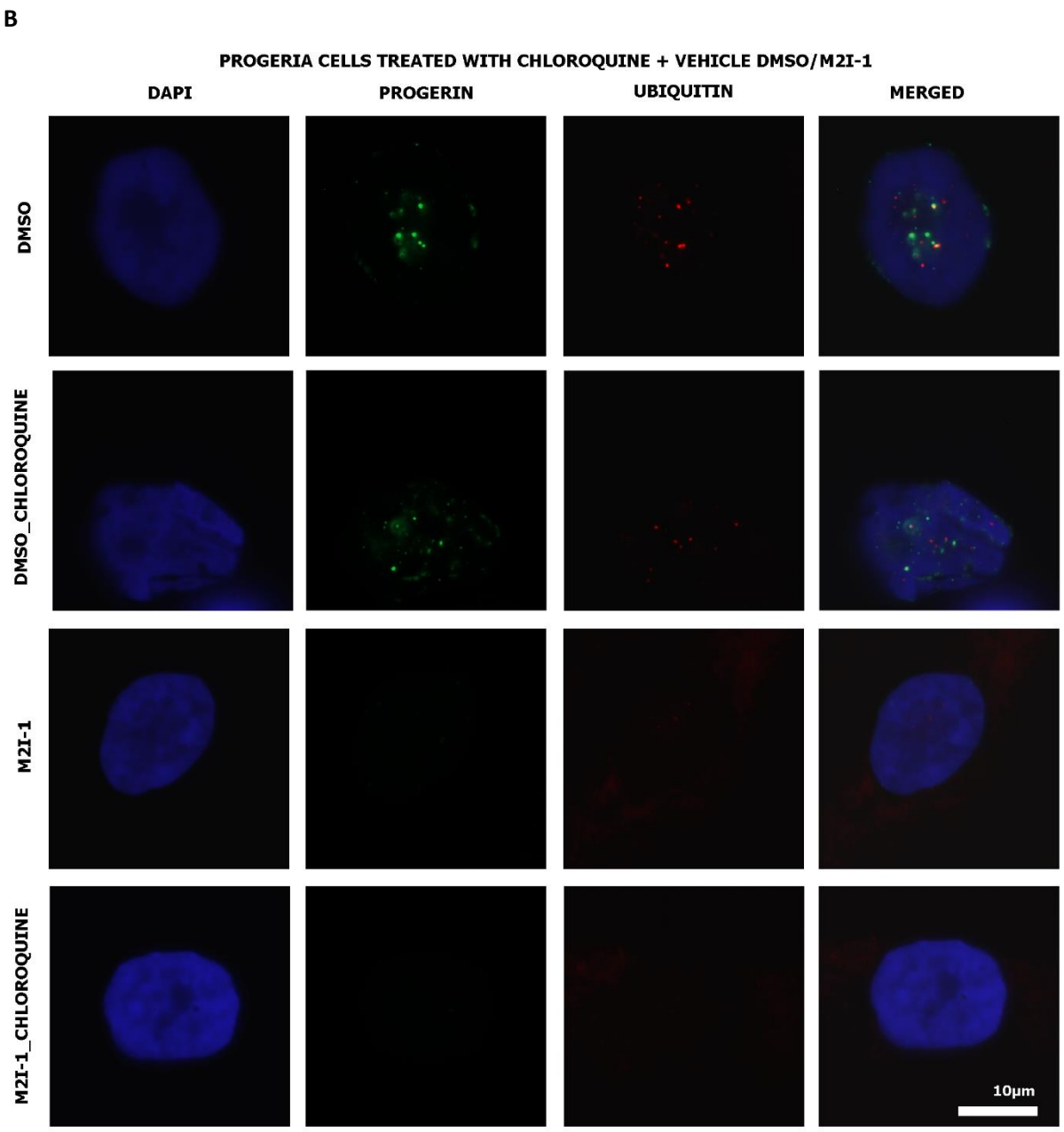

Figure 4.22 Assessment of signal colocalization between progerin and ubiquitin evaluated in the nuclei of HGADFN169 primary fibroblasts.

Fibroblasts grown in coverslips were treated with or without chloroquine in combination with DMSO (vehicle control) or 5 µMM2I-1. After 48 h, cells were fixed, permeabilized and immunolabeled with the primary antibody against progerin and ubiquitin. Images were collected and analyzed with IMAGEJ. A) Images collected at standard exposure times and B) Images collected at lower exposure times.
Green: Progerin Red: Ubiquitin Yellow: Colocalization.

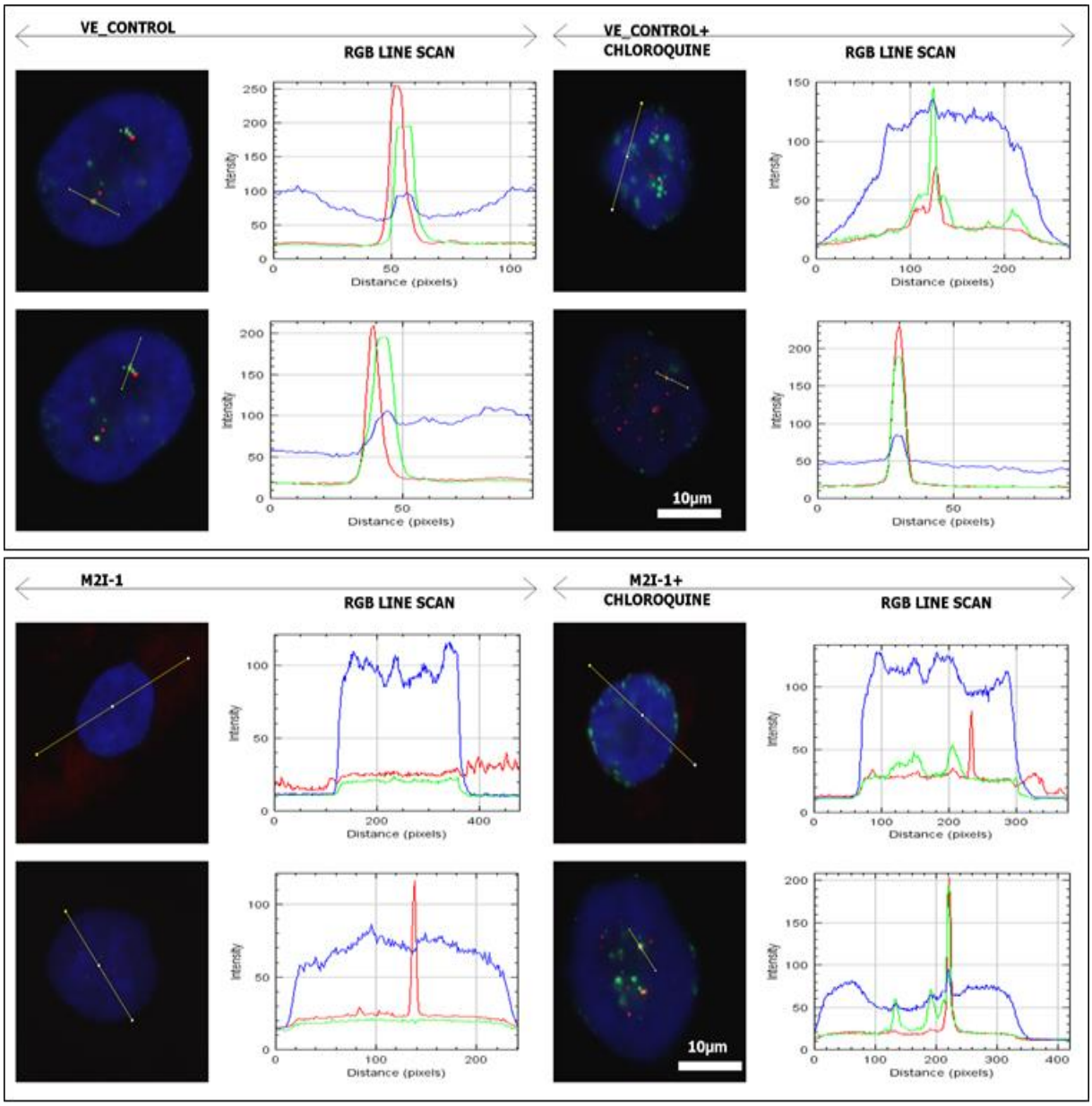

Figure 4.23 RGB linear scans to determine colocalization of progerin and ubiquitin.
HGADFN169 primary fibroblasts treated with vehicle control DMSO (VE_CONTROL), APC activator M2I-1 or chloroquine combined with DMSO (VE_CONTROL+CHLOROQUINE) or M2I-1(M2I-1+CHLOROQUINE), to determine the effect of autophagy inhibition on progerin accumulation.
Blue: DAPI; Green: Progerin; Red: Ubiquitin.

Contrary to our initial hypothesis, we did not observe progerin mobilization into the cytoplasm in HGPS primary fibroblasts. However, this could be due to the defective cycling of HGPS cells, which may result in progerin removal occurring primarily during mitosis when the APC is most active. To investigate this further, we used NB1-hTert fibroblasts that stably express GFP-tagged progerin to study changes in progerin localization upon autophagy inhibition. Our results showed that progerin accumulated in the cytoplasm of NB1-Δ50 cells (Figure 4.24). Specifically, cells treated with the vehicle and chloroquine exhibited foci of progerin in the cytoplasm in 14.9%, compared to 4.9% of cells treated with the vehicle without chloroquine. Similarly, 5.5% of cells treated with M2I-1 exhibited progerin foci in the cytoplasm, compared to 14.4% of cells treated with M2I-1 and chloroquine (Table 4.1).

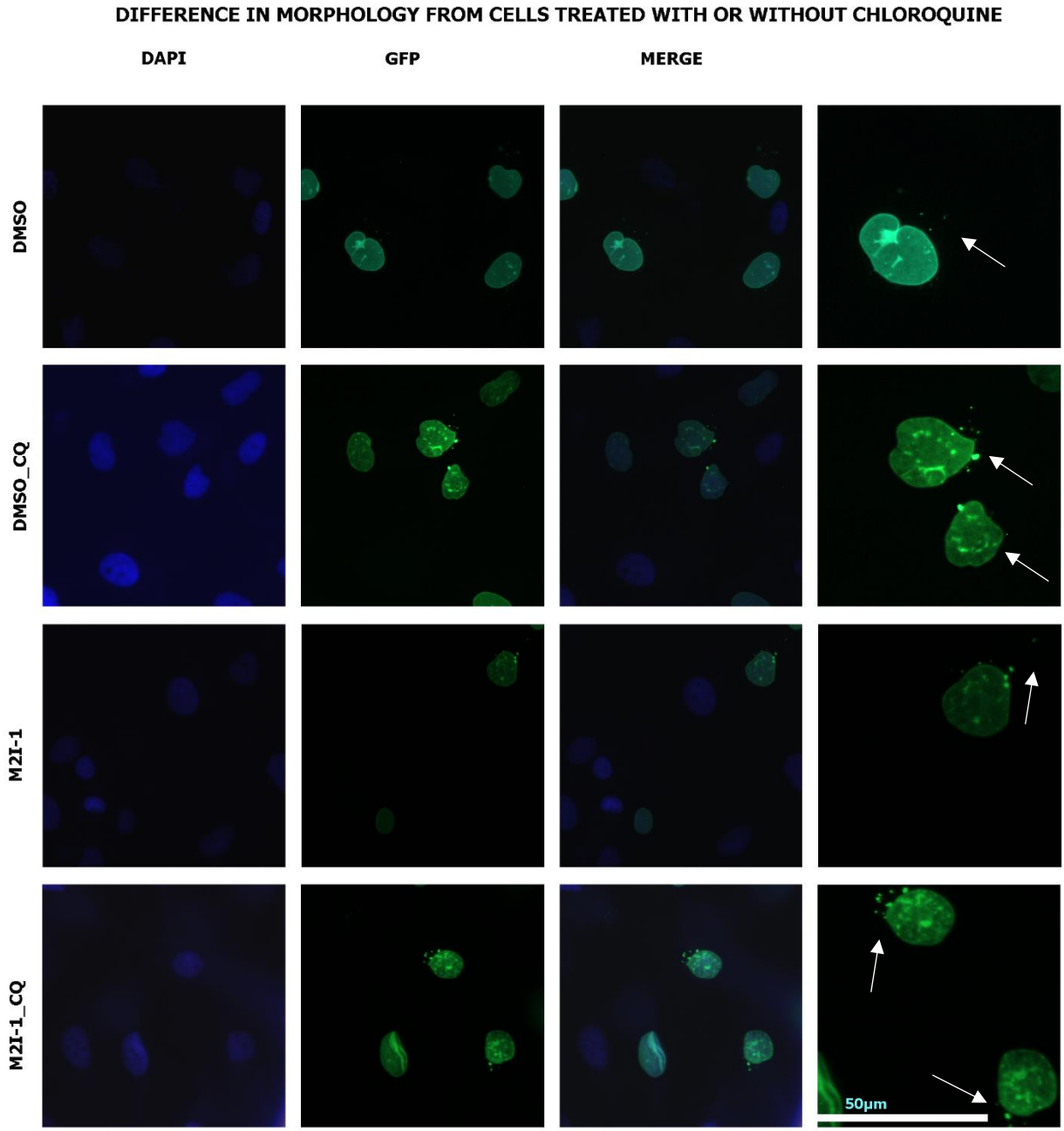

Figure 4.24 Changes in progerin localization upon autophagy inhibition.
NB1-hTERT cells stably expressing the D50 mutation that induces a deletion od 50 amino acids leading to the production of progerin. Cells were treated for 48 h with or without chloroquine in combination with the Vehicle control DMSO or APC activator M2I-1. Green: Progerin, Blue: DAPI staining chromatin**.**

Table 4.1 Quantification of progerin foci located in the cytoplasm of NB1-cells stably expressing progerin

TREATMENT / CELLS	DMSO	CQ_DMSO	M2I-1	CQ_M2I-1
Total number of counted cells	341	369	428	386
GFP-progerin positive cells	144	147	146	139
% of cells with progerin foci in cytoplasm	4.9%	14.9%	5.5%	14.4%

5. DISCUSSION

APC activation and its role in progerin removal and autophagy

In this research, we identified a novel mechanism by which progerin is degraded in HGPS primary fibroblasts. We found that APC, an E3 ubiquitin ligase, is involved in progerin removal from the nuclear lamina mediated by the activation of autophagy. We noted that after the APC is activated with M2I-1, progerin levels decreased, as observed by western blot and immunofluorescence analysis. To our knowledge, this is the first time that an interaction between the APC and progerin has been described. However, in yeast, interactions between the APC and inner nuclear membrane proteins have been observed by Koch and collaborators (2019), where the APC^{CDH1} complex regulates the degradation of the inner nuclear membrane protein Mps3. Similar with progerin accumulation, Mps3 accumulation in the inner nuclear membrane impairs nuclear morphology and cell division. Therefore, it is possible that the APC is an essential player in progerin turnover. There is evidence that Lamin A and progerin can be degraded by ubiquitination, where SMURF2 mediates autophagic-dependent turnover (Borroni *et al.,* 2018). Therefore, Lamin A and progerin ubiquitination and later degradation could be mediated by several cellular machineries to restore cellular health.

We observed that progerin reduction impacts nuclear morphology and population doubling times after the APC is activated. We observed that, on average, M2I-1 treated cells present longer doubling times over 4 passages, which was observed in previous research where primary fibroblasts treated with Rapamycin (inhibitor of Target of Rapamycin mTOR) reduced proliferation rates without inducing quiescence (Gillespie *et al.,* 2015). However, calculating the statistical power using Lehrt's rule, we determined that to produce an assay with 80% statistical of power for the t-test, at least two more observations (passages) would have been necessary (Lehr, 1992; Aberson, 2019). For this reason, it is recommended to start the assay, if possible, with earlier passages than 13. However, this factor is subject to progeria cell availability at the research facility. This assay should be considered as an initial estimation of the treatment's impact since it is subject to variation sources such as pipetting errors, counting errors, automatic cell counter accuracy in progeria cells, differences in counting times, and even the efficiency of cellular detachment when passaging and counting. Similarly, changes in growth rates have been associated with beneficial effects of pro-longevity, as observed by Zehfus *et al.* (2021), where phenolic extracts increased

PDTs with a decrease in intracellular free radicals. Furthermore, HGPS cells were observed to present a hyperproliferation rate before senescence (Bridger & Kill, 2004), so a decrease in doublings could mean that cells are repairing cellular defects or delaying quiescence. However, increased doubling times can also be caused by cellular senescence and premature aging (Scaffidi & Misteli, 2005). For instance, Harhouri and collaborators (2022) found that progerin levels decreased after treating HGPS cells with MG132 as proliferation rates increased. To address this issue, we recommend using flow cytometry to identify alterations in cell cycle progression and determine if cells are arrested in specific phases, such as the G0/G1 phase, to detect early cell senescence. This would also help elucidate whether defects occur during the proliferative state, such as G2/M (Zhang *et al*., 2014). Additionally, long-term passages could help determine an increased cellular lifespan, and positive effects of senescence, such as β-galactosidase activity, can be monitored.

When HGPS cells were treated with MG132, progerin levels decreased. We expected progerin levels to increase since MG132 inhibits the proteasome, and APC activation decreased what we thought was proteasome-dependent progerin destruction. A possible explanation could be that because of MG132, toxicity would not have been enough to be detected using western blots. However, considering this, we monitored protein levels and the total western blot load by ponceau total protein staining and TCE to ensure enough protein was loaded across all treatments. It is also possible that MG132 could have induced progerin clearance through autophagy (Harhouri *et al.*, 2017, 2022), as proteasomal inhibitors can induce autophagy as a compensatory mechanism to maintain proteostasis and degrade ubiquitinated proteins (Tang *et al.,* 2014). In our experiment, when MG132 was combined with M2I-1, we observed the most significant reduction of progerin levels. We used chloroquine as an autophagy inhibitor to assess whether autophagy is involved in progerin clearance after the APC is active. Chloroquine blocks autophagy primarily by inhibiting the fusion of autophagophores and lysosomes without altering the lysosomal acidification process. According to Mauthe *et al.* (2018), chloroquine induces morphological changes in the lysosomes, and causes disorganization of the Golgi apparatus. This disorganization involves relocating Trans-Golgi Network integral protein (TGOLN2) from its perinuclear position to the cytoplasm. As a result of impaired recruitment of Synaptosome Associated Protein 29 (SNAP29), which is necessary for lysosomal fusion, and the fusion of autophagophores and lysosomes to generate a mature autophagophore, is inhibited (Mauthe *et al.,* 2018). In our experiments, chloroquine alone

increased progerin levels in HGPS primary fibroblasts, and when combined with the APC activaror partially inhibited the effect of M2I-1, causing an increase in progerin levels (Figure 4.19, Figure 4.20, Figure 4.21). This indicates that some aspect of APC-progerin degradation depends on autophagy. However, MG132 alone or combined with with M2I-1, did not show increased progerin levels after chloroquine exposure. Harhouri and collaborators (2017) exposed fibroblasts to chloroquine and observed a partial inhibition of MG132 effects after a high chloroquine dose (25-50 μM). To recapitulate this findings we attempted higher doses of chloroquine; however, HGPS cells did not survive to this conditions. Therefore, we were unable to take advantage of higher chloroquine concentrations.

Regarding progerin removal and the role of autophagy, Rapamycin and Metformin have been reported to reduce progerin levels by autophagy induction (Niccoli & Partridge, 2012; Martin-Montalvo *et al*., 2013; Finley, 2018; Harhouri *et al.*, 2018; Belak *et al*., 2020; Lu *et al*., 2021); hence, we theorized that combining these drugs with M2I-1 would have synergistic effects in progerin clearance. From immunoblots, we observed a trend towards decreased progerin levels in the presence of Metformin (Figure 4.8). A similar trend was observed by immunofluorescence (Figure 4.10). Metformin mimics low-nutrient conditions decreasing hepatic gluconeogenesis and inducing autophagy. The most well-known mechanism of Metformin-induced autophagy is through the adenosine 5-monophosphate (AMP)-activated kinase (AMPK). It is proposed that Metformin inhibits mitochondrial complex 1 of the respiratory chain, which results in the suppression of ATP production. This increases the ADT:ATP and AMP:ATP ratios resulting in the activation of AMPK. AMPK activation impacts downstream AMPK-targets, such as inhibition of mammalian target of rapamycin (mTOR), activation of unc-51 like autophagy activating kinase (ULK1) (Hsu *et al.,* 2021; Lu *et al.,* 2021), and decreased protein kinase A (PKA) activity (Luo *et al.,* 2019). The latter affects APC activity. For instance, it was reported in yeast that PKA inhibits APC activity in nutrient abundance (Irniger et al., 2000; Bolte et al., 2003; Harkness, 2018). This inhibition could be caused by the phosphorylation of Cdc34, a component of the E3 ubiquitin ligase SCF, which targets CDH1 for degradation (Cocklin & Goebl, 2011). Therefore, Metformin could cause decreased activity of PKA, reducing SCF targeting of CDH1, facilitating the formation of the APC^{CDH1} complex. Consequently, APC^{CDC20} and APC^{CDH1} are active in distinct cell cycle stages; and since we worked with asynchronous cellular populations, it is possible that Metformin and promoting autophagy to remove progerin, increased APC activity during G1 stage by

promoting the formation of the APC^{CDH1} complex. Therefore, progerin clearance was induced during G2/M (with M2I-1) and G1 phase with Metformin, leading to an overall progerin decrease in the cellular population. Likewise, in primary fibroblasts, Metformin was reported to upregulate the expression of forkhead box O3a (FOXO3a), an essential regulator of metabolism, stress, and lifespan (Gillespie *et al.*, 2019). It is noted that in yeast, FOXO (Fkh1) genetically interacts with the APC to prolong lifespan. Yeast strains that carry a mutation in the APC gene *APC5* are temperature sensitive. Overexpression of *FKH* rescues the *apc5* mutant growth defect and helps cells respond to nutrient stress (Postnikoff *et al.*, 2012), meaning that FOXO proteins interact with the APC under stress. Hence, Metformin-M2I-1 treatment could have further boosted autophagy and longevity pathways to clear progerin.

We did not observe progerin clearance when Everolimus (a rapamycin analog) was combined with M2I-1. Even when both drugs elicit caloric restriction-like responses, they are not direct mimetics of each other. In fact, in primary drugs fibroblasts, these drugs have a different impact on the transcriptome level (Gillespie *et al.*, 2019). While Everolimus directly inhibited mTOR, Metformin would have had a broader range of action to induce autophagy and APC activity by AMPK and FOXO while downregulating PKA. However, assessing the effect of Metformin or Everolimus alone should be necessary at the same experimental conditions as the drugs combined with M2I-1. Additionally to this assay, transcriptome analysis should be carried out to determine how these combinations impact progerin clearance, DNA repair, and recovery of epigenetic markers.

Another aspect that should be noted is the significant variability among biological replicas of cellular treatments evaluated by western blot. Variability in western blot depends greatly on the normalization process, as data points originated from different replicas can not be directly compared (Degasperi *et al.*, 2014). In our protein quantification, we observed variability between biological replicates; however, the trends of protein abundance repeated. Nevertheless, some strategies have been proposed to account for this variability, such as a multi-strip blotting procedure described by Aksamitiene et al. (2007). In multi-strip blots, the proteins of interest of different replicates are cut from the gel and transferred to the same membrane, reducing the variability between blots. Still, this technique would require precision, and an error while cutting the gel would lead to losing the protein of interest. Another strategy includes the use of

normalization by an optimal alignment of the replicas. This means that the data should be scaled by a scaling factor such sum of square differences or mean coefficient of variation between replicates (Degasperi *et al.*, 2014). These methods require establishing a linear protein detection range between quantified intensities and protein amounts per biological replica. In our case, the amount of total protein that can be obtained with HGPS cells is the limiting factor, as well as the increased time and reagents required to generate linearization curves per each experiment. Another case of the influence of biological variation in our experiments was evidenced when the effect of autophagy inhibition was compared in two different HGPS cell lines, HGADFN169 and HGADFN167. Progerin levels decreased in both cell lines after M2I-1 treatments. However, the decrease levels vary depending on the cell line. In HGADFN169, fibroblast progerin was reduced by 20% compared to vehicle control treatments, while in HGADFN167, progerin decreased by 61%. In addition, when cells were incubated with chloroquine, progerin levels increased by 15% in HGADFN169 fibroblasts and 177% in HGADFN167 fibroblasts. In both cases, we observed differences in protein quantifications; however, we observed a consistent trend where progerin decreased upon APC activation and increased upon autophagy inhibition. Even when both cell lines were originated from similar age patients (~8yrs), there are individual variations that cannot be controlled, such as genetic background, epigenetic variations, and external influences that could impact the response to the treatments applied. Therefore, it would be necessary to complement the aforementioned experiments with genetic analysis as identification of individual single nucleotide polymorphisms (SNPs) and analysis expression levels for APC, lamins A/C, or autophagy genes.

APC and progerin interactome

One of our main goals was to determine if progerin interacts with the APC and if this interaction could cause progerin clearance from the nuclear lamina. Fluorescence imaging helps determine protein interactions in their natural environment (Fontana *et al.*, 2010). With PLA assays, we identified the presence of fluorescent foci in the reactions APC2 with progerin, CDC20, and progerin; this could mean an interaction in-situ between constitutive components of the APC and progerin, or at least they are close enough to produce a signal. This signal increases when APC is activated with M2I-1. PLA provides evidence of this protein interaction, and the utilization of specific antibodies provides specificity since it uses probes conjugated with oligonucleotides when

proteins in approximately 40nm from each other (Lönn & Landegren, 2017). Each fluorescent foci or the rolling circle of amplification (RCA) helps to visualize where the reaction is happening in the cell (Söderberg *et al.,* 2006). With this in mind, we mainly counted for interactions occurring in the nuclei since progerin is anchored to the nuclear lamina. However, we also observed RCAs in the cytoplasm, which can indicate where progerin may be mobilized for its degradation by autophagy. Little is known about the specific compartmentalization of the APC, yet evidence suggests this process is compartmentalized. For example, securin turnover occurs in the cytoplasm when the APC-CDC20 complex is active (Shindo *et al.*, 2012). On the other hand, APC could also mediate progerin degradation in the nuclei. Evidence shows that laminas can be degraded by ubiquitin-mediated autophagy-lysosomal activity, where the E3 ligase SMURF2 binds and ubiquitinates Lamin A and progerin. Overexpression of SMURF2 in HGPS cells reduced nuclear morphological aberrations, similar to what we observed after activating the APC with M2I-1 (Borroni *et al.*, 2018). Moreover, in yeast, the APC-mediated clearance of the inner nuclear membrane protein Mps3 is carried out in nucleus-localized proteasomes (Koch *et al.,* 2019). Therefore, from the data presented, it can be concluded that the APC interacts with progerin in the nuclei of HGPS primary fibroblasts.

Besides PLA interactions between APC and progerin, we found that the APC precipitates with Lamin A/C and progerin in Co-IP. This also provides evidence that APC and these laminas could form a complex, as it was visualized in western blot probing for CDC20. Additionally, we identified by PLA a possible interaction between progerin and ubiquitin, contrary to what Serebryannyy & Misteli (2019) observed using high-throughput PLA imaging. This difference could be because PLA signals highly depend on the affinity and concentration of the antibodies used; a negative PLA signal does not mean that these protein interactions are not happening in the cell (Barateau & Buendia, 2016; Serebryannyy & Misteli, 2019). This is evidenced in our research since we used higher concentrations of antibodies, different cell lines, and amplification times than Serebryannyy & Misteli. However, several antibodies should be analyzed against progerin and ubiquitin and compare PLA signals to rule out false positives or negatives due to antibody specificity. To address this issue, we performed colocalization analyses. We identified (although in fewer cells) colocalization of ubiquitin and progerin by immunofluorescence, especially when autophagy is inhibited. Since ubiquitination is transient and a rapid process, it may not be detectable in all the cells (Peng *et al.,* 2003); further analysis should be performed to query the role

of progerin ubiquitination further after the APC is activated. For example, APC components like APC2, CDC27, and APC10 might be compared among non-diseased cells vs. HGPS before and after M2I-1 and autophagy inhibition, accompanied by the observation of autophagy markers. Additionally, like Borroni and collaborators (2018), we could assess progerin ubiquitination using protein synthesis blockers like cycloheximide and in vivo ubiquitination after M2I-1 treatments.

Finally, one of the hallmarks of age is the dysregulation of proteins and the UPS system; in HGPS this is not the exception; protein clearance and proteasome are compromised (Lopez-Otin *et al.*, 2013). We observed that the PLA reaction between two constitutive components of the APC2 and CDC27 decreases in HGPS cells compared to nondiseased fibroblasts. This indicates that the APC may be impaired in HGPS, and the re-establishment of this function by M2I-1 is a player in progerin clearance.

6. CONCLUSIONS

Hutchinson-Gilford progeria syndrome is a devastating disease with no known cure. One of the main causes of cellular defects and loss of proteostasis in HGPS is the accumulation of progerin in the nuclear lamina. However, normally aging individuals also produce this protein. Understanding how progerin is removed from cells can help bridge the knowledge gap regarding protein accumulation in the nuclear lamina and the disease.

We observed that the activation of APC plays a significant role in progerin removal for the first time. This increased the population doubling times and number of doublings in primary HGPS fibroblasts, which could potentially have beneficial pro-longevity effects, as previously observed in the Eskiw lab. Additionally, progerin clearance induced by M2I-1 enhanced physical morphology by increasing the number of cells with a smoother surface that resembled nondiseased cells.

Interactome assays revealed that the APC is in close proximity to progerin. Decreased interactions between APC2 and CDC27 in HGPS cells compared to NB1 provide evidence that the APC may be impaired in HGPS. Colocalization assays further suggest that progerin may be ubiquitinated. This was supported by the fact that the number of foci increased upon APC activation, and these interactions decreased when apcin was applied.

Our research also shows that APC interacts with autophagy to remove progerin from cells. However, whether APC activation directly removes progerin from cells or promotes autophagy in HGPS cells requires further investigation.

7. FUTURE DIRECTIONS.

One of the significant difficulties for this project was the limiting factor of utilizing HGPS patient fibroblasts since they senesce faster, can be difficult to culture, have higher stress sensitivity, low growth, and protein yield. For some assays, the protein concentrations obtained were insufficient using HGPS cells; therefore, to test mechanistic answers of how progerin is degraded, we could implement the use of non-immortalized fibroblasts that stability express progerin in an inducible manner, tetracycline-controlled systems or Tet-On and Tet-Off for instance, to study the mechanism of action of APC activation in progerin removal. Furthermore, stable cell lines could be engineered to overexpress either APC2 or APC10 to provide further evidence of APC's role in progerin clearance, followed by ontology analysis. These cell lines would also help obtain higher cell numbers and more biological replicas to increase statistical power. Another advantage of monoclonal cell population stability expressing progerin lines instead of progeria cells could be a more effortless population synchronization. Since the APC activity depends highly on cell cycle, studying a synchronous cell population could provide further insight into when progerin is degraded after APC activation.

The effect of APC activation using small synthetic peptides that impact APC function on HGPS diseased and nondiseased cells should also be observed. Previously identified by yeast 2-hybrid yeast and developed by the Harkness lab, these peptides induced increased lifespans and stress resistance in yeast. Activation of APC with these compounds would provide further information about the mechanism of action of progerin removal. Hence, this will enable us to address if APC activity is impaired in HGPS cells or if activation of APC through binding of its units would reduce progerin levels and increase cellular lifespan and health span. It should also be considered if this approach would increase stress resistance by exposing cells to peroxide or UV light stressors. Then cell survival could be monitored with cell proliferation reagents such as WST-1 kit (Roche, Indianapolis, IN, USA). Finally, in the future, it should be explored the impact of APC activation on multicellular organisms such as *C. elegans* and HGPS mice models $Lmna^{G609G/G609G}$.

8. LITERATURE CITED

Aberson, C. L. (2019). *Applied power analysis for the behavioral sciences* (Second). Routledge.

Aksamitiene, E., Hoek, J. B., Kholodenko, B., & Klyatkin, A. (2007). Multi-strip Western blotting to increase quantitative data output. *Electrophoresis*, *28*(18), 3163. https://doi.org/10.1002/ELPS.200700002

Alexandru, G., Zachariae, W., Schleiffer, A., & Nasmyth, K. (1999). Sister chromatid separation and chromosome re-duplication are regulated by different mechanisms in response to spindle damage. *EMBO Journal*, *18*(10), 2707–2721. https://doi.org/10.1093/EMBOJ/18.10.2707

Alkuraya, F. S., Saadi, I., Lund, J. J., Turbe-Doan, A., Morton, C. C., & Maas, R. L. (2006). SUMO1 haploinsufficiency leads to cleft lip and palate. *Science (New York, N.Y.)*, *313*(5794), 1751. https://doi.org/10.1126/SCIENCE.1128406

Almeida, A., Bolaños, J. P., & Moreno, S. (2005). *Cellular/Molecular Cdh1/Hct1-APC Is Essential for the Survival of Postmitotic Neurons*. https://doi.org/10.1523/JNEUROSCI.1143-05.2005

Almendáriz-Palacios, C., Gillespie, Z. E., Janzen, M., Martinez, V., Bridger, J. M., Harkness, T. A. A., Mousseau, D. D., & Eskiw, C. H. (2020). The nuclear lamina: Protein accumulation and disease. In *Biomedicines* (Vol. 8, Issue 7). MDPI AG. https://doi.org/10.3390/BIOMEDICINES8070188

Arnason, T. G., MacDonald-Dickinson, V., Davies, J. F., Lobanova, L., Gaunt, C., Trost, B., Waldner, M., Baldwin, P., Borrowman, D., Marwood, H., Gillespie, Z. E., Vizeacoumar, F. S., Vizeacoumar, F. J., Eskiw, C. H., Kusalik, A., & Harkness, T. A. A. (2020). Activation of the Anaphase Promoting Complex reverses multiple drug resistant cancer. *BioRxiv*, 2020.05.26.115337. https://doi.org/10.1101/2020.05.26.115337

Arnason, T. G., MacDonald-Dickinson, V., Gaunt, M. C., Davies, G. F., Lobanova, L., Trost, B., Gillespie, Z. E., Waldner, M., Baldwin, P., Borrowman, D., Marwood, H., Vizeacoumar, F. S., Vizeacoumar, F. J., Eskiw, C. H., Kusalik, A., & Harkness, T. A. A. (2022). Activation of the Anaphase Promoting Complex Reverses Multiple Drug Resistant Cancer in a Canine Model of Multiple Drug Resistant Lymphoma. *Cancers*, *14*(17). https://doi.org/10.3390/cancers14174215

Barateau, A., & Buendia, B. (2016). In situ detection of interactions between nuclear envelope proteins and partners. *Methods in Molecular Biology*, *1411*, 147–158. https://doi.org/10.1007/978-1-4939-3530-7_9/FIGURES/6

Belak, Z. R., Pickering, J. A., Gillespie, Z. E., Audette, G., Eramian, M., Mithcell, J. A., Bridger, J. M., Anthony, K., & Eskiw, C. H. (2020). Genes responsive to rapamycin and serum deprivation are clustered on chromosomes and undergo re-organization within local chromatin environments. *Biochem Cell Biology*, *98*(2), 178–190. https://doi.org/10.1139/bcb-2019-0096

Blank, M. (2020). Targeted Regulation of Nuclear Lamins by Ubiquitin and Ubiquitin-Like Modifiers. *Cells*, *9*(6). https://doi.org/10.3390/CELLS9061340

Bolte, M., Dieckhoff, P., Krause, C., Braus, G. H., & Irniger, S. (2003). Synergistic inhibition of APC/C by glucose and activated Ras proteins can be mediated by each of the Tpk1-3 proteins in Saccharomyces cerevisiae. *Microbiology*, *149*(5), 1205–1216. https://doi.org/10.1099/MIC.0.26062-0/CITE/REFWORKS

Borroni, A. P., Emanuelli, A., Shah, P. A., Ilić, N., Apel-Sarid, L., Paolini, B., Manikoth Ayyathan, D., Koganti, P., Levy-Cohen, G., & Blank, M. (2018). Smurf2 regulates stability and the autophagic–lysosomal turnover of lamin A and its disease-associated form progerin. *Aging Cell*, *17*(2), e12732. https://doi.org/10.1111/ACEL.12732

Boudreau, É., Labib, S., Bertrand, A. T., Decostre, V., Bolongo, P. M., Sylvius, N., Bonne, G., & Tesson, F. (2012). Lamin A/C Mutants Disturb Sumo1 Localization and Sumoylation in Vitro and in Vivo. *PLOS ONE*, *7*(9), e45918. https://doi.org/10.1371/JOURNAL.PONE.0045918

Bridger, J. M., & Kill, I. R. (2004). Aging of Hutchinson-Gilford progeria syndrome fibroblasts is characterised by hyperproliferation and increased apoptosis. *Experimental Gerontology*, *39*(5), 717–724. https://doi.org/10.1016/j.exger.2004.02.002

Bruston, F., Delbarre, E., Östlund, C., Worman, H. J., Buendia, B., & Duband-Goulet, I. (2010). Loss of a DNA binding site within the tail of prelamin A contributes to altered heterochromatin anchorage by progerin. *FEBS Letters*, *584*(14), 2999–3004. https://doi.org/10.1016/J.FEBSLET.2010.05.032

Capell, B. C., & Collins, F. S. (2006). Human laminopathies: Nuclei gone genetically awry. In *Nature Reviews Genetics* (Vol. 7, Issue 12, pp. 940–952). https://doi.org/10.1038/nrg1906

Casasola, A., Scalzo, D., Nandakumar, V., Halow, J., Recillas-Targa, F., Groudine, M., & Rincón-Arano, H. (2016). Prelamin A processing, accumulation and distribution in normal cells and laminopathy disorders. *Nucleus*, *7*(1), 84–102. https://doi.org/10.1080/19491034.2016.1150397

Castro, A., Bernis, C., Vigneron, S., Labbé, J. C., & Lorca, T. (2005). The anaphase-promoting complex: A key factor in the regulation of cell cycle. *Oncogene*, *24*(3), 314–325.

https://doi.org/10.1038/sj.onc.1207973

Chakravarti, D., LaBella, K. A., & DePinho, R. A. (2021). Telomeres: history, health, and hallmarks of aging. *Cell*, *184*(2), 306–322. https://doi.org/10.1016/J.CELL.2020.12.028

Chi, Y.-H., Chen, Z.-J., & Jeang, K.-T. (2009). The nuclear envelopathies and human diseases. *Journal of Biomedical Science*, *16*(1), 96. https://doi.org/10.1186/1423-0127-16-96

Chojnowski, A., Ong, P. F., Wong, E. S. M., Lim, J. S. Y., Mutalif, R. A., Navasankari, R., Dutta, B., Yang, H., Liow, Y. Y., Sze, S. K., Boudier, T., Wright, G. D., Colman, A., Burke, B., Stewart, C. L., & Dreesen, O. (2015). Progerin reduces LAP2α-telomere association in hutchinson-gilford progeria. *ELife*, *4*(AUGUST2015), 1–21. https://doi.org/10.7554/ELIFE.07759

Cocklin, R., & Goebl, M. (2011). Nutrient Sensing Kinases PKA and Sch9 Phosphorylate the Catalytic Domain of the Ubiquitin-Conjugating Enzyme Cdc34. *PLOS ONE*, *6*(11), e27099. https://doi.org/10.1371/JOURNAL.PONE.0027099

Cook, P. R. (2001). *Principles of nuclear structure and function / Peter R. Cook. | Wellcome Collection*. wiley-Liss. https://wellcomecollection.org/works/n6nstv24

David, D. C., Ollikainen, N., Trinidad, J. C., Cary, M. P., Burlingame, A. L., & Kenyon, C. (2010). Widespread Protein Aggregation as an Inherent Part of Aging in C. elegans. *PLoS Biology*, *8*(8), e1000450. https://doi.org/10.1371/journal.pbio.1000450

De Sandre-Giovannoli, A., Bernard, R., Cau, P., Navarro, C., Amiel, J., Boccaccio, I., Lyonnet, S., Stewart, C. L., Munnich, A., Le Merrer, M., & Lévy, N. (2003). Lamin A truncation in Hutchinson-Gilford progeria. *Science*, *300*(5628), 2055. https://doi.org/10.1126/SCIENCE.1084125/SUPPL_FILE/DESANDRE.SOM.PDF

Deboy, E., Puttaraju, M., Jailwala, P., Kasoji, M., Cam, M., & Misteli, T. (2017). Identification of novel RNA isoforms of LMNA. *Nucleus*, *VOL. 8*(NO. 5,), 573–582. https://doi.org/10.1080/19491034.2017.1348449

Dechat, T., Adam, S. A., & Goldman, R. D. (2009). Nuclear Lamins and Chromatin: When Structure Meets Function. *Advances in Enzyme Regulation*, *49*(1), 157. https://doi.org/10.1016/J.ADVENZREG.2008.12.003

Dechat, T., Adam, S. A., Taimen, P., Shimi, T., & Goldman, R. D. (2010). Nuclear lamins. *Cold Spring Harbor Perspectives in Biology*, *2*(11), 1–22. https://doi.org/10.1101/cshperspect.a000547

Dechat, T., Pfleghaar, K., Sengupta, K., Shimi, T., Shumaker, D. K., Solimando, L., & Goldman, R. D. (2008). Nuclear lamins: major factors in the structural organization and function of the nucleus and chromatin. *Genes & Development*, *22*(7), 832. https://doi.org/10.1101/GAD.1652708

Degasperi, A., Birtwistle, M. R., Volinsky, N., Rauch, J., Kolch, W., & Kholodenko, B. N. (2014). Evaluating Strategies to Normalise Biological Replicates of Western Blot Data. *PLoS ONE*, *9*(1), 87293. https://doi.org/10.1371/JOURNAL.PONE.0087293

Dittmer, T., & Misteli, T. (2011). The lamin protein family. *Genome Biology*, *12*(5), 1–14. https://doi.org/10.1186/GB-2011-12-5-222/FIGURES/6

Dobrzynska, A., Gonzalo, S., Shanahan, C., & Askjaer, P. (2016). The nuclear lamina in health and disease. *Nucleus*, *7*(3), 233–248. https://doi.org/10.1080/19491034.2016.1183848

Dou, Z., Xu, C., Donahue, G., Shimi, T., Pan, J. A., Zhu, J., Ivanov, A., Capell, B. C., Drake, A. M., Shah, P. P., Catanzaro, J. M., Ricketts, M. D., Lamark, T., Adam, S. A., Marmorstein, R., Zong, W. X., Johansen, T., Goldman, R. D., Adams, P. D., & Berger, S. L. (2015). Autophagy mediates degradation of nuclear lamina. *Nature*, *527*(7576), 105–109. https://doi.org/10.1038/nature15548

Egesipe, A. L., Blondel, S., Cicero, A. Lo, Jaskowiak, A. L., Navarro, C., De Sandre-Giovannoli, A., Levy, N., Peschanski, M., & Nissan, X. (2016). Metformin decreases progerin expression and alleviates pathological defects of hutchinson–gilford progeria syndrome cells. *Npj Aging and Mechanisms of Disease*, *2*(1), 16026. https://doi.org/10.1038/npjamd.2016.26

Eissenberg, J. C., & Gonzalo, S. (2020). Pushing the limit on laminopathies. In *Nature Materials* (Vol. 19, Issue 4, pp. 378–380). Nature Research. https://doi.org/10.1038/s41563-020-0648-1

Eriksson, M., Brown, W. T., Gordon, L. B., Glynn, M. W., Singer, J., Scott, L., Erdos, M. R., Robbins, C. M., Moses, T. Y., Berglund, P., Dutra, A., Pak, E., Durkin, S., Csoka, A. B., Boehnke, M., Glover, T. W., & Collins, F. S. (2003). Recurrent de novo point mutations in lamin A cause Hutchinson-Gilford progeria syndrome. *Nature*, *423*(6937), 293–298. https://doi.org/10.1038/NATURE01629

Field, M. C., & Rout, M. P. (2019). Pore timing: the evolutionary origins of the nucleus and nuclear pore complex. *F1000Research*, *8*. https://doi.org/10.12688/F1000RESEARCH.16402.1

Finley, J. (2018). Cellular stress and AMPK activation as a common mechanism of action linking the effects of metformin and diverse compounds that alleviate accelerated aging defects in Hutchinson-Gilford progeria syndrome. *Medical Hypotheses*, *118*, 151–162. https://doi.org/10.1016/j.mehy.2018.06.029

Fontana, L., Partridge, L., & Longo, V. D. (2010). Extending healthy life span-from yeast to humans. *Science*, *328*(5976), 321–326. https://doi.org/10.1126/SCIENCE.1172539/SUPPL_FILE/PLAYLIST.XML

Fujita, H., Sasaki, T., Miyamoto, T., Akutsu, S. N., Sato, S., Mori, T., Nakabayashi, K., Hata, K., Suzuki, H., Kosaki, K., Matsuura, S., Matsubara, Y., Amagai, M., & Kubo, A. (2020). Premature aging syndrome showing random chromosome number instabilities with CDC20 mutation. *Aging Cell*, *19*(11). https://doi.org/10.1111/ACEL.13251

Gabriel, D., Gordon, L. B., & Djabali, K. (2016). Temsirolimus partially rescues the Hutchinson-Gilford progeria cellular phenotype. *PLoS ONE*, *11*(12). https://doi.org/10.1371/journal.pone.0168988

Gaillard, M. C., & Reddy, K. L. (2018). The Nuclear Lamina and Genome Organization. *Nuclear Architecture and Dynamics*, 321–343. https://doi.org/10.1016/B978-0-12-803480-4.00014-4

Geiss-Friedlander, R., & Melchior, F. (2007). Concepts in sumoylation: a decade on. *Nature Reviews Molecular Cell Biology 2007 8:12*, *8*(12), 947–956. https://doi.org/10.1038/nrm2293

Gerace, L., & Huber, M. D. (2012). Nuclear lamina at the crossroads of the cytoplasm and nucleus. In *Journal of Structural Biology* (Vol. 177, Issue 1, pp. 24–31). https://doi.org/10.1016/j.jsb.2011.11.007

Ghosh, S., & Zhou, Z. (2014). Genetics of aging, progeria and lamin disorders. *Current Opinion in Genetics and Development*, *26*, 41–46. https://doi.org/10.1016/j.gde.2014.05.003

Gilbert, S. F. (Ed.). (2000). Aging: The Biology of Senescence - Developmental Biology - NCBI Bookshelf. In *Developmental Biology* (6th editio). Sinauer Associates. https://www.ncbi.nlm.nih.gov/books/NBK10041/

Gillespie, Z. E., Mackay, K., Sander, M., Trost, B., Dawicki, W., Wickramarathna, A., Gordon, J., Eramian, M., Kill, I. R., Bridger, J. M., Kusalik, A., Mitchell, J. A., & Eskiw, C. H. (2015). *Rapamycin reduces fibroblast proliferation without causing quiescence and induces STAT5A/B-mediated cytokine production*. *6*(6). https://doi.org/10.1080/19491034.2015.1128610

Gillespie, Z. E., Wang, C., Vadan, F., Yu, T. Y., Ausió, J., Kusalik, A., & Eskiw, C. H. (2019). Metformin induces the AP-1 transcription factor network in normal dermal fibroblasts OPEN. *Scientific Reports*. https://doi.org/10.1038/s41598-019-41839-1

Goldberg, M. W., Huttenlauch, I., Hutchison, C. J., & Stick, R. (2008). Filaments made from A- and B-type lamins differ in structure and organization. *Journal of Cell Science*, *121*(2), 215–225.

https://doi.org/10.1242/JCS.022020

Goldman, R. D., Shumaker, D. K., Erdos, M. R., Eriksson, M., Goldman, A. E., Gordon, L. B., Gruenbaum, Y., Khuon, S., Mendez, M., Varga, R., & Collins, F. S. (2004). Accumulation of mutant lamin A causes progressive changes in nuclear architecture in Hutchinson–Gilford progeria syndrome. *Proceedings of the National Academy of Sciences*, *101*(24), 8963–8968. https://doi.org/10.1073/PNAS.0402943101

González Morán, M. G. (2014). Síndrome de Progeria de Hutchinson-Gilford. Causas, investigación y tratamientos farmacológicos. *Educacion Quimica*, *25*(4), 432–439. https://doi.org/10.1016/S0187-893X(14)70063-1

Gordon, L. B., Rothman, F. G., López-Otín, C., & Misteli, T. (2014). Progeria: A Paradigm for Translational Medicine. *HHS Public Access*, *156*(3), 400–407. https://doi.org/10.1016/j.cell.2013.12.028

Gruenbaum, Y., Margalit, A., Goldman, R. D., Shumaker, D. K., & Wilson, K. L. (2005). The nuclear lamina comes of age. *Nature Reviews Molecular Cell Biology 2005 6:1*, *6*(1), 21–31. https://doi.org/10.1038/nrm1550

Guerville, F., De Souto Barreto, P., Ader, I., Andrieu, S., Casteilla, L., Dray, C., Fazilleau, N., Guyonnet, S., Langin, D., Liblau, R., Parini, A., Valet, P., Vergnolle, N., Rolland, Y., & Vellas, B. (2019). Revisiting the Hallmarks of Aging to Identify Markers of Biological Age. *The Journal of Prevention of Alzheimer's Disease 2019 7:1*, *7*(1), 56–64. https://doi.org/10.14283/JPAD.2019.50

Gütgemann, I., Lehman, N. L., Jackson, P. K., & Longacre, T. A. (2008). Emi1 protein accumulation implicates misregulation of the anaphase promoting complex/cyclosome pathway in ovarian clear cell carcinoma. *Modern Pathology 2008 21:4*, *21*(4), 445–454. https://doi.org/10.1038/modpathol.3801022

Harhouri, K., Cau, P., Casey, F., Guedenon, K. M., Doubaj, Y., Van, L., Mejia-baltodano, G., Bartoli, C., Sandre-giovannoli, A. De, & Nicolas, L. (2022). MG132 Induces Progerin Clearance and Improves Disease Phenotypes in HGPS-like Patients ' Cells. *Cells*, *11*(4), 610. https://doi.org/10.3390/cells11040610

Harhouri, K., Frankel, D., Bartoli, C., Roll, P., De Sandre-Giovannoli, A., Lévy, N., & Evy, N. L. (2018). An overview of treatment strategies for hutchinson-gilford progeria syndrome. *Nucleus*, *9*(1), 265–276. https://doi.org/10.1080/19491034.2018.1460045

Harhouri, K., Navarro, C., Depetris, D., Mattei, M., Nissan, X., Cau, P., De Sandre-Giovannoli, A., & Lévy, N. (2017). MG 132-induced progerin clearance is mediated by autophagy activation and splicing regulation . *EMBO Molecular Medicine*, *9*(9), 1294–1313. https://doi.org/10.15252/emmm.201607315

Harkness, T. (2006). The Anaphase Promoting Complex and Aging: The APCs of Longevity. *Current Genomics*, *7*(4), 263–272. https://doi.org/10.2174/138920206778426997

Harkness, T. A. A. (2018). *Activating the Anaphase Promoting Complex to Enhance Genomic Stability and Prolong Lifespan*. https://doi.org/10.3390/ijms19071888

Harkness, T. A. A. A., Shea, K. A., Legrand, C., Brahmania, M., & Davies, G. F. (2004). A Functional Analysis Reveals Dependence on the Anaphase-Promoting Complex for Prolonged Life Span in Yeast. *Genetics*, *168*(2), 759–774. https://doi.org/10.1534/genetics.104.027771

Hars, E. S., Qi, H., Ryazanov, A. G., Jin, S., Cai, L., Hu, C., & Liu, L. F. (2006). Autophagy Regulates Ageing in C. elegans. *Http://Dx.Doi.Org/10.4161/Auto.3636*, *3*(2), 93–95. https://doi.org/10.4161/AUTO.3636

Hershko, A., & Ciechanover, A. (1998). THE UBIQUITIN SYSTEM. In *Annu. Rev. Biochem* (Vol. 67). www.annualreviews.org

Hipp, M. S., Kasturi, P., & Hartl, F. U. (2019). The proteostasis network and its decline in ageing. *Nature Reviews Molecular Cell Biology 2019 20:7*, *20*(7), 421–435. https://doi.org/10.1038/s41580-019-0101-y

Hochstrasser, M. (2009). Origin and Function of Ubiquitin-like Protein Conjugation. *Nature*, *458*(7237), 422. https://doi.org/10.1038/NATURE07958

Hommen, F., Bilican, S., & Vilchez, D. (2021). Protein clearance strategies for disease intervention. *Journal of Neural Transmission 2021 129:2*, *129*(2), 141–172. https://doi.org/10.1007/S00702-021-02431-Y

Hsu, S. K., Cheng, K. C., Mgbeahuruike, M. O., Lin, Y. H., Wu, C. Y., Wang, H. M. D., Yen, C. H., Chiu, C. C., & Sheu, S. J. (2021). New Insight into the Effects of Metformin on Diabetic Retinopathy, Aging and Cancer: Nonapoptotic Cell Death, Immunosuppression, and Effects beyond the AMPK Pathway. *International Journal of Molecular Sciences*, *22*(17), 9453. https://doi.org/10.3390/IJMS22179453

Irniger, S., Bäumer, M., & Braus, G. H. (2000). Glucose and Ras Activity Influence the Ubiquitin Ligases

APC/C and SCF in Saccharomyces cerevisiae. *Genetics*, *154*(4), 1509–1521. https://doi.org/10.1093/GENETICS/154.4.1509

Jana, N. R. (2012). Protein homeostasis and aging: Role of ubiquitin protein ligases. In *Neurochemistry International* (Vol. 60, Issue 5, pp. 443–447). Elsevier Ltd. https://doi.org/10.1016/j.neuint.2012.02.009

Janin, A., Bauer, D., Ratti, F., Millat, G., & Méjat, A. (2017). Nuclear envelopathies: A complex LINC between nuclear envelope and pathology. In *Orphanet Journal of Rare Diseases* (Vol. 12, Issue 1, pp. 1–16). BioMed Central Ltd. https://doi.org/10.1186/s13023-017-0698-x

Johnson, T. E. (1990). Increased Life-Span of age-1 Mutants in Caenorhabditis elegans and Lower Gompertz Rate of Aging. *Science*, *249*(4971), 908–912. https://doi.org/10.1126/SCIENCE.2392681

Kalukula, Y., Stephens, A. D., Lammerding, J., & Gabriele, S. (2022). Mechanics and functional consequences of nuclear deformations. *Nature Reviews Molecular Cell Biology 2022 23:9*, *23*(9), 583–602. https://doi.org/10.1038/s41580-022-00480-z

Kane, A. E., & Sinclair, D. A. (2019). Epigenetic changes during aging and their reprogramming potential. *Https://Doi.Org/10.1080/10409238.2019.1570075*, *54*(1), 61–83. https://doi.org/10.1080/10409238.2019.1570075

Karoutas, A., & Akhtar, A. (2021). Functional mechanisms and abnormalities of the nuclear lamina. In *Nature Cell Biology* (Vol. 23, Issue 2, pp. 116–126). Nature Research. https://doi.org/10.1038/s41556-020-00630-5

Kastl, J., Braun, J., Prestel, A., Möller, H. M., Huhn, T., & Mayer, T. U. (2015). Mad2 Inhibitor-1 (M2I-1): A Small Molecule Protein-Protein Interaction Inhibitor Targeting the Mitotic Spindle Assembly Checkpoint. *ACS Chemical Biology*, *10*(7), 1661–1666. https://doi.org/10.1021/acschembio.5b00121

Kataria, M., & Yamano, H. (2019). Interplay between Phosphatases and the Anaphase-Promoting Complex/Cyclosome in Mitosis. *Cells 2019, Vol. 8, Page 814*, *8*(8), 814. https://doi.org/10.3390/CELLS8080814

Khanna, R., Krishnamoorthy, V., & Parnaik, V. K. (2018). E3 ubiquitin ligase RNF123 targets lamin B1 and lamin-binding proteins. *The FEBS Journal*, *285*(12), 2243–2262. https://doi.org/10.1111/FEBS.14477

Klass, M. R. (1983). A method for the isolation of longevity mutants in the nematode Caenorhabditis

elegans and initial results. *Mechanisms of Ageing and Development*, *22*(3–4), 279–286. https://doi.org/10.1016/0047-6374(83)90082-9

Koch, B. A., Jin, H., Tomko, R. J., & Yu, H.-G. G. (2019). The anaphase-promoting complex regulates the degradation of the inner nuclear membrane protein Mps3. *Journal of Cell Biology*, *218*(3), 839–854. https://doi.org/10.1083/jcb.201808024

Labbadia, J., & Morimoto, R. I. (2014). Proteostasis and longevity: when does aging really begin? *F1000 Prime Reports*. https://doi.org/10.12703/P6-7

Lammerding, J. (2011). Mechanics of the Nucleus. *Comprehensive Physiology*, *1*(2), 783. https://doi.org/10.1002/CPHY.C100038

LE, L., & JV, R. (2002). Identification of a new APC/C recognition domain, the A box, which is required for the Cdh1-dependent destruction of the kinase Aurora-A during mitotic exit. *Genes & Development*, *16*(17), 2274–2285. https://doi.org/10.1101/GAD.1007302

Lehr, R. (1992). Sixteen S-squared over D-squared: A relation for crude sample size estimates. *Statistics in Medicine*, *11*(8), 1099–1102. https://doi.org/10.1002/sim.4780110811

Leidal, A. M., Levine, B., & Debnath, J. (2018). Autophagy and the cell biology of age-related disease. *Nature Cell Biology 2018 20:12*, *20*(12), 1338–1348. https://doi.org/10.1038/s41556-018-0235-8

Li, M., Shin, Y.-H., Hou, L., Huang, X., Wei, Z., Klann, E., & Zhang, P. (2008). The Adaptor Protein of the Anaphase Promoting Complex Cdh1 Plays An Essential Role in Maintaining Replicative Lifespan and in Learning and Memory. In *Nat Cell Biol* (Vol. 10, Issue 9).

Longo, V. D., Antebi, A., Bartke, A., Barzilai, N., Brown-Borg, H. M., Caruso, C., Curiel, T. J., De Cabo, R., Franceschi, C., Gems, D., Ingram, D. K., Johnson, T. E., Kennedy, B. K., Kenyon, C., Klein, S., Kopchick, J. J., Lepperdinger, G., Madeo, F., Mirisola, M. G., … Fontana, L. (2015). Interventions to slow aging in humans: Are we ready? *Aging Cell*, *14*(4), 497–510. https://doi.org/10.1111/ACEL.12338

Lönn, P., & Landegren, U. (2017). Close Encounters – Probing Proximal Proteins in Live or Fixed Cells. *Trends in Biochemical Sciences*, *42*(7), 504–515. https://doi.org/10.1016/J.TIBS.2017.05.003

The hallmarks of aging, 153 Cell 1194 (2013). https://doi.org/10.1016/j.cell.2013.05.039

Lu, G., Wu, Z., Shang, J., Xie, Z., Chen, C., & zhang, C. (2021). The effects of metformin on autophagy. *Biomedicine & Pharmacotherapy*, *137*, 111286. https://doi.org/10.1016/J.BIOPHA.2021.111286

Luo, Z., Zhu, T., Luo, W., Lv, Y., Zhang, L., Wang, C., Li, M., Wu, W., & Shi, S. (2019). Metformin induces apoptotic cytotoxicity depending on AMPK/PKA/GSK-3β-mediated c-FLIPL degradation in non-small cell lung cancer. *Cancer Management and Research*, *11*, 681. https://doi.org/10.2147/CMAR.S178688

Mackenzie, M. E., Postnikoff, S. D. . L., Arnason, T. G., Harkness, T. . A. A., Malo, E., Postnikoff, S. D. . L., Arnason, T. G., Harkness, T. . A. A., Mackenzie, M. E., Postnikoff, S. D. . L., Arnason, T. G., & Harkness, T. . A. A. (2016). Mitotic degradation of yeast Fkh1 by the Anaphase Promoting Complex is required for normal longevity, genomic stability and stress resistance. *AGING*, *8*(4), 810–828. www.impactaging.com

Malashicheva, A., & Perepelina, K. (2021). Diversity of Nuclear Lamin A/C Action as a Key to Tissue-Specific Regulation of Cellular Identity in Health and Disease. *Frontiers in Cell and Developmental Biology*, *9*, 2834. https://doi.org/10.3389/FCELL.2021.761469/BIBTEX

Malo, E., Postnikoff, S. D. L., Arnason, T. G., & Harkness, T. A. A. (2016). *Mitotic degradation of yeast Fkh1 by the Anaphase Promoting Complex is required for normal longevity , genomic stability and stress resistance*. *8*(4), 810–830.

Martin-Montalvo, A., Mercken, E. M., Mitchell, S. J., Palacios, H. H., Mote, P. L., Scheibye-Knudsen, M., Gomes, A. P., Ward, T. M., Minor, R. K., Blouin, M. J., Schwab, M., Pollak, M., Zhang, Y., Yu, Y., Becker, K. G., Bohr, V. A., Ingram, D. K., Sinclair, D. A., Wolf, N. S., … De Cabo, R. (2013). Metformin improves healthspan and lifespan in mice. *Nature Communications 2013 4:1*, *4*(1), 1–9. https://doi.org/10.1038/ncomms3192

Mauthe, M., Orhon, I., Rocchi, C., Zhou, X., Luhr, M., Hijlkema, K. J., Coppes, R. P., Engedal, N., Mari, M., & Reggiori, F. (2018). Chloroquine inhibits autophagic flux by decreasing autophagosome-lysosome fusion. *Autophagy*, *14*(8), 1435–1455. https://doi.org/10.1080/15548627.2018.1474314/SUPPL_FILE/KAUP_A_1474314_SM5890.ZIP

McClintock, D., Ratner, D., Lokuge, M., Owens, D. M., Gordon, L. B., Collins, F. S., & Djabali, K. (2007). The Mutant Form of Lamin A that Causes Hutchinson-Gilford Progeria Is a Biomarker of Cellular Aging in Human Skin. *PLoS ONE*, *2*(12), e1269. https://doi.org/10.1371/journal.pone.0001269

McCord, R. P., Nazario-Toole, A., Zhang, H., Chines, P. S., Zhan, Y., Erdos, M. R., Collins, F. S., Dekker, J., & Cao, K. (2013). Correlated alterations in genome organization, histone methylation, and DNA-lamin A/C interactions in Hutchinson-Gilford progeria syndrome. *Genome Research*,

23(2), 260–269. https://doi.org/10.1101/GR.138032.112

Medvar, B., Raghuram, V., Pisitkun, T., Sarkar, A., & Knepper, M. A. (2016). Comprehensive database of human E3 ubiquitin ligases: application to aquaporin-2 regulation. *Physiological Genomics*, *48*(7), 502. https://doi.org/10.1152/PHYSIOLGENOMICS.00031.2016

Meraldi, P., Honda, R., & Nigg, E. A. (2002). Aurora-A overexpression reveals tetraploidization as a major route to centrosome amplification in p53–/– cells. *The EMBO Journal*, *21*(4), 483. https://doi.org/10.1093/EMBOJ/21.4.483

Metzger, M. B., Hristova, V. A., & Weissman, A. M. (2012). HECT and RING finger families of E3 ubiquitin ligases at a glance. *Journal of Cell Science*, *125*(3), 531–537. https://doi.org/10.1242/JCS.091777/-/DC1

Meuleman, W., Peric-Hupkes, D., Kind, J., Beaudry, J. B., Pagie, L., Kellis, M., Reinders, M., Wessels, L., & Van Steensel, B. (2013). Constitutive nuclear lamina–genome interactions are highly conserved and associated with A/T-rich sequence. *Genome Research*, *23*(2), 270–280. https://doi.org/10.1101/GR.141028.112

Meyer, H. J., & Rape, M. (2014). Enhanced protein degradation by branched ubiquitin chains. *Cell*, *157*(4), 910–921. https://doi.org/10.1016/j.cell.2014.03.037

Misteli, T., & Scaffidi, P. (2005). *Genome instability in progeria: when repair gets old* (Vol. 718). http://www.nature.com/naturemedicine

Niccoli, T., & Partridge, L. (2012). Ageing as a Risk Factor for Disease. *Current Biology*, *22*(17), R741–R752. https://doi.org/10.1016/J.CUB.2012.07.024

Orioli, D., & Dellambra, E. (2018). Epigenetic regulation of skin cells in natural aging and premature aging diseases. *Cells*, *7*(12), 1–30. https://doi.org/10.3390/cells7120268

Ottaviano, Y., & Gerace, L. (1985). Phosphorylation of the nuclear lamins during interphase and mitosis. *Journal of Biological Chemistry*, *260*(1), 624–632. https://doi.org/10.1016/S0021-9258(18)89778-2

Ottens, F., Franz, A., & Hoppe, T. (2021). Build-UPS and break-downs: metabolism impacts on proteostasis and aging. *Cell Death & Differentiation 2021 28:2*, *28*(2), 505–521. https://doi.org/10.1038/s41418-020-00682-y

Pandey, U. B., Batlevi, Y., Baehrecke, E. H., & Taylor, J. P. (2007). HDAC6 at the Intersection of Autophagy, the Ubiquitin-proteasome System, and Neurodegeneration.

Https://Doi.Org/10.4161/Auto.5050, *3*(6), 643–645. https://doi.org/10.4161/AUTO.5050

Paschal, B. M., & Kelley, J. B. (2013). Nuclear Lamina. *Encyclopedia of Biological Chemistry: Second Edition*, 310–313. https://doi.org/10.1016/B978-0-12-378630-2.00477-1

Passmore, L. A., & Barford, D. (2004). Getting into position: the catalytic mechanisms of protein ubiquitylation. *Biochem. J*, *379*, 513–525.

Peng, J., Schwartz, D., Elias, J. E., Thoreen, C. C., Cheng, D., Marsischky, G., Roelofs, J., Finley, D., & Gygi, S. P. (2003). A proteomics approach to understanding protein ubiquitination. *Nature Biotechnology 2003 21:8*, *21*(8), 921–926. https://doi.org/10.1038/nbt849

Perez-Hernandez, D., Mendez, M. L., & Dittmar, G. (2020). Ubiquitin Proteasome Patway. In Z. Xianquan (Ed.), *Intech* (p. 124). IntechOpen. https://doi.org/10.5772/intechopen.87547

Pérez, V. I., Buffenstein, R., Masamsetti, V., Leonard, S., Salmon, A. B., Mele, J., Andziak, B., Yang, T., Edrey, Y., Friguet, B., Ward, W., Richardson, A., & Chaudhuri, A. (2009). Protein stability and resistance to oxidative stress are determinants of longevity in the longest-living rodent, the naked mole-rat. *Proceedings of the National Academy of Sciences of the United States of America*, *106*(9), 3059–3064. https://doi.org/10.1073/pnas.0809620106

Peters, J. M. (2006). The anaphase promoting complex/cyclosome: A machine designed to destroy. *Nature Reviews Molecular Cell Biology*, *7*(9), 644–656. https://doi.org/10.1038/nrm1988

Pickart, C. M. (2001). *MECHANISMS UNDERLYING UBIQUITINATION*. www.annualreviews.org

Pollard, T. D., Earnshaw, W. C., Lippincott-Schwartsz, J., & Jonson, G. T. (2017). Introduction to the Cell Cycle. In T. Pollard, W. Earnshaw, J. Lippincott-Schwartz, & G. Johnson (Eds.), *Cell Biology* (Third, pp. 697–711). Elsevier. https://doi.org/10.1016/b978-0-323-34126-4.00040-2

Postnikoff, S. D. L., Malo, M. E., Wong, B., & Harkness, T. A. A. (2012). The Yeast Forkhead Transcription Factors Fkh1 and Fkh2 Regulate Lifespan and Stress Response Together with the Anaphase-Promoting Complex. *PLOS Genetics*, *8*(3), e1002583. https://doi.org/10.1371/JOURNAL.PGEN.1002583

Quek, L. S., Grasset, N., Jasmen, J. B., Robinson, K. S., & Bellanger, S. (2018). Dual Role of the Anaphase Promoting Complex/Cyclosome in Regulating Stemness and Differentiation in Human Primary Keratinocytes. *Journal of Investigative Dermatology*, *138*(8), 1851–1861. https://doi.org/10.1016/j.jid.2018.02.033

Romo-Tena, J., Rajme-López, S., Aparicio-Vera, L., Alcocer-Varela, J., & Gómez-Martín, D. (2018). Lys63-polyubiquitination by the E3 ligase casitas B-lineage lymphoma-b (Cbl-b) modulates peripheral regulatory T cell tolerance in patients with systemic lupus erythematosus. *Clinical and Experimental Immunology*, *191*(1), 42–49. https://doi.org/10.1111/CEI.13054

Sadowski, M., & Sarcevic, B. (2010). Mechanisms of mono- and poly-ubiquitination: Ubiquitination specificity depends on compatibility between the E2 catalytic core and amino acid residues proximal to the lysine. *Cell Division*, *5*(1), 1–5. https://doi.org/10.1186/1747-1028-5-19/FIGURES/2

Scaffidi, P., & Misteli, T. (2005). Reversal of the cellular phenotype in the premature aging disease Hutchinson-Gilford progeria syndrome. *Nature Medicine*, *11*(4), 440–445. https://doi.org/10.1038/nm1204

Scaffidi, P., & Misteli, T. (2007). Lamin A-Dependent Nuclear Defects in Human Aging. *National Institute of Health*. https://doi.org/10.1126/science.1084125

Schwitzgebel, V. M. (2014). Many faces of monogenic diabetes. *J Diabetes Invest*, *5*, 121–133. https://doi.org/10.1111/jdi.12197

Serebryannyy, L., & Misteli, T. (2018). Protein sequestration at the nuclear periphery as a potential regulatory mechanism in premature aging. *Journal of Cell Biology*, *217*(1), 21–38. https://doi.org/10.1083/jcb.201706061

Serebryannyy, L., & Misteli, T. (2019). HiPLA: High-throughput imaging proximity ligation assay. *Methods*, *157*, 80–87. https://doi.org/10.1016/j.ymeth.2018.11.004

Shimi, T., Pfleghaar, K., Kojima, S. I., Pack, C. G., Solovei, I., Goldman, A. E., Adam, S. A., Shumaker, D. K., Kinjo, M., Cremer, T., & Goldman, R. D. (2008). The A- and B-type nuclear lamin networks: microdomains involved in chromatin organization and transcription. *Genes & Development*, *22*(24), 3409–3421. https://doi.org/10.1101/GAD.1735208

Shimia, T., Kittisopikul, M., Tran, J., Goldman, A. E., Adam, S. A., Zheng, Y., Jaqaman, K., & Goldman, R. D. (2015). Structural organization of nuclear lamins A, C, B1, and B2 revealed by superresolution microscopy. *Molecular Biology of the Cell*, *26*(22), 4075–4086. https://doi.org/10.1091/MBC.E15-07-0461/ASSET/IMAGES/LARGE/MBC-26-4075-G005.JPEG

Shindo, N., Kumada, K., & Hirota, T. (2012). Separase Sensor Reveals Dual Roles for Separase Coordinating Cohesin Cleavage and Cdk1 Inhibition. *Developmental Cell*, *23*(1), 112–123. https://doi.org/10.1016/J.DEVCEL.2012.06.015

Shumaker, D. K., Dechat, T., Kohlmaier, A., Adam, S. A., Bozovsky, M. R., Erdos, M. R., Eriksson, M., Goldman, A. E., Khuon, S., Collins, F. S., Jenuwein, T., & Goldman, R. D. (2006). Mutant nuclear lamin A leads to progressive alterations of epigenetic control in premature aging. *Proceedings of the National Academy of Sciences of the United States of America*, *103*(23), 8703–8708. https://doi.org/10.1073/PNAS.0602569103

Simon, D. N., & Wilson, K. L. (2013). Partners and post-translational modifications of nuclear lamins. *Chromosoma 2013 122:1*, *122*(1), 13–31. https://doi.org/10.1007/S00412-013-0399-8

Skaar, J. R., & Pagano, M. (2009). Control of cell growth by the SCF and APC/C ubiquitin ligases. *National Institute of Health*, *21*(6), 816–824. https://doi.org/10.1016/j.ceb.2009.08.004

Söderberg, O., Gullberg, M., Jarvius, M., Ridderstråle, K., Leuchowius, K. J., Jarvius, J., Wester, K., Hydbring, P., Bahram, F., Larsson, L. G., & Landegren, U. (2006). Direct observation of individual endogenous protein complexes in situ by proximity ligation. *Nature Methods 2006 3:12*, *3*(12), 995–1000. https://doi.org/10.1038/nmeth947

Somech, R. R. A., Shaklai, S., Amariglio, N., Rechavi, G., & Simon, A. J. (2005). Nuclear Envelopathies—Raising the Nuclear Veil. In *Pediatric Research* (Vol. 57, Issue 5, pp. 8R-15R). Nature Publishing Group. https://doi.org/10.1203/01.PDR.0000159566.54287.6C

Statistics Canada. (2021). *The Daily — Canada's population estimates: Age and sex, July 1, 2021*. Canada's Population Estimates: Age and Sex, July 1, 2021. https://doi.org/https://doi.org/10.25318/1710000501-eng

Stierlé, V., Couprie, J., Östlund, C., Krimm, I., Zinn-Justin, S., Hossenlopp, P., Worman, H. J., Courvalin, J. C., & Duband-Goulet, I. (2003). The carboxyl-terminal region common to lamins A and C contains a DNA binding domain. *Biochemistry*, *42*(17), 4819–4828. https://doi.org/10.1021/BI020704G

Strieter, E. R., & Korasick, D. A. (2011). *Unraveling the Complexity of Ubiquitin Signaling*. https://doi.org/10.1021/cb2004059

Tamburri, S., Lavarone, E., Fernández-Pérez, D., Conway, E., Zanotti, M., Manganaro, D., & Pasini, D. (2020). Histone H2AK119 Mono-Ubiquitination Is Essential for Polycomb-Mediated Transcriptional Repression. *Molecular Cell*, *77*(4), 840-856.e5. https://doi.org/10.1016/J.MOLCEL.2019.11.021

Tang, B., Cai, J., Sun, L., Li, Y., Qu, J., Snider, B. J., & Wu, S. (2014). Proteasome inhibitors activate

autophagy involving inhibition of PI3K-Akt-mTOR pathway as an anti-oxidation defense in human RPE cells. *PLoS ONE*, *9*(7). https://doi.org/10.1371/JOURNAL.PONE.0103364

Tsakiri, E. N., & Trougakos, I. P. (2015). The amazing ubiquitin-proteasome system: Structural components and implication inaging. In *International Review of Cell and Molecular Biology* (Vol. 314). Elsevier Ltd. https://doi.org/10.1016/bs.ircmb.2014.09.002

Uhlmann, F., Wernic, D., Poupart, M. A., Koonin, E. V., & Nasmyth, K. (2000). Cleavage of Cohesin by the CD Clan Protease Separin Triggers Anaphase in Yeast. *Cell*, *103*(3), 375–386. https://doi.org/10.1016/S0092-8674(00)00130-6

Varshavsky, A. (2012). The Ubiquitin System, an Immense Realm. *Annual Review of Biochemistry*, *81*(1), 167–176. https://doi.org/10.1146/annurev-biochem-051910-094049

Vodermaier, H. C. (2004). APC/C and SCF: Controlling each other and the cell cycle. In *Current Biology* (Vol. 14, Issue 18, pp. R787–R796). https://doi.org/10.1016/j.cub.2004.09.020

von Mikecz, A. (2006). The nuclear ubiquitin-proteasome system. In *Journal of Cell Science* (Vol. 119, Issue 10, pp. 1977–1984). The Company of Biologists Ltd. https://doi.org/10.1242/jcs.03008

Wang, X. J., Yu, J., Wong, S. H., Cheng, A. S., Chan, F. K., Ng, S. S., Cho, C. H., Sung, J. J., & Wu, W. K. (2013). A novel crosstalk between two major protein degradation systems: regulation of proteasomal activity by autophagy. *Autophagy*, *9*(10), 1500–1508. https://doi.org/10.4161/AUTO.25573

Wei, W., Ayad, N. G., Wan, Y., Zhang, G.-J., Kirschner, M. W., & Kaelin, W. G. (2004). *Degradation of the SCF component Skp2 in cell-cycle phase G1 by the anaphase-promoting complex*. www.nature.com/nature

Wente, S. R. (2000). Gatekeepers of the nucleus. *Science (New York, N.Y.)*, *288*(5470), 1374–1377. https://doi.org/10.1126/SCIENCE.288.5470.1374

Wheaton, K., Campuzano, D., Ma, W., Sheinis, M., Ho, B., Brown, G. W., & Benchimol, S. (2017). *Progerin-Induced Replication Stress Facilitates Premature Senescence in Hutchinson-Gilford Progeria Syndrome*. https://doi.org/10.1128/MCB.00659-16

World Health Organization. (2021). *Ageing and health*. https://www.who.int/news-room/fact-sheets/detail/ageing-and-health

Wu, X., & Karin, M. (2015). Emerging roles of Lys63-linked polyubiquitylation in immune responses.

Immunological Reviews, *266*(1), 161–174. https://doi.org/10.1111/imr.12310

Ye, Q., Callebaut, I., Pezhman, A., Courvalin, J. C., & Worman, H. J. (1997). Domain-specific Interactions of Human HP1-type Chromodomain Proteins and Inner Nuclear Membrane Protein LBR *. *Journal of Biological Chemistry*, *272*(23), 14983–14989. https://doi.org/10.1074/JBC.272.23.14983

Zastrow, M. S., Vlcek, S., & Wilson, K. L. (2004). Proteins that bind A-type lamins: integrating isolated clues. *Journal of Cell Science*, *117*(7), 979–987. https://doi.org/10.1242/JCS.01102

Zehfus, L. R., Gillespie, Z. E., Almendáriz-palacios, C., Low, N. H., & Eskiw, C. H. (2021). Haskap berry phenolic subclasses differentially impact cellular stress sensing in primary and immortalized dermal fibroblasts. *Cells*, *10*(10), 2643. https://doi.org/10.3390/CELLS10102643/S1

Zhang, H., Xiong, Z. M., & Cao, K. (2014). Mechanisms controlling the smooth muscle cell death in progeria via down-regulation of poly(ADP-ribose) polymerase 1. *Proceedings of the National Academy of Sciences of the United States of America*, *111*(22), E2261. https://doi.org/10.1073/PNAS.1320843111/-/DCSUPPLEMENTAL

Zhang, Y. Q., & Sarge, K. D. (2008). *Sumoylation regulates lamin A function and is lost in lamin A mutants associated with familial cardiomyopathies*. *182*(1). https://doi.org/10.1083/JCB.200712124

Zhou, Z., He, M., Shah, A. A., & Wan, Y. (2016). Insights into APC/C: From cellular function to diseases and therapeutics. *Cell Division*, *11*(1), 1–18. https://doi.org/10.1186/s13008-016-0021-6